BROOKHAVEN NATIONAL LABORATORY

BNL-98984-2012-IR

BWR Anticipated Transients Without SCRAM in the MELLLA+ Expanded Operating Domain

Part 4: Sensitivity Studies for Events Leading to Emergency Depressurization

L-Y Cheng, J-S Baek, A. Cuadra, A. Aronson, D. Diamond

January 2013

Nuclear Science & Technology Department

Brookhaven National Laboratory

U.S. Department of Energy
U.S Nuclear Regulatory Commission
Office of Nuclear Regulatory Research

DISCLAIMER

BROOKHAVEN NATIONAL LABORATORY

BNL-98984-2012-IR

BWR ANTICIPATED TRANSIENTS WITHOUT SCRAM IN THE MELLLA+ EXPANDED OPERATING DOMAIN

Part 4: Sensitivity Studies for Events Leading to Emergency Depressurization

Manuscript Completed:
January 22, 2013

Prepared by:
Lap-Yan Cheng, Joo-Seok Baek, Arantxa Cuadra, Arnold Aronson,
David Diamond
Nuclear Science and Technology Department
Brookhaven National Laboratory

and

Peter Yarsky
Office of Nuclear Regulatory Research
U.S. Nuclear Regulatory Commission

Prepared for:

Tarek Zaki, NRC Project Manager
Office of Nuclear Regulatory Research
U.S. Nuclear Regulatory Commission
Washington, DC 20555-0001
NRC Job Codes V6150, F6018

ABSTRACT

This is the fourth in a series of reports on the response of a boiling water reactor (BWR) to anticipated transients without reactor scram (ATWS) when operating in the expanded operating domain MELLLA+ (maximum extended load line limit analysis plus). In this report ATWS events initiated by closure of main steam isolation valves are analyzed at beginning-of-cycle, and end-of-full-power-life, conditions. These events include emergency depressurization (ED). The objective is to understand the sensitivity of ATWS-ED events to the initial operating core flow and to the spectrally corrected moderator density history (void history). Different water level control strategies are considered.

The ATWS events are simulated for a sufficiently long time (2500 s) to understand the response of key components and the potential for fuel damage or failure of the containment. These events lead to the automatic trip of recirculation pumps; and operator actions to manually activate the automatic depressurization system (ADS) when the wetwell (suppression pool) has reached the heat capacity temperature limit, and to control power through water level control and the injection of soluble boron.

The simulations were carried out using the TRACE/PARCS code system and models developed for a previous study with all relevant BWR systems.

TABLE OF CONTENTS

LIST OF FIGURES

LIST OF TABLES

ACKNOWLEDGEMENTS

This project was a joint effort of Brookhaven National Laboratory (BNL) and U.S. Nuclear Regulatory Commission staff. The authors wish to thank the Project Manager Tarek Zaki, and his predecessor Istvan Frankl, for their support, and the staff in the Office of Nuclear Regulatory Research, Reactor Systems Code Branch, for their efforts to quickly assess and rectify problems, identified by BNL, in the computer codes used in the project. We also appreciate the work done by Lynda Fitz to finalize this document and provide administrative support.

ACRONYMS

3D	Three dimensional
ADF	Assembly Discontinuity Factor
ADS	Automatic Depressurization System
ATWS	Anticipated Transient Without SCRAM
ATWS-ED	Anticipated Transient Without SCRAM with Emergency Depressurization
ATWS-I	Anticipated Transient Without SCRAM with Instability
BNL	Brookhaven National Laboratory
BOC	Beginning of Cycle
BWR	Boiling Water Reactor
CB	Control Block in TRACE Input
CONTAN	Containment Component in TRACE Input
DC	Downcomer
DW	Drywell
DWO	Density-Wave Oscillation
ED	Emergency Depressurization
EOFPL	End of Full Power Life
FCT	Fuel Centerline Temperature
FW	Feedwater
GE	General Electric
GEH	GE Hitachi
HCTL	Heat Capacity Temperature Limit
LP	Lower Plenum
MELLLA+	Maximum Extended Load Line Limit Analysis Plus
MSIV	Main Steam Isolation Valve
NEM	Nodal Expansion Method

NRC	Nuclear Regulatory Commission
OLTP	Original Licensed Thermal Power
PARCS	Purdue Advanced Reactor Core Simulator
PCT	Peak Clad Temperature
PHE	Peak Hot Excess
RPS	Reactor Protection System
RPT	Recirculation Pump Trip
RPV	Reactor Pressure Vessel
RWL	Reactor Water Level
SETS	Stability Enhancing Two-Step method
S-I	Semi-Implicit Numerics
SLCS	Standby Liquid Control System
SP	Suppression Pool
SRV	Safety Relief Valve
TAF	Top of Active Fuel
TRACE	TRAC-RELAP Advanced Computational Engine
UH	Void History
UHSPH	Void History Spectrally Corrected

1 INTRODUCTION

1.1 Background

Boiling Water Reactors (BWRs) have in recent years been increasing operating power; sometimes to 120% of their original licensed thermal power (OLTP). This places them in an expanded operating domain and changes how they maneuver in the power-flow operating map. One option being pursued, "maximum extended load line limit analysis plus" (MELLLA+) operation [1], raises questions about how the plant will respond to anticipated transients without scram (ATWS). This report is one of several Brookhaven National Laboratory (BNL) reports that describe how these events were simulated with state-of-the-art codes, and the results of that analysis.

In a previous report [2] a discussion is given of how MELLLA+ operation affects the power-flow operating map and the impact of this in an ATWS event. If the initiating event is a turbine trip, then after the automatic trip of the recirculation pumps, the reactor evolves to a relatively high power to flow condition and specifically to a region of the power-flow map where unstable power oscillations are likely to occur. The occurrence of these power oscillations, if left unmitigated, may result in fuel damage. Additionally, the severity of the power oscillations may hamper the effectiveness of mitigation strategies. For example, ATWS events are typically mitigated through the injection of dissolved neutron absorber (boron) through the standby liquid control system (SLCS). The occurrence of oscillation induced core inlet flow reversal may reduce the rate at which this soluble absorber is delivered to the active region of the reactor core. The results of studies of these ATWS events with core instability (ATWS-I) are given in [2, 3].

If the initiating event is the closure of main steam isolation valves (MSIVs) the concern is the amount of energy placed into containment during the mitigation period. This thermal load may exhaust available pressure suppression capacity of the containment wetwell, which would prompt the operators to conduct a manual emergency depressurization according to standard emergency operating procedures. The emergency depressurization raises several concerns: (1) the reactor has undergone a beyond-design-basis event, and fuel damage may have occurred, (2) the pressure suppression capacity of the containment has been exhausted, and (3) the reactor coolant pressure boundary has been bypassed by manually opening the automatic depressurization system valves. One study of these ATWS events with emergency depressurization (ATWS-ED) is discussed in a companion report [4].

1.2 Objectives

ATWS-ED events were studied in a previous report [4] for a typical BWR/5 plant for the simulation of ATWS-ED events, the TRACE BWR/5 model was modified to become a BWR/4-like model with lower plenum SLCS injection. Significant insight was gained as to reactor behavior and the ability to mitigate these events. In the present study, the

objective is to understand the sensitivity of ATWS-ED events to operating core flow and spectrally corrected moderator density history (void history). The correction to the moderator history is to take into account the impact of factors such as leakage or control state, on the neutron energy spectrum. The study considers different water level control strategies (top of active fuel (TAF) ± a given number of feet) and different times in the fuel cycle (beginning of cycle (BOC) and end of full-power life (EOFPL)). The specific cases considered are summarized in Table 1.1. In the context of this study the nominal core flows for the BOC and the EOFPL conditions are assumed to be 85% and 105% of rated flow, respectively. In this report, results of the sensitivity cases listed in Table 1.1 are compared with results of the corresponding reference cases presented in a previous report [4].

Table 1.1 Simulation Conditions of ATWS-ED Cases

Case ID	Exposure	Core Flow Rate, %	Reactor Water Level Strategy	SLCS Injection
4B	BOC	75*	TAF+5	Lower Plenum
10D	EOFPL	75*	TAF-2	Lower Plenum
10A	EOFPL	85**	TAF+5	Lower Plenum
11A	EOFPL	85**	TAF	Lower Plenum
12A	EOFPL	85**	TAF-2	Lower Plenum
10C	EOFPL UHSPH#	105	TAF+5	Lower Plenum

* No adjustment made to control rod bank to achieve criticality (requested by NRC)

** Upper-peaked power shape in the allowable operating domain

Void history spectrally corrected (UHSPH)

1.3 Methodology

The methodology used in the present study is the same as used in the previous studies [2, 4] where it is explained in detail. The basic tool is TRACE/PARCS which couples the modeling of thermal-hydraulics throughout all relevant reactor components (TRACE) with the modeling of neutronics in the core (PARCS). The code package has been assessed for its applicability to ATWS [5] and the previous studies [2, 4] provided additional insights into its capability. Indeed, one of the objectives of those studies was to further assess the capabilities of TRACE/PARCS to calculate the phenomena associated with BWR ATWS events at MELLLA+ conditions.

Reactor systems/components that are modeled are: the steam line, including turbine bypass and stop valves, safety/relief valves, and main steam isolation valves; the recirculation loop, including recirculation pumps; feedwater and reactor water level control; reactor core isolation cooling with an option to draw from the condensate

storage tank or the suppression pool; standby liquid control system; primary containment (drywell and wetwell) with pool cooling; and the vessel including core, steam separator/dryer, and jet pumps.

The core requires special attention and each fuel bundle is individually represented in the neutronics model. In the thermal-hydraulic model the bundles are lumped into 27 thermal-hydraulic channel groups. Nuclear data for each bundle are a function of thermal-hydraulic variables and the presence of control blades and soluble boron. Models for three different times in the fuel cycle are available: BOC, peak hot excess reactivity (PHE), and EOFPL. Within each bundle four different types of fuel rods are modeled.

The validity of these models is in part assessed by comparing steady state results for power distributions with those obtained by the vendor, GE-Hitachi (GEH). They are also compared with results obtained using 382 thermal-hydraulic channel groups as used for the ATWS-I studies. Those results are documented in [4].

1.4 Organization of Report

The analysis of the sensitivity calculations is given in Chapter 2. This includes consideration of the effect of reduced core operating flow and the effect of spectrally corrected moderator density history (void history). Conclusions are provided in Chapter 3 and references in Chapter 4. Appendix A contains a comparison of results from two versions of the TRACE executable that had been used in this study. Appendix B explores the sensitivity of the ATWS-ED results to two aspects of the TRACE numerical computation, the numerical scheme used and the time-step size. Appendix C, on CD, has input files and copies of all plots shown in Chapter 2 and Appendices A and B. It also includes a set of plots of time-dependent parameters for all cases listed in Table 1.1.

2 SENSITIVITY STUDIES FOR MSIV CLOSURE EVENTS

2.1 Introduction

Sensitivity studies have been conducted to evaluate the effects of reduced core flow and the effect of spectrally corrected moderator density history (void history). Table 2.1 lists all ATWS-ED transients that have been analyzed. Results of the first eleven cases in the table have been presented in a previous report [4] and are considered the base reference cases. The remaining six cases are the sensitivity cases (as listed in Table 1.1) and are the subject of the current report.

Table 2.1 Simulation Conditions of ATWS-ED Cases

Case ID	Exposure	Core Flow Rate, %	Reactor Water Level Strategy	SLCS Injection
6	BOC	85	TAF-2	Lower Plenum
7	PHE	85	TAF+5	Lower Plenum
4	BOC	85	TAF+5	Lower Plenum
7C	PHE	85	TAF+5	Upper Plenum
5	BOC	85	TAF	Lower Plenum
10	EOFPL	105	TAF+5	Lower Plenum
12	EOFPL	105	TAF-2	Lower Plenum
EDSI#	BOC	85	TAF	Lower Plenum
9	PHE	85	TAF-2	Lower Plenum
8	PHE	85	TAF	Lower Plenum
11	EOFPL	105	TAF	Lower Plenum
Listed Below are the Current Sensitivity Cases				
4B	BOC	75*	TAF+5	Lower Plenum
10D	EOFPL	75*	TAF-2	Lower Plenum
10A	EOFPL	85**	TAF+5	Lower Plenum
11A	EOFPL	85**	TAF	Lower Plenum
12A	EOFPL	85**	TAF-2	Lower Plenum
10C	EOFPL UHSPH##	105	TAF+5	Lower Plenum

Simulation with semi-implicit (S-I) numerics
Void history spectrally corrected (UHSPH)
* No adjustment made to control rod bank to achieve criticality (requested by the NRC)
** Upper-peaked power shape in the allowable operating domain

The analysis of the sensitivity cases utilized the same TRACE/PARCS models as those used in the previous ATWS-ED studies [4]. The models, summarized in Section 1.3, are

explained in detail in [4]. The same input model was used in all six sensitivity cases however they were analyzed using three different versions (executable) of TRACE. The executable used for each case is indicated in Table 2.2.

Table 2.2 Version of TRACE Executable Used

Case ID	Exposure	Core Flow Rate, %	Reactor Water Level Strategy	TRACE Executable
4B	BOC	75	TAF+5	V5.540_fxValveChoke.x
10D	EOFPL	75	TAF-2	V5.0p3P32m07co_x64.exe
10A	EOFPL	85	TAF+5	V5.540_fxValveChoke.x
11A	EOFPL	85	TAF	V5.540_fxValveChoke.x
12A	EOFPL	85	TAF-2	V5.0p3P32m07co.x
10C	EOFPL UHSPH	105	TAF+5	V5.540_fxValveChoke.x

The Linux and Windows executables are identified by filename extensions ".x" and ".exe" respectively. All eleven of the base reference cases were analyzed using V5.540_fxValveChoke.x, a version that is very similar to the latest released version of TRACE (V5.541 is V5 Patch 3). However, this version of the executable failed to complete two of the EOFPL cases at reduced flow (75% and 85%) with water level reduction to TAF-2. The difficulty appears to be related to failure of PARCS to converge when the reactor power is at decay heat levels. A revised version of TRACE, V5.0p3P32m07co, was subsequently used to complete the two TAF-2 sensitivity cases. Two of the relevant changes made in the PARCS module of TRACE that enable the completion of the TAF-2 simulations are:

1. A limiter was added to the assembly discontinuity factor (ADF) adjustment factor, on the left and right faces of the considered node.
2. For the nodal expansion method (NEM) kernel, a limit was also placed on the lowest value for the surface flux.

Further discussion on the use of different TRACE executables in the simulation of ATWS-ED transients is given in Appendix A.

In addition to using a modified version of TRACE, the simulation of the two TAF-2 sensitivity cases required the following changes in the execution of the transient:

1. For the EOFPL 85% flow TAF-2 case, the Linux executable, V5.0p3P32m07co.x, terminated due to a failure in the thermal-hydraulic calculation for the CONTAN component. A change in the CSTEP input for the CONTAN from 1.0 to 0.5 was successful in eliminating the execution error. It is noted that no error was experienced in the Windows executable, even without the input change.

2. A power spike was observed at about 700 s in the EOFPL 75% flow TAF-2 case using the Linux executable, V5.0p3P32m07co.x. While the cause of the anomaly is under investigation the transient was simulated to completion successfully by using the equivalent executable for the Windows platform, namely V5.0p3P32m07co_x64.exe.
3. All three EOFPL TAF-2 cases, 105% (base reference case), 85% and 75% flow, were analyzed using the semi-implicit (S-I) numerical scheme with a maximum time-step size of 0.02 s. Attempts to run the cases using the stability enhancing two-step method (SETS) with a maximum time-step size of 0.01 s failed. Appendix B examines the sensitivity of the results to the numerical scheme and the maximum time-step size. It includes results of a sensitivity study, cited in footnote b in [4], examining the impact of time-step size and numerics on the natural circulation flow through the core and the downcomer.

The ATWS with emergency depressurization (ATWS-ED) of interest is initiated by a spurious closure of the main steam isolation valves (MSIV) with subsequent failure of the reactor protection system (RPS) to SCRAM the reactor. The same ATWS-ED scenario, as used in the previous report [4] and summarized in Table 2.3, was applied to the sensitivity cases.

Table 2.3 ATWS-ED Scenario

Event	Timing/Setpoint
Begin transient simulation	0.0 s
MSIV closure	10.0 s (0.5 s delay + 4 s closure time)
Recirculation pump trip (2RPT)	Reactor pressure vessel (RPV) pressure exceeds 7.651 MPa
SRVs cycling	See Table 2.4 in [4]
Reactor water level reduction	130.0 s
Begin boron injection	211.0 s
Emergency depressurization	Suppression pool temperature exceeds 344.26 K
Reactor water level recovery	2180.0 s
End of simulation	2500.0 s

It is noted that the scenario includes four operator actions [4]:

1. Water level control to top of active fuel (TAF), TAF plus five feet (TAF+5) or TAF minus two feet (TAF-2). This is accomplished at 130 s by artificially raising the calculated water level by a fixed amount (over a 0.1 s interval) and feeding it to the water level control system.

2. Boron injection. This is initiated at 211 s and linearly ramped to full flow in 60 s.

3. Emergency depressurization (ED). Operator actuation of the automatic depressurization system (ADS) is triggered when the heat capacity temperature

limit (HCTL) of the suppression pool reaches a simulated setpoint at a temperature of 344.26 K.

4. Water level recovery to normal water level. This is accomplished at 2180 s by reducing the artificial water level adjustment to zero over a 100 s period.

All transient cases were run as a restart case from a TRACE/PARCS coupled steady-state. Details of the code execution can be found in Section 2.1 of [4]. The initial steady-state conditions for the sensitivity cases have been established earlier and reported in [4]. Table 2.4 identifies the corresponding sections in [4] that provide the initial steady-state results for the sensitivity cases.

Table 2.4 Reference for the Initial Steady-State

Case ID	Exposure	Core Flow Rate, %	Reactor Water Level Strategy	Sections in [4] that Describe the Initial Steady-State Conditions
4B	BOC	75	TAF+5	Section 3.1.4
10D	EOFPL	75	TAF-2	Section 3.3.5
10A	EOFPL	85	TAF+5	Section 3.3.5
11A	EOFPL	85	TAF	Section 3.3.5
12A	EOFPL	85	TAF-2	Section 3.3.5
10C	EOFPL UHSPH	105	TAF+5	Section 3.3.4

The general progression of all cases is quite similar and a synopsis of the ATWS-ED transient has been provided in Section 4.1 of [4]. Descriptions of the representative base cases for the BOC and EOPFL cycle conditions are in Sections 4.2 and 4.4 of [4] respectively.

Results of the six sensitivity cases are discussed in comparison with their corresponding base reference cases and with each other. In the context of the sensitivity study the base reference cases will have the following initial core flows as defined in [4]:

BOC = 85% of rated flow
EOFPL = 105% of rated flow

Section 2.2 compares Case 4B to Case 4 [BOC TAF+5: 75% and 85% flow (the reference case)]. Section 2.3 discusses the effect of the spectrally corrected void history, comparing Cases 10C and 10 [EOFPL TAF+5: UHSPH and UH (the reference case)]. Section 2.4 examines the effects of reduced core flow at the EOFPL, comparing Cases 10D, 12A and 12 [EOFPL TAF-2: 75%, 85% and 105% (the reference case) flow]. Finally Section 2.5 compares the three EOFPL cases at 85% flow, Cases 10A, 11A and 12A (EOFPL 85% flow: TAF+5, TAF and TAF-2).

2.2 Effect of Reduced Core Flow for the BOC

The effect of reduced core flow at BOC is examined by an ATWS-ED case (Case 4B) with initial core flow at 75% rated (which is lower than, and thus bounding of, the lowest core flow allowable along the MELLLA+ upper boundary in the power-flow operating map at the highest allowable power level) and a water level strategy of TAF+5. A complete set of plots for this case is available in Appendix C .This sensitivity case is compared with the results of the reference case, Case 4, which have been presented previously in [4]. The implementation of the reduced core flow at BOC in the TRACE BWR model has been discussed in Section 3.1.4 in [4]. Figure 2.1 and Figure 2.2, reproduced from [4], show the steady-state axial power distribution and the axial moderator density distribution as calculated by PARCS for different initial core flows at the BOC condition. The results demonstrate that reducing the core flow shifts the boiling boundary downward axially in the core. The boiling boundary shift also shifts the power generation downward axially within the core.

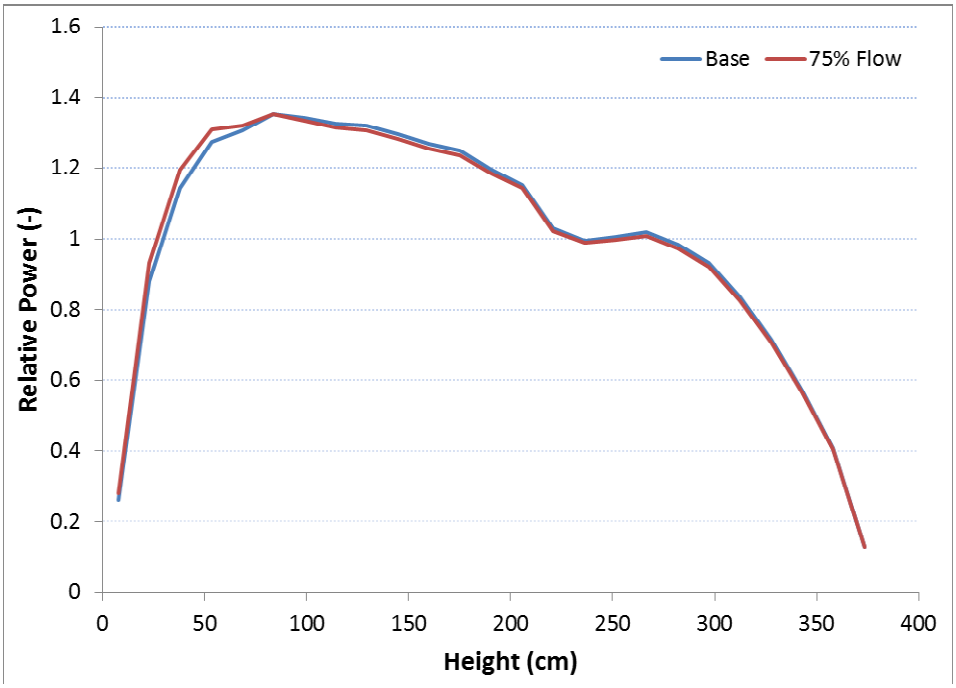

Figure 2.1 Radially Averaged Axial Power Distribution at BOC, Effect of Reduced Flow

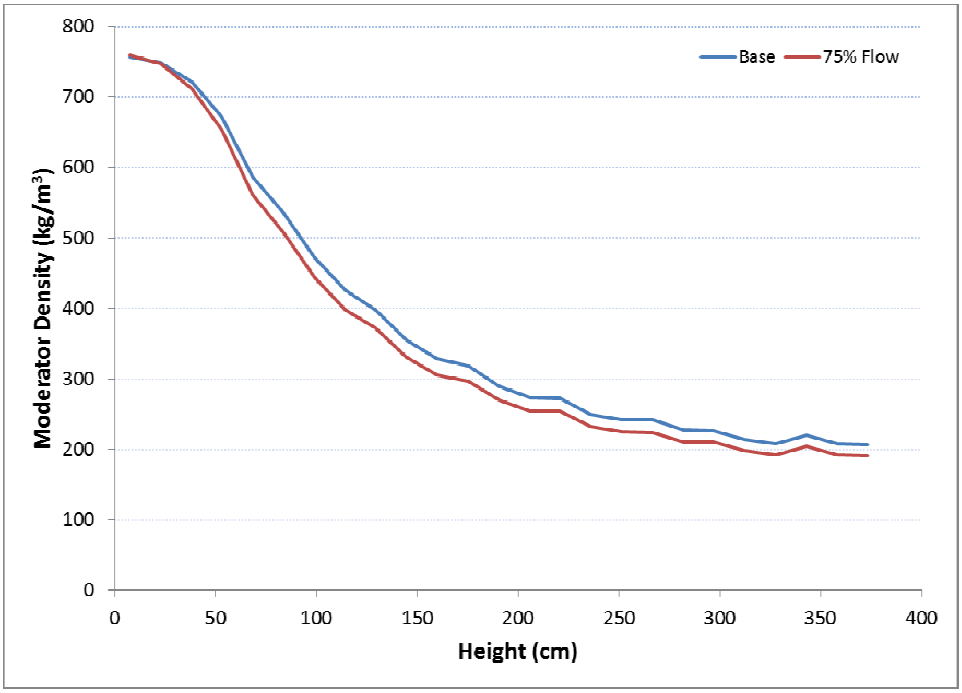

Figure 2.2 Radially Averaged Axial Moderator Density at BOC, Effect of Reduced Flow

The progression of the ATWS-ED transient exhibited by the sensitivity case is in general similar to the reference case. Table 2.5 compares some of the key results for the two cases. The most significant difference between the two cases is in the maximum peak clad temperature (PCT); the sensitivity case reaches a PCT of 1388.9 K, compared to 639.0 K for the reference case. A select set of plots (Figure 2.3 to Figure 2.13) is used to compare and contrast the transient responses of the two cases.

Table 2.5 Comparison of Key Results for BOC TAF+5 Cases

Key Event	75% Flow	85% Flow
Maximum PCT (trhmax-100)	1388.9 K (157.8 s)	639.0 K (146.8 s)
Core Boron Inventory (CB 359) > 0.01 kg	245 s	245 s
Emergency Depressurization	266.4 s	296.7 s
Maximum Drywell Pressure	0.174 MPa (793 s)	0.170 MPa (772 s)
Reactor Shutdown (Power Remains < 3.25% of Initial Power)	1046.4 s	974.8 S
Maximum Suppression Pool Temperature	372.0 (1902 s)	368.0 K (2156 s)

The reactor power, as shown in Figure 2.3 and in Figure 2.4 on an expanded time scale, generally exhibits similar responses for the two cases. However, in the early phase of the transient, the sensitivity case (75% core flow) shows a slightly higher power than the reference case (85% flow). The higher core power after the recirculation pump trip (2RPT) for the reduced flow case is a result of its higher total reactivity (see Figure 2.5) compared to the reference case. The higher core power for the sensitivity case is also reflected in the earlier depressurization time and higher maximum drywell pressure and higher maximum suppression pool temperature (see Table 2.5).

There is a break point in the power response for the reference case at about 500 s while the sensitivity case shows a smoother decay in reactor power after depressurization. A review of the total reactivity for the two cases, shown in Figure 2.5, reveals slightly different behavior after the emergency depressurization. For the reference case the total reactivity fluctuates very close to zero (null reactivity) between about 450 to 500 s and then stays negative for the rest of the transient. For the sensitivity case the total reactivity stays negative for the whole time period after the emergency depressurization. The power transients are different most likely due to the differences in the void reactivity response to the void formation as a result of the depressurization. Other components of the core reactivity, including void reactivity (dm, moderator density), fuel reactivity (Tf, Doppler) and boron reactivity, are shown in Figure 2.6 for the sensitivity case. Overall the reactivity components all exhibit similar time responses for the two cases.

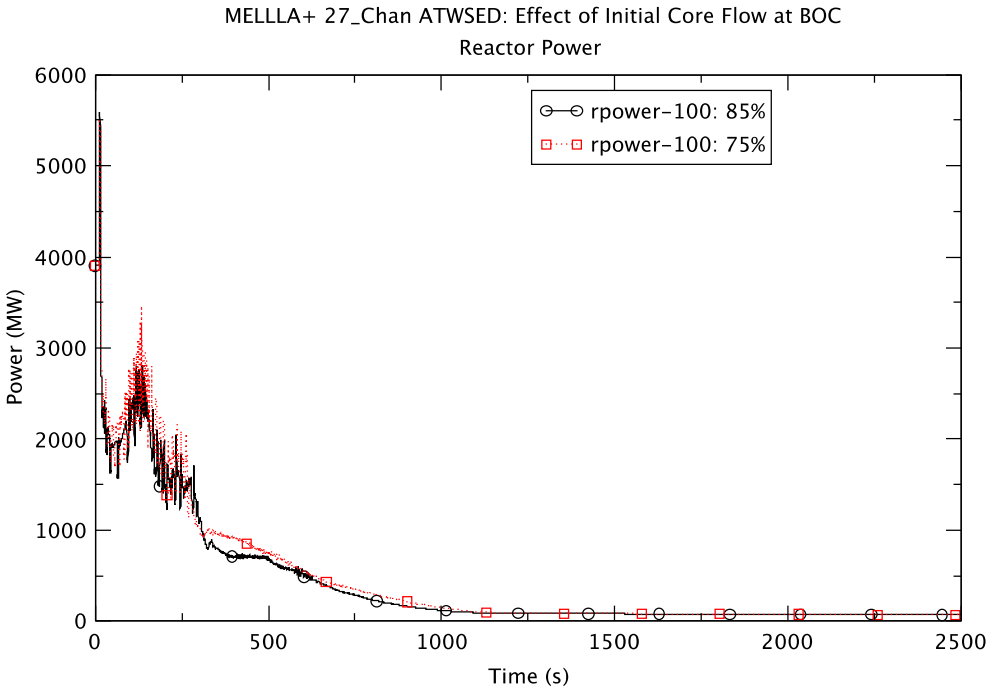

Figure 2.3 Reactor Power - BOC TAF+5 85% & 75% Flow

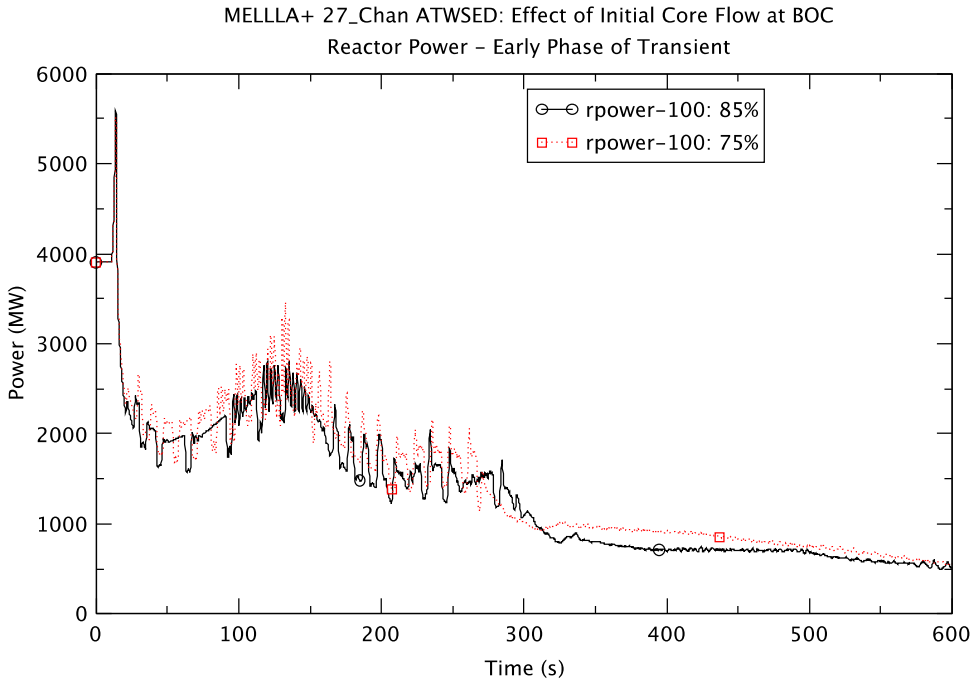

Figure 2.4 Reactor Power – Early Phase of Transient

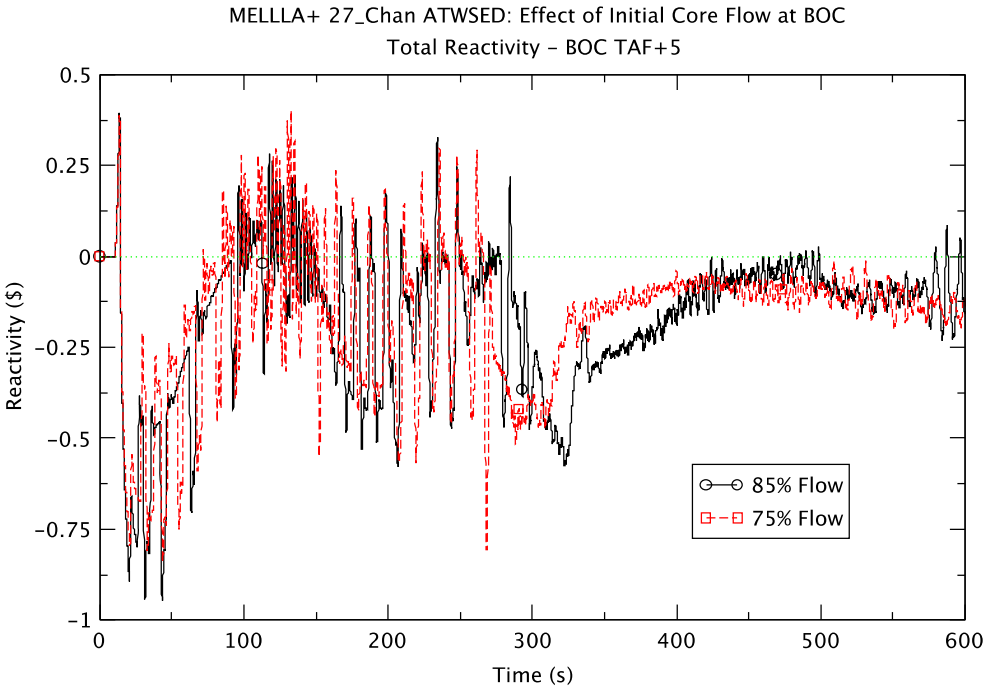

Figure 2.5 Total Reactivity – BOC TAF+5 85% & 75% Flow

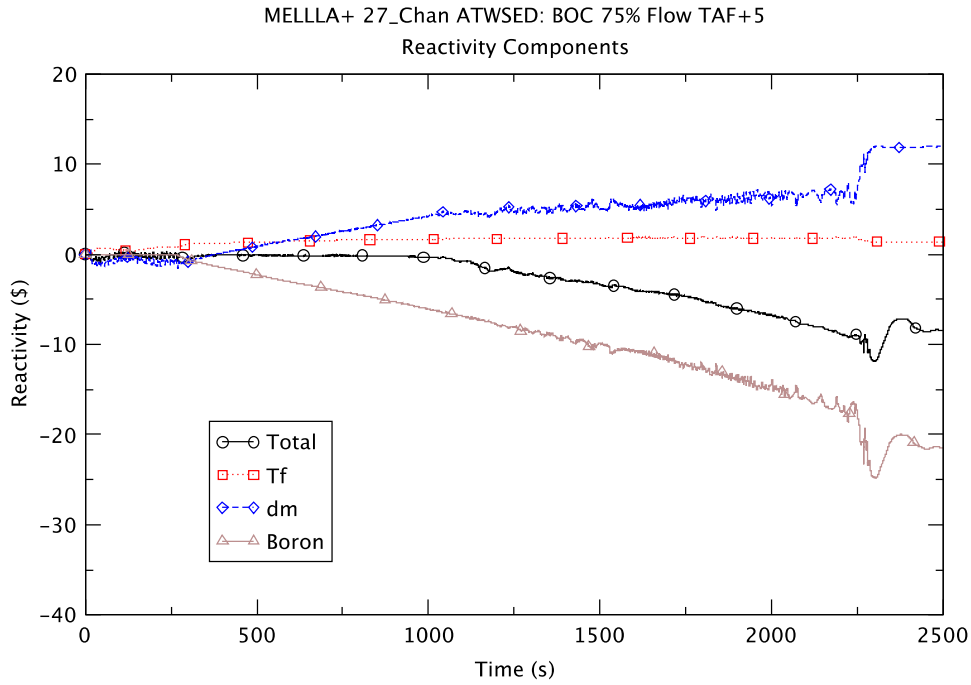

Figure 2.6 Core Reactivity – BOC TAF+5 75% Flow

Reactor pressure is shown in Figure 2.7 for the two cases. An earlier depressurization time for the sensitivity case is consistent with its higher reactor power relative to the reference case.

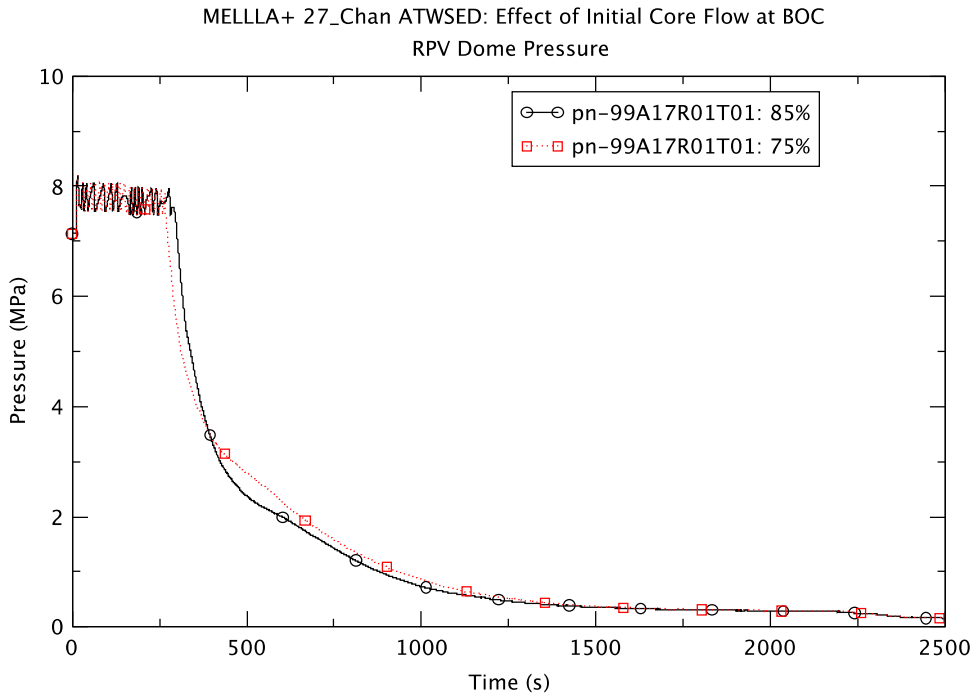

Figure 2.7 Reactor Pressure – BOC TAF+% 85% & 75% Flow

Results of the core flow and the downcomer water level for the two cases are compared in Figure 2.8 and Figure 2.9, respectively. The sudden decrease in flow shortly after the closure of the MSIVs at 10 s is due to the 2RPT. A further drop in core flow is noticed after the initiation of water level control to TAF+5 at 130 s. Natural circulation flow appears to be preserved for both cases after emergency depressurization, at 266.4 s and 296.7 s for the sensitivity case and the reference case, respectively. At about 1000 s, the core power in both cases has dropped sufficiently for the core region to be refilled with water. This sets up a manometer-type oscillation (driven by difference in the density head between the downcomer and the core) in the downcomer water level. The oscillation is evident in the fluctuations in the water level (Figure 2.9) between about 1000 s and 1500 s. During that time period the oscillating core flow (Figure 2.8) also shows a decreasing trend.

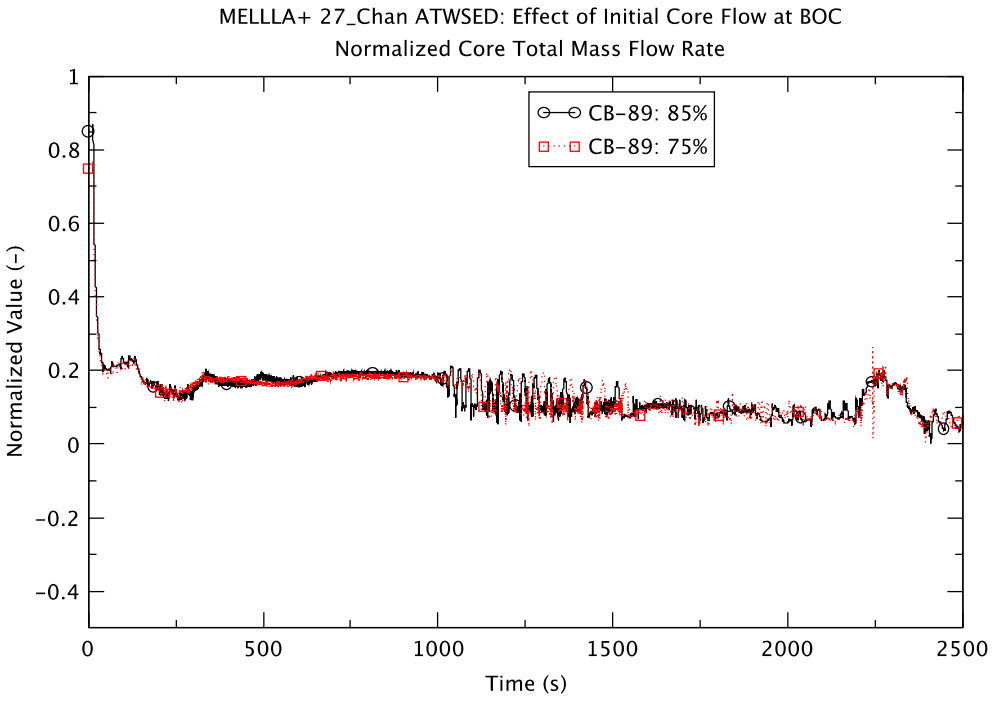

Figure 2.8 Core Flow – BOC TAF+5 85% & 75% Flow

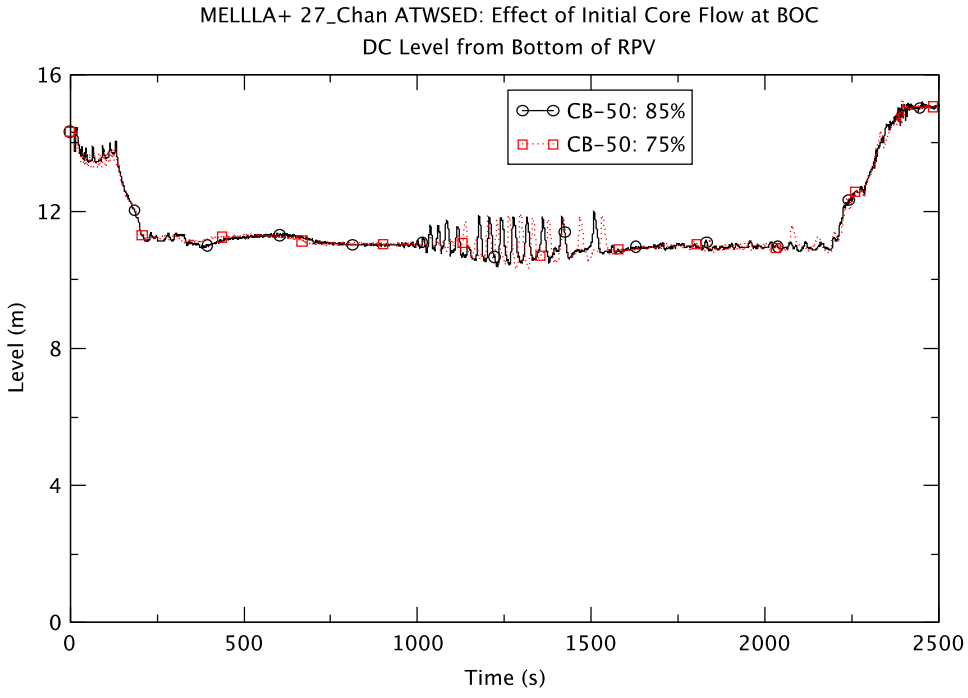

Figure 2.9 Downcomer Water Level – BOC TAF+5 85% & 75% Flow

Boron inventory in the core region is shown in Figure 2.10 for both cases. For both cases boron inventory is increasing with time. During the mitigation the operators maintain a downcomer water level that is sufficiently high to maintain natural circulation flow through the lower plenum. This flow is sufficient to entrain all of the borated solution injected into the lower plenum through the SLCS, resulting in the steady increase of boron inventory in the core region.

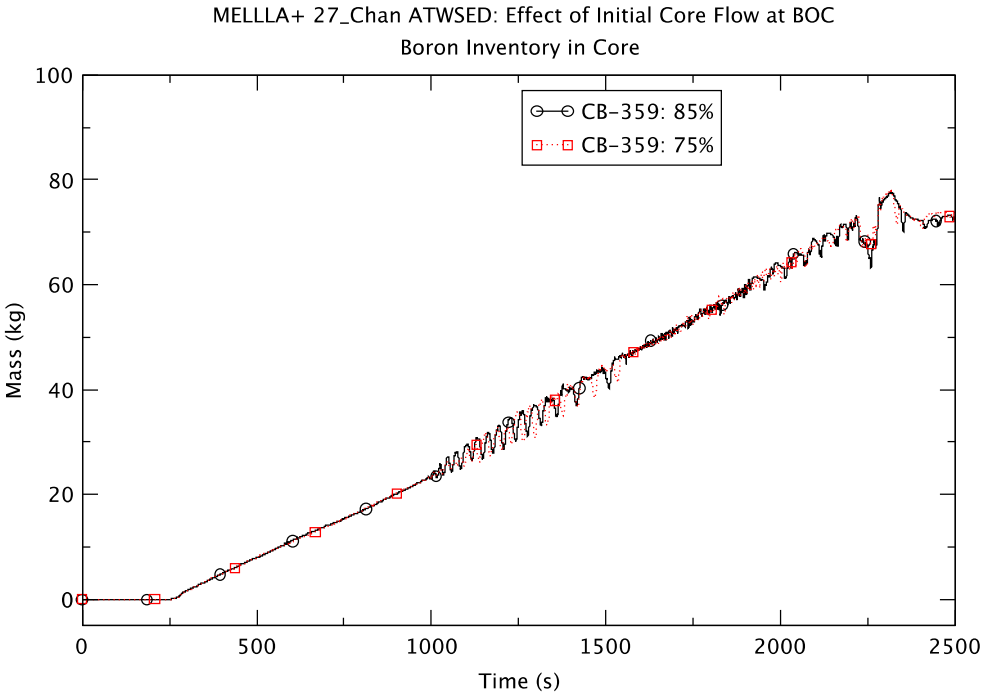

Figure 2.10 Boron Inventory in the Core Region – BOC TAF+5 85% & 75% Flow

As indicated earlier, the maximum PCT for the sensitivity case is more limiting than the reference case. Figure 2.11 shows the maximum PCT for both cases. Both cases actually show the incidence of dryout at similar times, right after level control is initiated when core flow is decreasing. In the lower flow case the cladding surface fails to rewet for a period of several hundred seconds whereas the higher flow case shows some periodic heatup and rewet. The behavior of the PCT is consistent with the higher power for the lower flow case as compared to the power for the higher flow case. The maximum PCT for the core remains almost identical for the two cases after rewet is complete for all fuel rods.

The suppression pool water temperature (Figure 2.12) is a gauge for quantifying the cumulative energy relieved to the pool via the SRVs. The higher pool temperature exhibited by the sensitivity case is indicative of higher power relative to the reference case.

The transient response of the drywell pressure (Figure 2.13), with a higher maximum pressure for the sensitivity case, is again consistent with the observation that at reduced core flow (75%) the transient core power is higher than that in the reference case (85% flow).

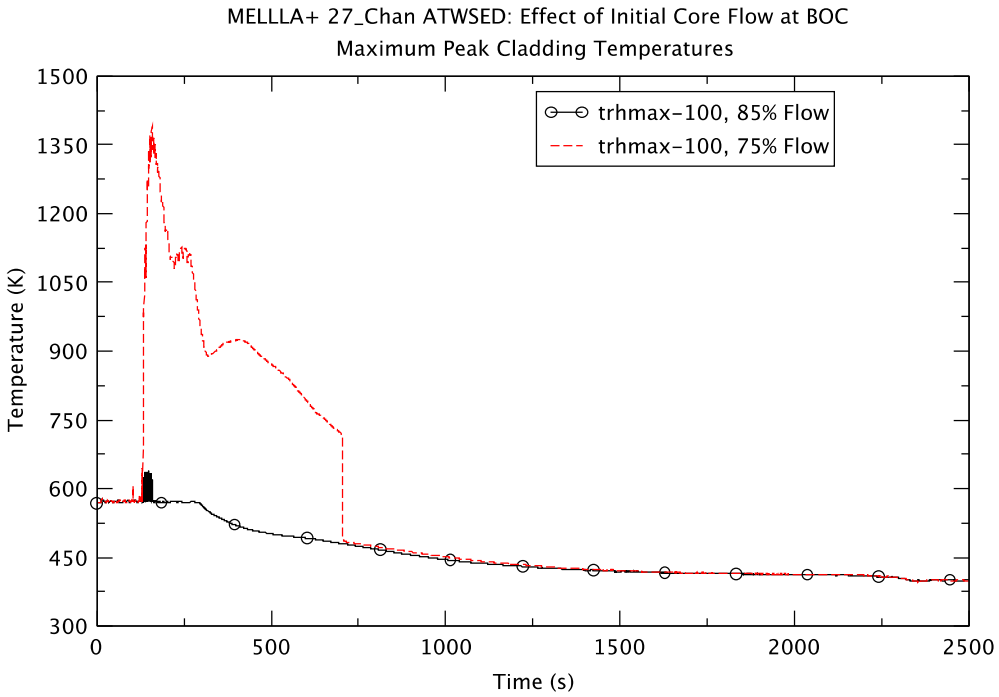

Figure 2.11 Peak Clad Temperature – BOC TAF+5 85% & 75% Flow

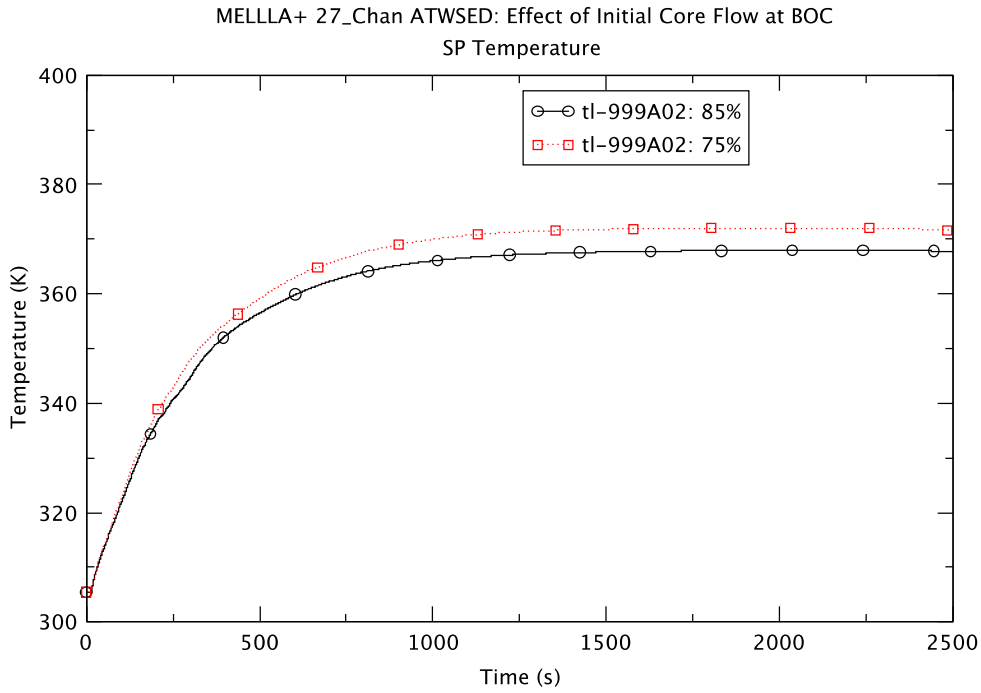

Figure 2.12 Suppression Pool Temperature – BOC TAF+5 85% & 75% Flow

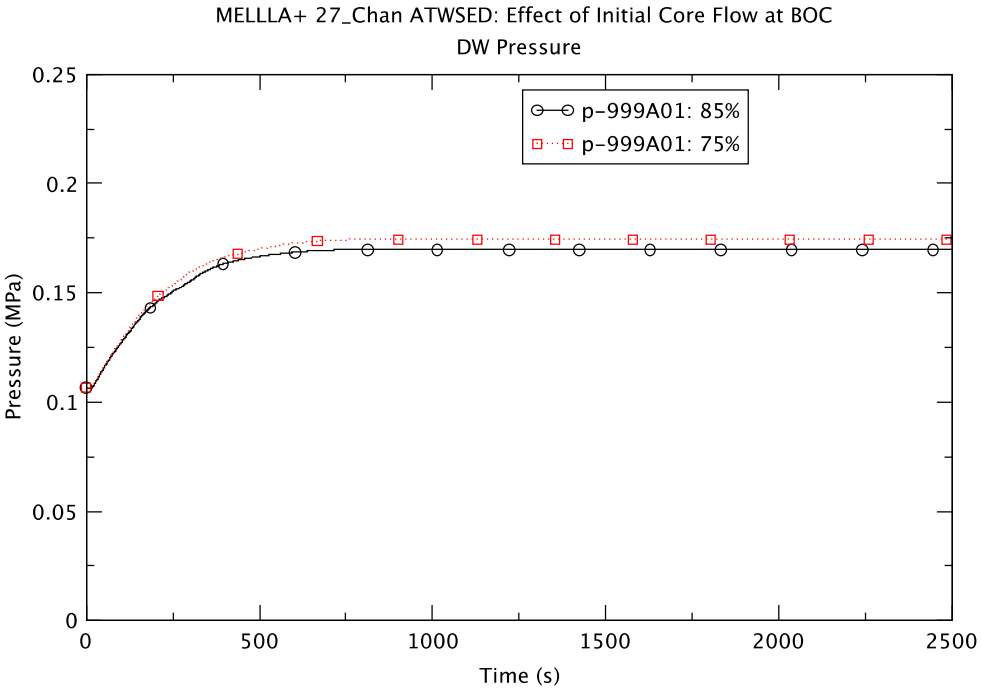

Figure 2.13 Drywell Pressure - BOC TAF+5 85% & 75% Flow

Results of the TRACE analysis indicate that even at reduced core flow the reactor remains shutdown by the injected boron. There is no recriticality observed due to either repressurization of the reactor vessel or dilution of boron. Though the maximum PCT shows a significant increase at reduced core flow relative to the reference case, its magnitude is still 89 K below the 1478 K (2200°F) limit[a]. Both the suppression pool temperature and the drywell pressure stay below associated limits.

2.3 Effect of Void History Modeling for the EOFPL

The cross sections used by PARCS depend on several instantaneous variables, namely, control rod insertion, moderator density, fuel temperature and boron concentration. They also depend on exposure to take into account burnup, and one or more other "history" parameters to correct for the effect of the neutron energy spectrum during burnup on the instantaneous cross-sections. The history parameter used to generate the cross sections for PARCS is moderator density history (equivalent to void history, UH). However, another history parameter that might be important is the control rod position history. GEH has developed an approach accounting for the spectral history of the node by changing the void history artificially to provide an equivalent spectral effect.

In order to assess the effect of this correction, an EOFPL sensitivity case is run, replacing the UH distribution used with the cross section set in PARCS by a "void history spectrally corrected" (UHSPH) distribution provided by GEH. The implementation of the spectrally-corrected moderator density history in the TRACE BWR model has been discussed in Section 3.3.4 in [4]. Figure 2.14, reproduced from [4], shows a comparison of the steady-state axial power distribution calculated by PARCS for the EOFPL condition using the UH moderator density history and the UHSPH moderator density history. The results are essentially the same for the two void histories.

[a] For beyond design basis ATWS events, there is not an explicit temperature limit applied by the regulations. The acceptance criteria for ATWS evaluations are discussed in the NRC staff's standard review plan (NUREG-0800). The 1478 K temperature acceptance criterion in NUREG-0800 for ATWS is applicable only to new plants [6] but is used herein as a reasonable informal limit.

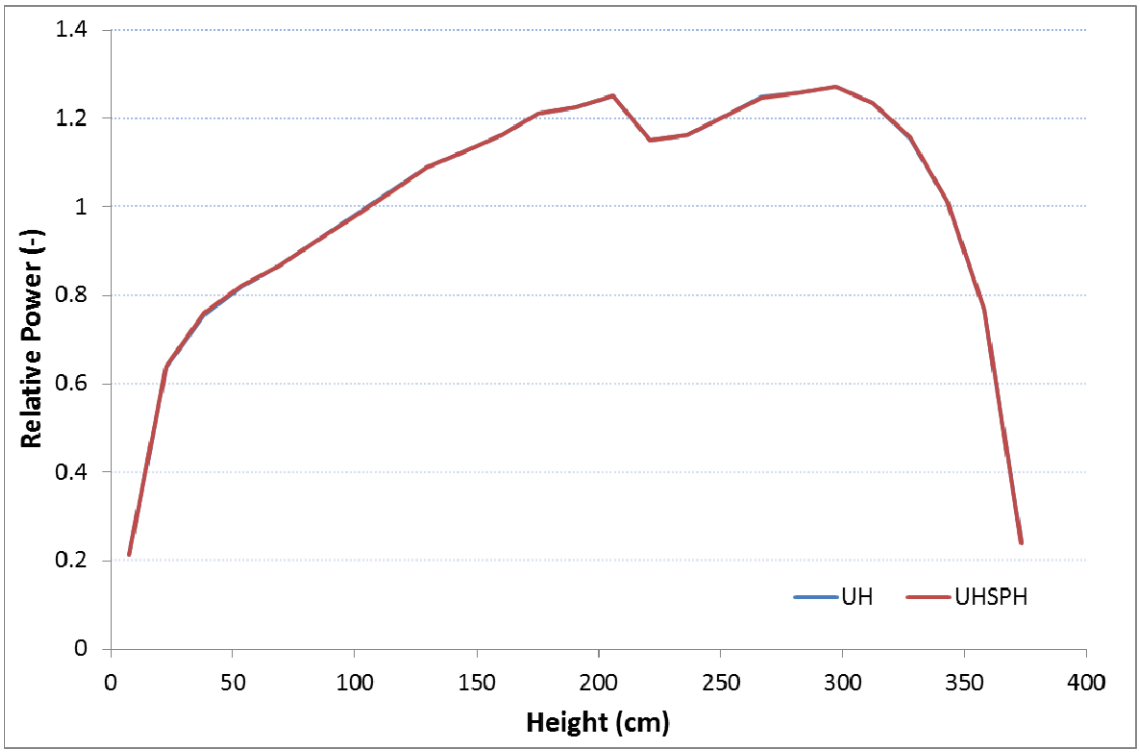

Figure 2.14 Radially Averaged Axial Power Distribution at EOFPL, Effect of Spectrally Corrected Void History

The EOFPL sensitivity case that utilized the UHSPH moderator density history is Case 10C, a case with TAF+5 water level control strategy. The corresponding reference case is Case 10, one of the base cases already presented in [4]. A complete set of plots for the sensitivity case is available in APPENDIX C .

Table 2.6 compares some of the key results for the two cases. A select set of plots (Figure 2.15 to Figure 2.22) is used to compare and contrast the transient responses of the two cases. The progression of the ATWS-ED transient exhibited by the sensitivity case is essentially the same as the reference case. Discussions of the EOFPL ATWS-ED cases found in Section 4.4 in [4] are thus applicable to the sensitivity case and will not be repeated here.

Based on the simulation results the two cases (UH and UHSPH) are essentially the same and thus the EOFPL ATWS-ED TAF+5 case is not sensitive to the spectral correction to the void history (moderator density history).The assessment of the correctness of the GEH approach to the void history correction is outside the scope of the current analysis.

Table 2.6 Comparison of Key Results for EOFPL TAF+5 Cases

Key Event	UHSPH	UH
Maximum PCT (trhmax-100)	576.9 K (14.3 s)	576.9 K (14.3 s)
Core Boron Inventory (CB 359) > 0.01 kg	245.5 s	246 s
Emergency Depressurization	403.5 s	403.2 s
Maximum Drywell Pressure	0.162 MPa (588 s)	0.162 MPa (588 s)
Reactor Shutdown (Power Remains < 3.25% of Initial Power)	949.5 s	937 s
Maximum Suppression Pool Temperature	358.7 (2298 s)	358.8 K (2288 s)

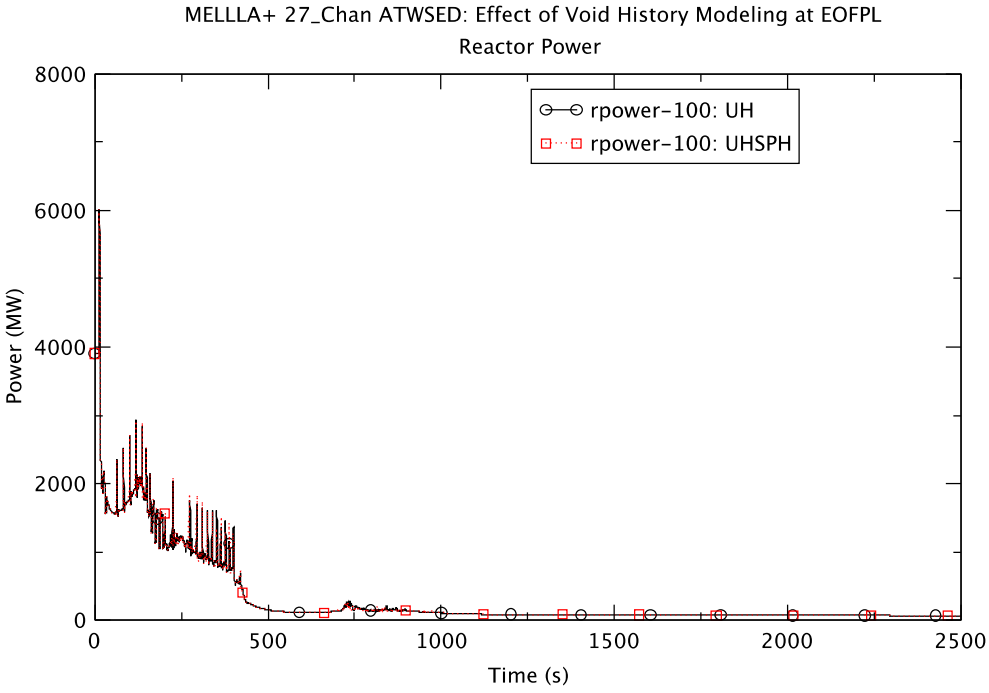

Figure 2.15 Reactor Power – EOFPL TAF+5 UH & UHSPH

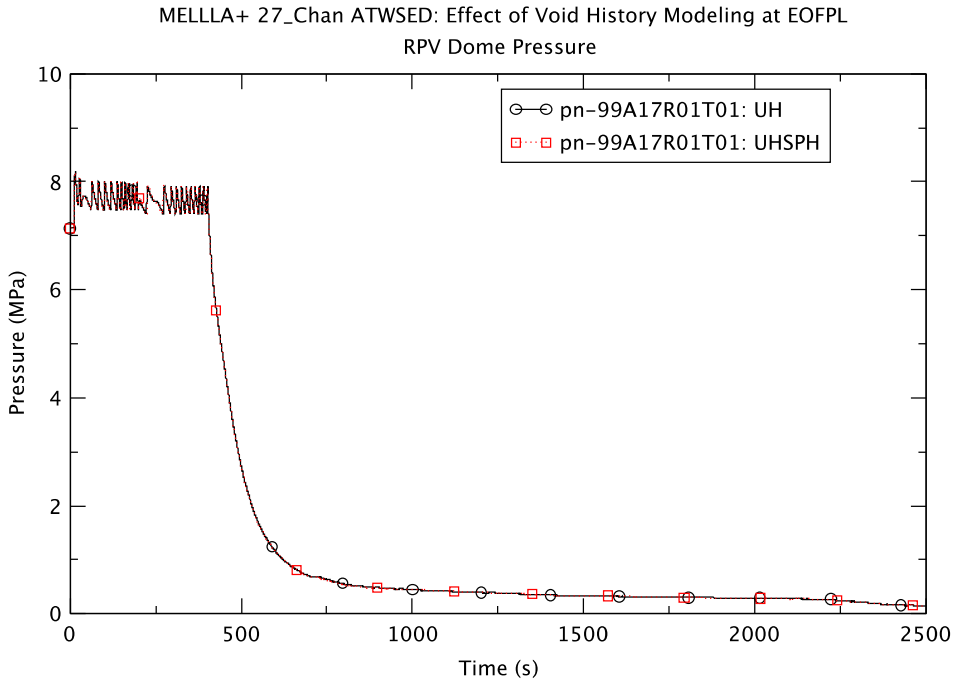

Figure 2.16 Reactor Pressure – EOFPL TAF+5 UH & UHSPH

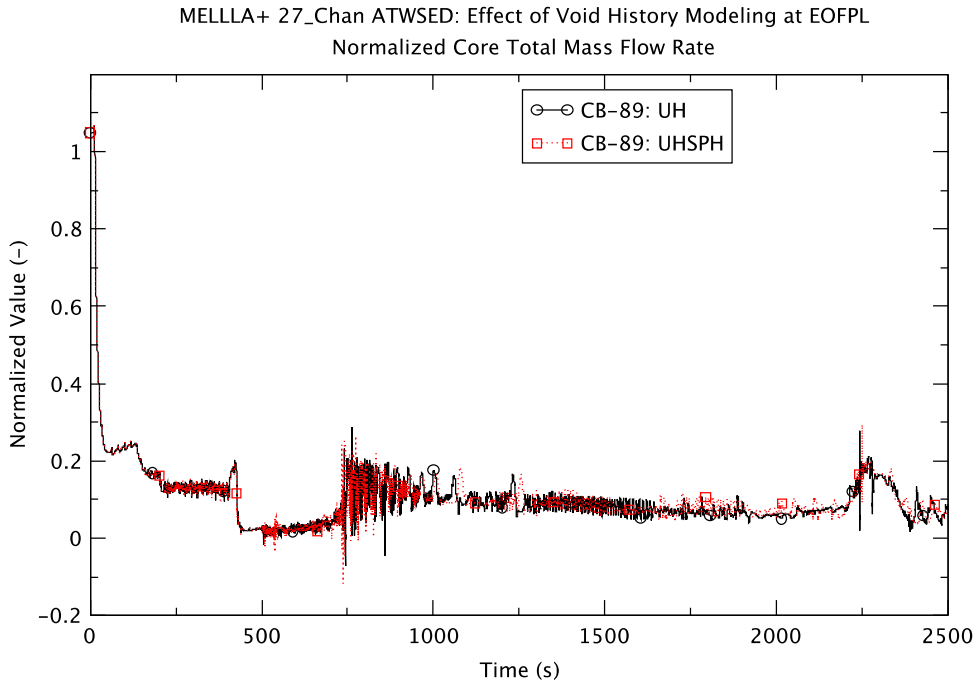

Figure 2.17 Core Flow – EOFPL TAF+5 UH & UHSPH

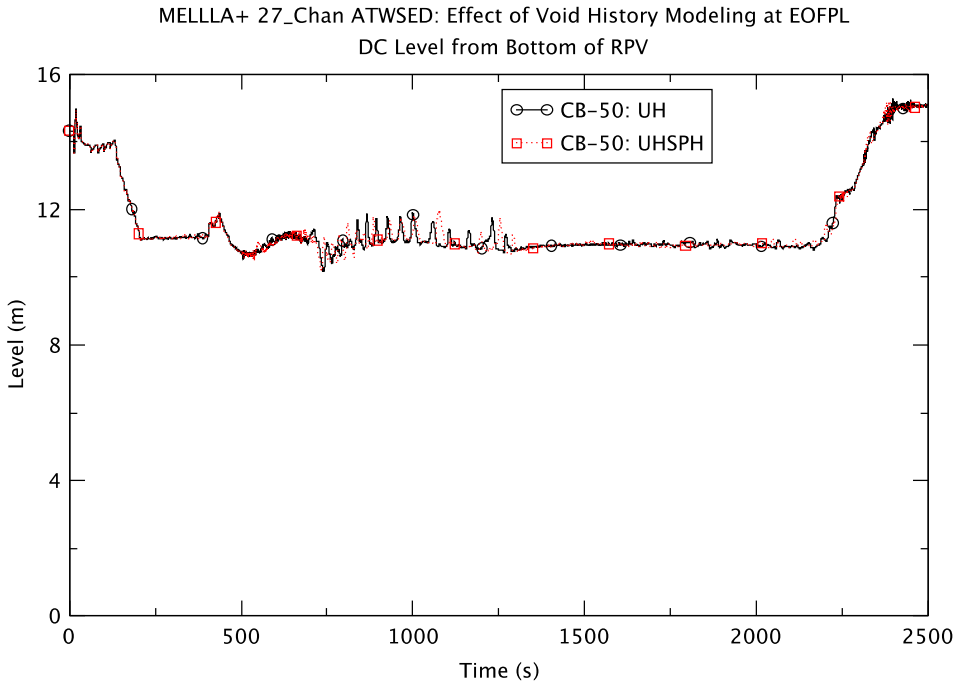

Figure 2.18 Downcomer Water Level – EOFPL TAF+5 UH & UHSPH

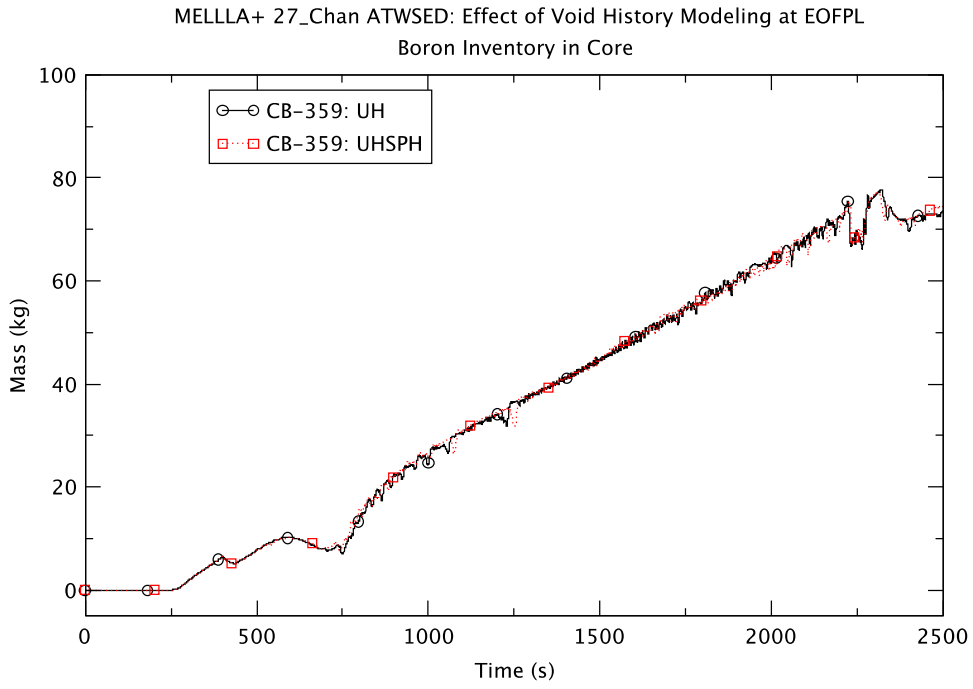

Figure 2.19 Boron Inventory in the Core Region – EOFPL TAF+5 UH & UHSPH

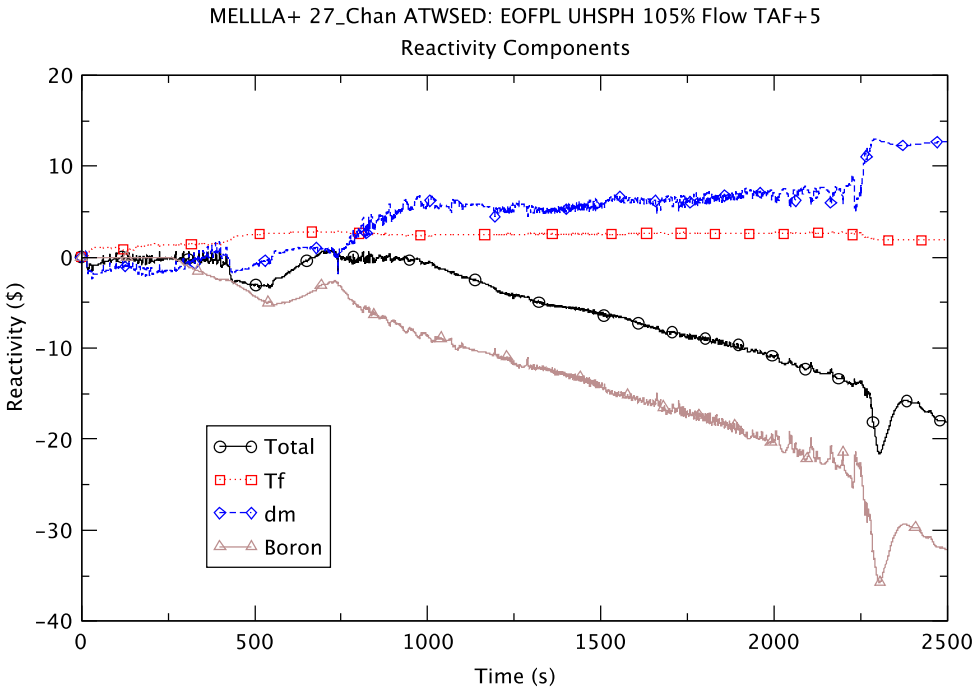

Figure 2.20 Core Reactivity – EOFPL TAF+5 UHSPH

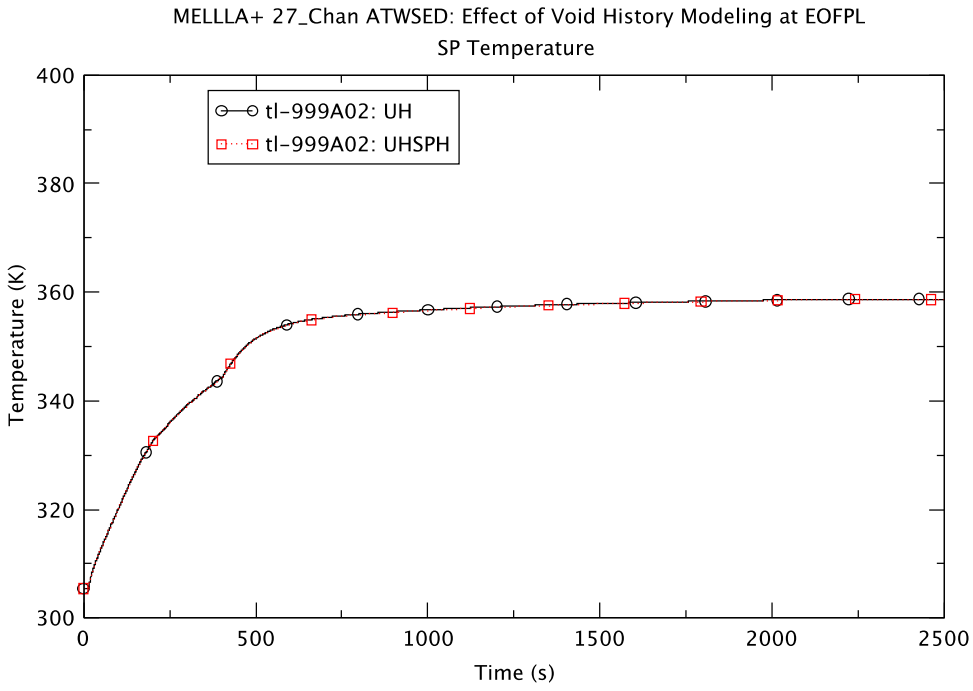

Figure 2.21 Suppression Pool Temperature – EOFPL TAF+5 UH & UHSPH

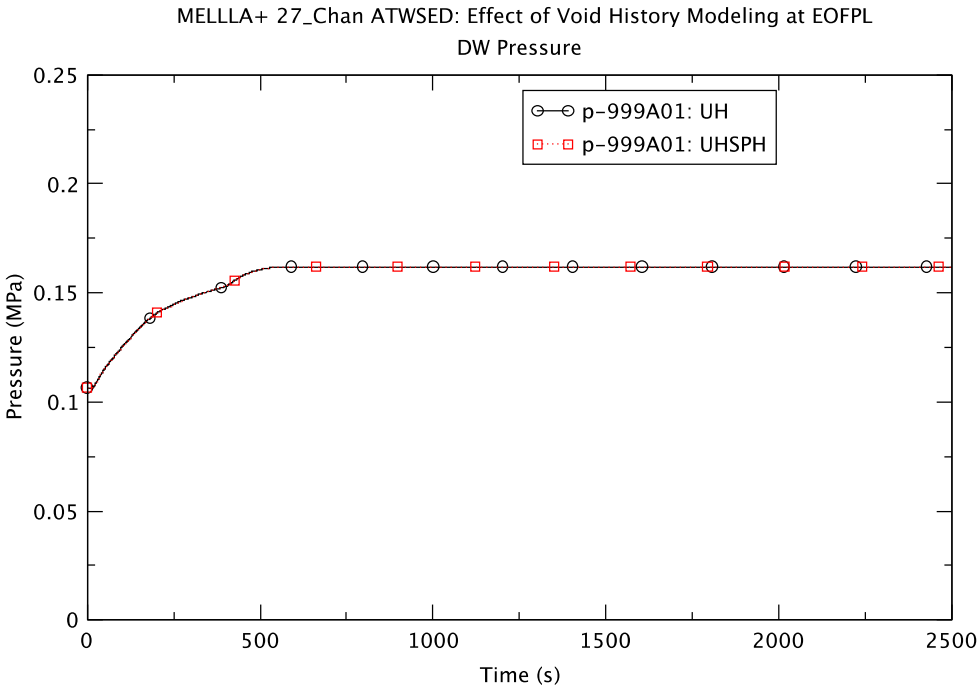

Figure 2.22 Drywell Pressure – EOFPL TAF+5 UH & UHSPH

2.4 Effect of Reduced Core Flow for the EOFPL

Two sensitivity cases are presented in this section to illustrate the effect of reduced core flow on the ATWS-ED transient at EOFPL with water level control to TAF-2. The initial core flows assumed for the two cases are 75% (Case 10D) and 85% (Case 12A) of rated core flow. The reference case, Case 12, is at 105% flow and results for this case have been presented in [4]. The 85% flow corresponds to the lowest core flow allowable along the upper boundary of the MELLLA+ operating domain on the power/flow map. The 75% flow represents a low-low flow condition that bounds the MELLLA+ domain. Simulation of the low-low flow case requires “eigenvalue offset” by PARCS (i.e. the predicted eigenvalue is less than unity and PARCS resets it to unity initially) to achieve criticality. In effect the analysis treats the artificial low-low flow condition as being artificially critical.

A complete set of plots for the two sensitivity cases is available in Appendix C. The implementation of the reduced core flow at EOFPL in the TRACE BWR model has been discussed in Section 3.3.5 in [4]. Figure 2.23 and Figure 2.24, reproduced from [4], show the steady-state axial power distribution and the axial moderator density distribution as calculated by PARCS for different initial core flows at the EOFPL condition. The results confirm that reducing the core flow shifts the boiling boundary

downward (towards core inlet) and also affects the axial power peaking (shifting more power to the lower core).

The progression of the ATWS-ED transient exhibited by the sensitivity cases is in general similar to the reference case. Table 2.7 compares some of the key results for the three cases.

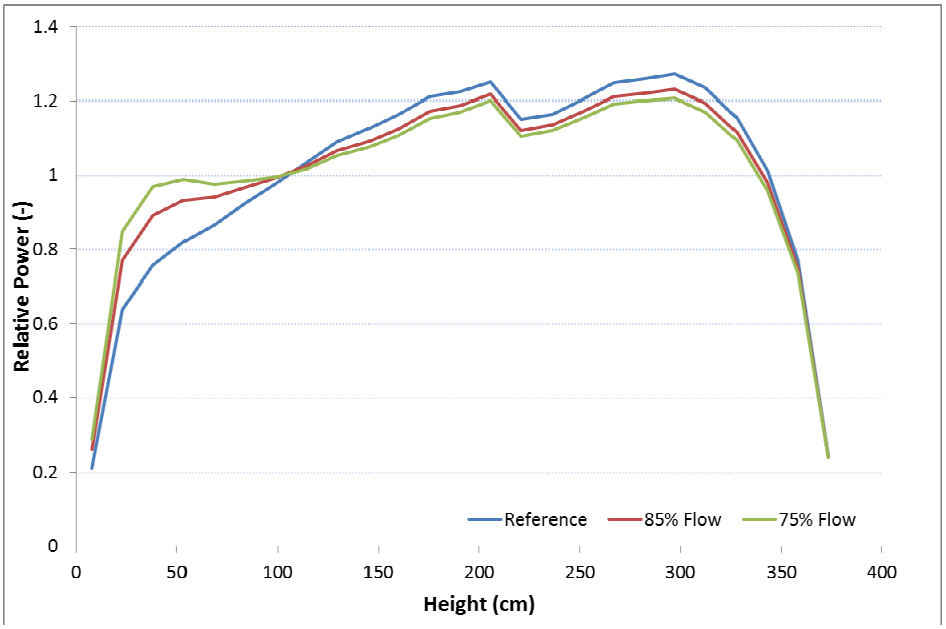

Figure 2.23 Radially Averaged Axial Power Distribution at EOFPL, Effect of Reduced Core Flow

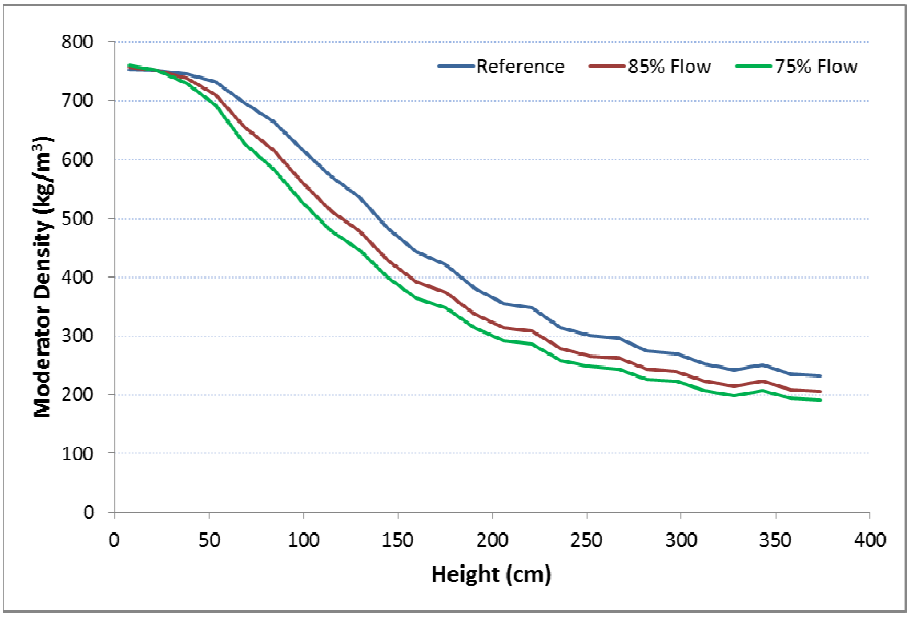

Figure 2.24 Radially Averaged Axial Moderator Density Distribution at EOFPL, Effect of Reduced Core Flow

Table 2.7 Comparison of Key Results for EOFPL TAF-2 Cases

Key Event	75% Flow	85% Flow	105% Flow
Maximum PCT (trhmax-100)	1380.5 K (145.8 s)	979.7 K (151.4 s)	639.0 K (699.3 s)
Core Boron Inventory (CB 359) > 0.01 kg	251 s	255 s	264 s
Emergency Depressurization	309.1 s	346.8 s	450 s
Maximum Drywell Pressure	0.163 MPa (501 s)	0.162 MPa (541 s)	0.160 MPa (648 s)
Reactor Shutdown (Power Remains < 3.25% of Initial Power)	1354 s	1188 s	887 s
Maximum Suppression Pool Temperature	361.5 (2190 s)	358.2 K (2205 s)	356.6 K (2191 s)

The most significant difference between the two sensitivity cases and the reference case is in the maximum peak clad temperature where the sensitivity cases reach temperatures of 1380.5 K and 979.7 K, compared to 639.0 K for the reference case. It is observed that the reactor power following the 2RPT trends inversely with the initial core flow because the 2RPT reduces the core flow (and hence reactivity) by a smaller amount when the initial core flow is lower. A higher reactor power generally leads to a higher PCT. Thus the trend of the PCT is consistent with the simulation results, a higher PCT for a lower initial core flow. Furthermore, the higher reactor power at a lower initial core flow leads to more energy relieved to the containment during an ATWS-ED transient, resulting in an earlier emergency depressurization, a higher suppression pool temperature, and a higher drywell pressure. The timing of the maximum PCT is also very different between the sensitivity cases and the reference case. For the two sensitivity cases the maximum PCT occurs much earlier, shortly after the initiation of water level control at 130 s and before emergency depressurization while the core flow is still relatively high. During this stage, the fuel is predicted to enter dryout under relatively low-quality conditions, fails to rewet, and experiences extended heatup. For the reference case the fuel rewets during the early transient stage and the maximum PCT occurs after emergency depressurization (i.e., at higher quality). By then the core flow for the reference case is relatively low because of water level control to TAF-2.

A select set of plots (Figure 2.25 to Figure 2.40) is used to compare and contrast the transient responses of the two sensitivity cases against the reference case.

The transient response of the reactor power for all three cases is shown in Figure 2.25. All three power traces show similar responses; a power spike after MSIV closure and power decreases after the dual recirculation pump trip (2RPT), lowering of water level

and depressurization. Figure 2.26 shows the reactor power for the first 600 s of the ATWS-ED transient. The simulation results show that a lower initial core flow leads to higher transient reactor power that also oscillates with higher amplitude (between roughly 110 s and 170 s) before the level reduction suppresses the reactor power. For a lower initial core flow rate, the reactor power level after 2RPT (i.e., under natural circulation conditions) is higher. The higher power to flow ratio for the cases with lower initial core flow rate evolve into more unstable conditions as core inlet subcooling increases during the event. The amplitude of power oscillations trends with increasing power to flow ratio as expected for density wave driven, unstable power oscillations.

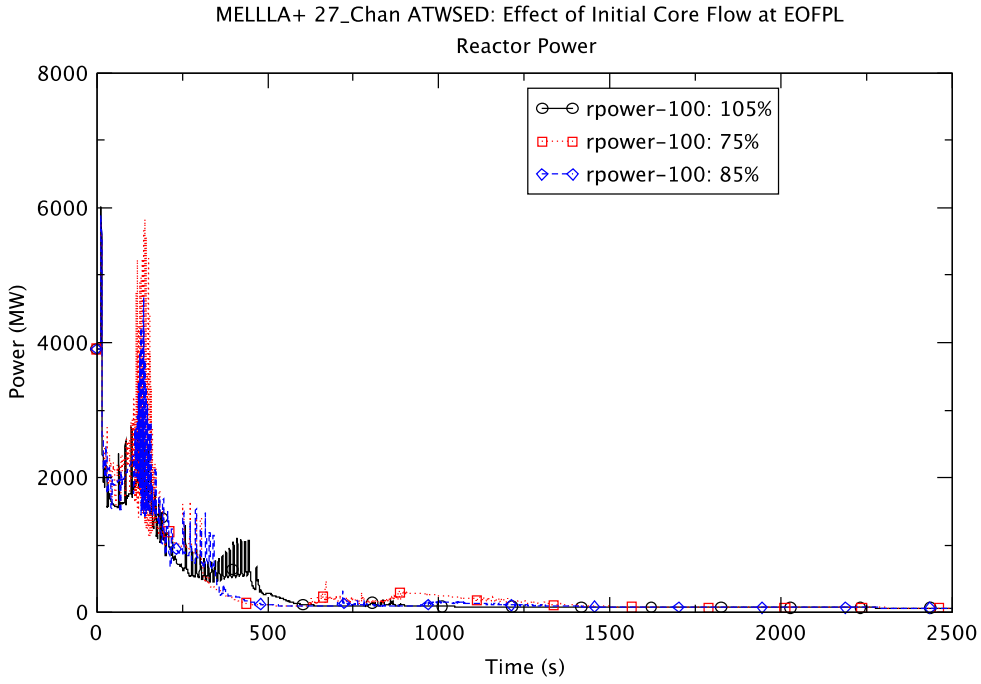

Figure 2.25 Reactor Power – EOFPL TAF-2 Cases

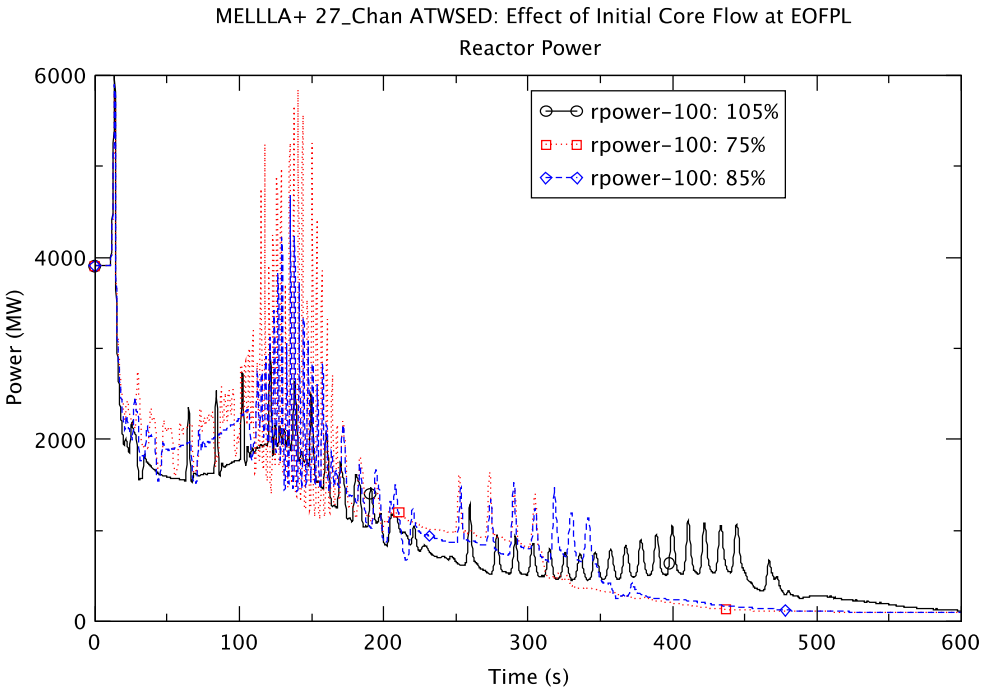

Figure 2.26 Reactor Power (0 to 600 s) – EOFPL TAF-2 Cases

Between roughly 110 s and 170 s the two sensitivity cases appear to exhibit unstable density-wave oscillations (DWO) in the core. It is during this period when the reactor power to flow ratio is high that the maximum PCT is reached for the two sensitivity cases.

With a higher reactor power (due to higher total reactivity) after the 2RPT and the initiation of water level control, the two sensitivity cases have an earlier emergency depressurization (ED) time than the reference case. The reactor pressure is shown in Figure 2.27. The rate of depressurization is similar for all three cases, and there is voiding in the lower plenum. The presence of void in the lower plenum and the core (due to flashing) disrupts the natural circulation flow from the downcomer to the core and the core flow is reduced (see Figure 2.28). It is noted that the core flow is higher for the two sensitivity cases after level control has been accomplished and before depressurization. The higher core flow is consistent with a higher core power for the sensitivity cases before the ED.

Downcomer level swell associated with the ED is evident in Figure 2.29 which shows the water level for all three cases. Fluctuations in core flow and water level are generally related to refilling of the lower plenum and the core region, and the injection of feedwater. Figure 2.30 and Figure 2.31 show the feedwater flow rate for the two sensitivity cases. It is observed that the flow of feedwater correlates qualitatively with perturbations in core flow and downcomer water level, around 1500 s for the 75% flow case and around 2000 s for the 85% flow case.

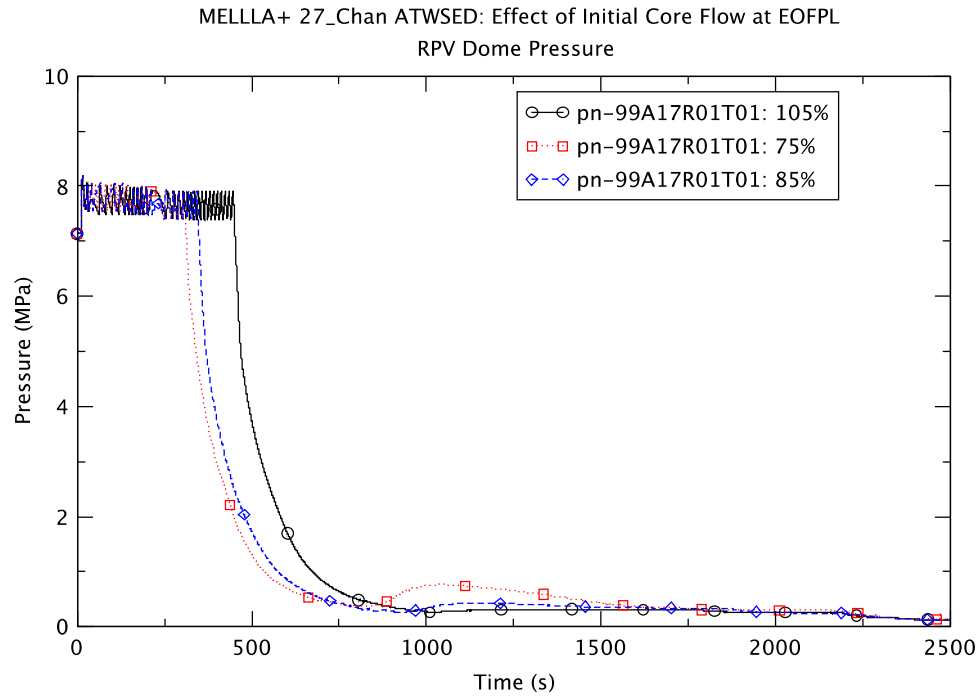

Figure 2.27 Reactor Pressure – EOFPL TAF-2 Cases

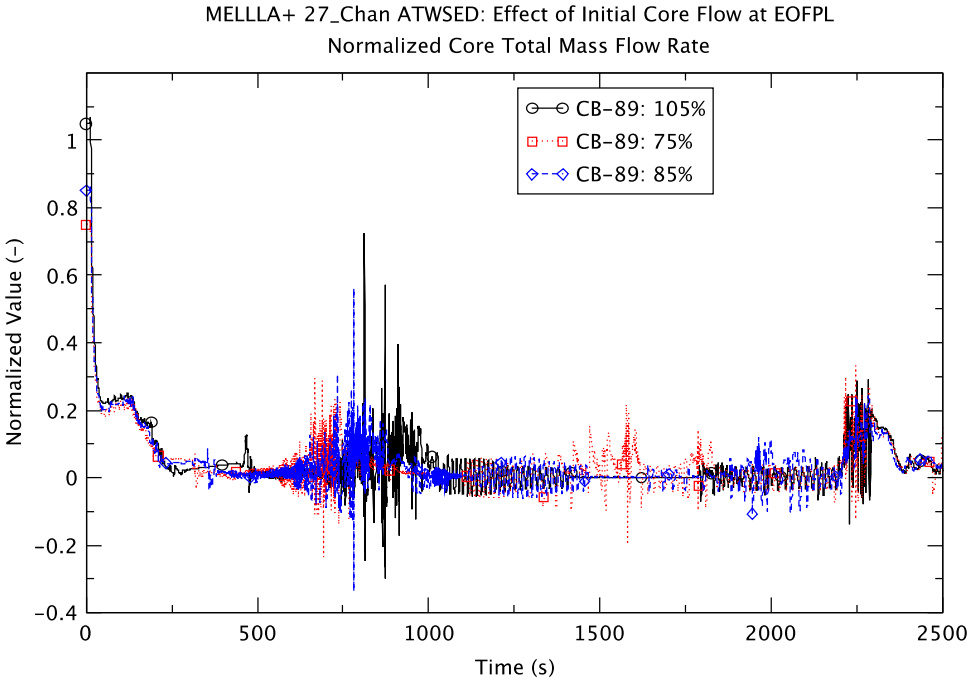

Figure 2.28 Core Flow – EOFPL TAF-2 Cases

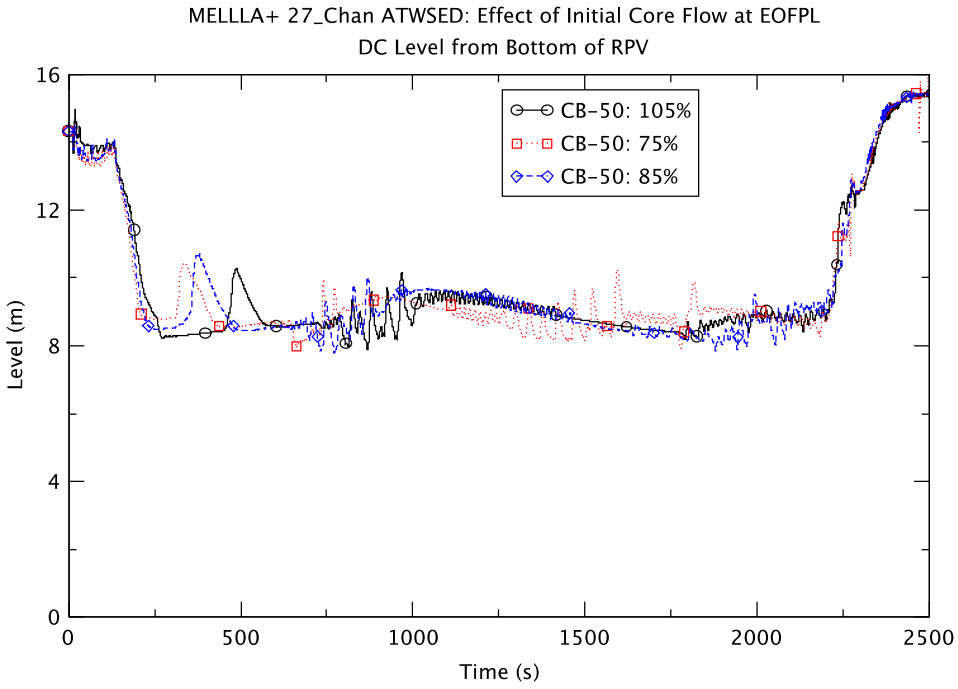

Figure 2.29 Downcomer Water Level – EOFPL TAF-2 Cases

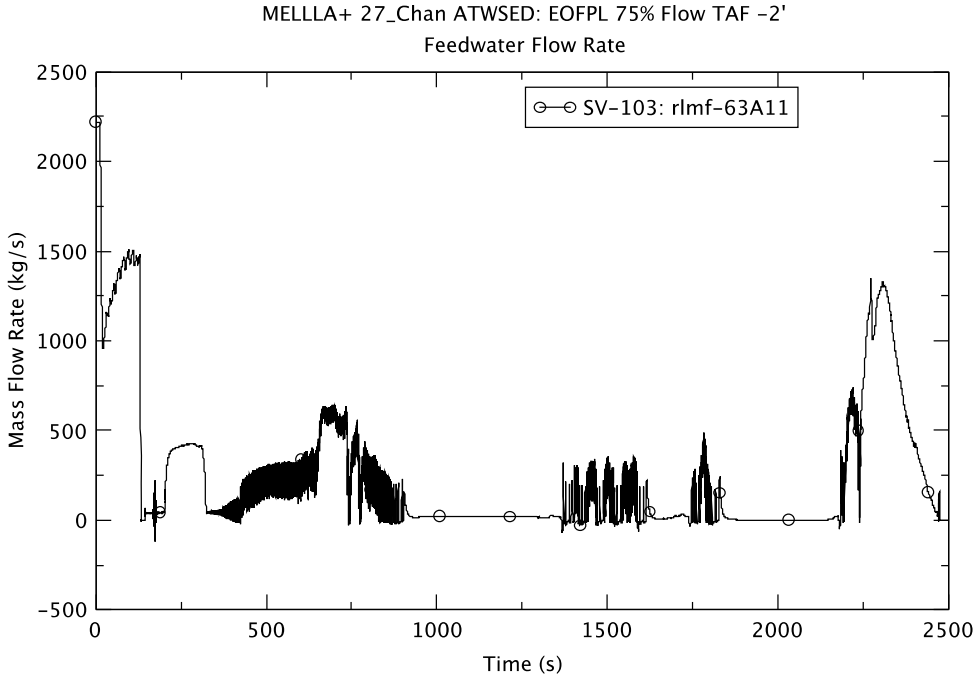

Figure 2.30 Feedwater Flow Rate – EOFPL TAF-2 75% Flow

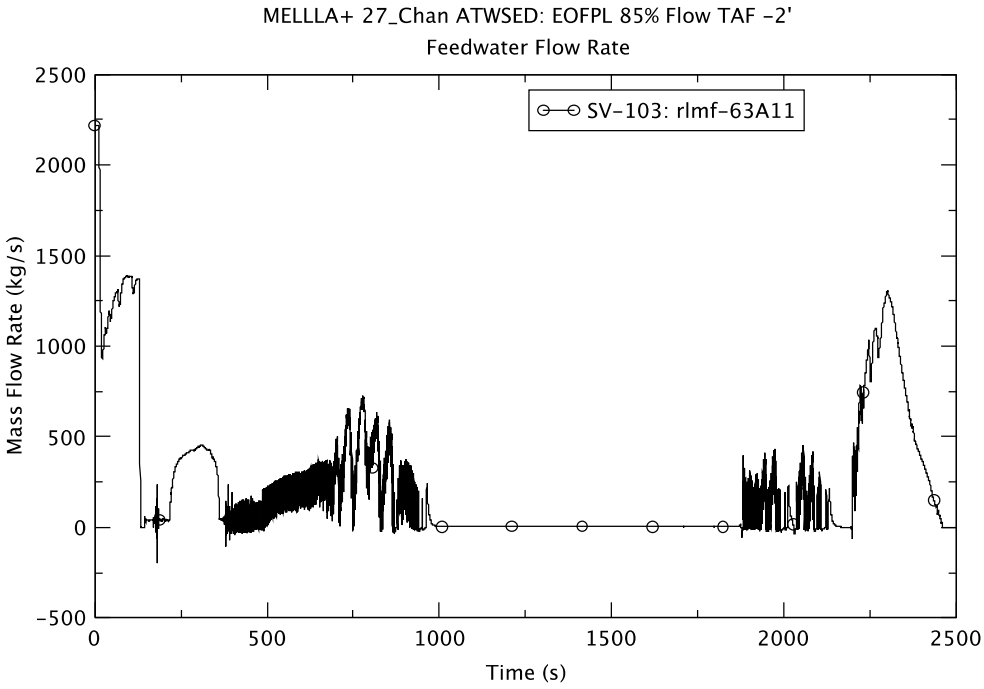

Figure 2.31 Feedwater Flow Rate – EOFPL TAF-2 85% Flow

For the sensitivity case with 75% flow, it is observed from Figure 2.28 and Figure 2.29 that for a roughly 200 s period around 1000 s the water level and core flow are quite stable and there is a slight increase in reactor power. The increase in reactor power is confirmed by observing an increase in reactor pressure (Figure 2.27) and steamline flow (Figure 2.32) at about 1000 s. To a lesser extent, an increase in pressure is also observed in the case of 85% flow at about 1200 s.

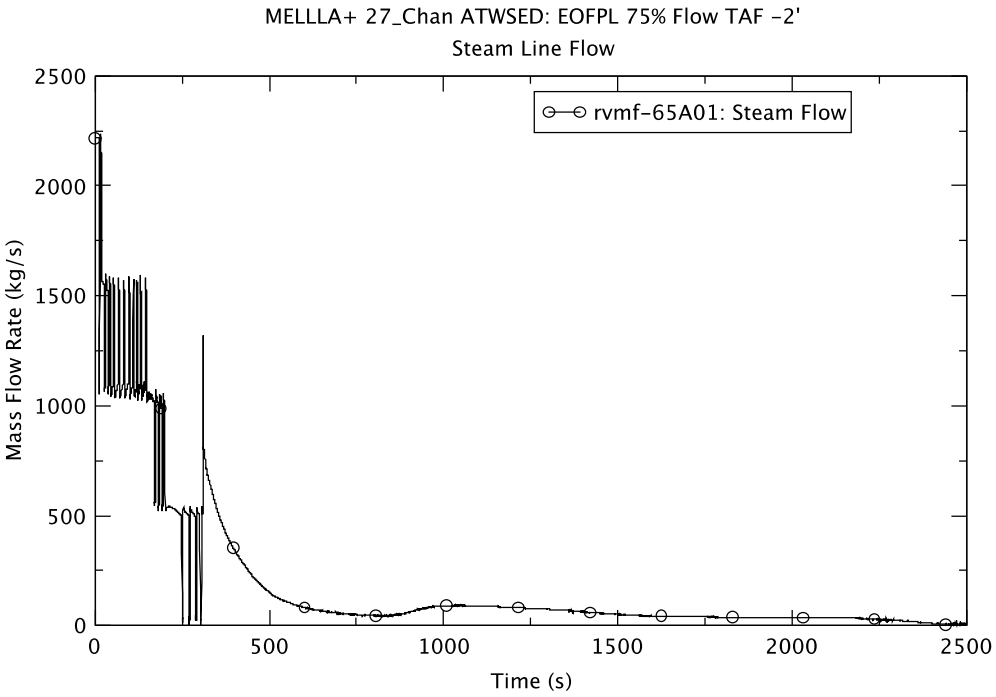

Figure 2.32 Steam Line Flow – EOFPL TAF-2 75% Flow

For the 75% flow case the core flow and downcomer water level begin to oscillate again after 1000 s. Further evidence of oscillatory conditions for the 75% flow case is in the core bypass void fraction, shown in Figure 2.33. Between 1000 s and 1700 s the magnitude of oscillation in core flow and downcomer water level is lower for the 85% flow case and the reference case (105% flow), which is expected since power level is higher in the 75% flow case. Also, no voiding in the lower nodes of the core bypass region is observed in these two cases during that time period.

The boron inventory in the core region is shown in Figure 2.34 for the three cases. The boron injection starts at 211 s and in all three cases it takes about 40 to 50 s for the boron to reach the core region. The rate of change in the boron inventory appears to be affected by the emergency depressurization due to its impact on core flow and voiding in the core. After that there is a period of slow growth in the boron inventory. Then at about 750 s, coincident with the refilling of the lower plenum, there is a marked increase in the boron inventory. The subsequent increase in boron at 1500 s and 2000 s for the 75% case and 85% case, respectively is associated with effective re-mixing of stratified boron in the bottom of the lower plenum. This is taken into account in the TRACE simulation through an increase in the concentration of the injected boron, as calculated by the boron transport control scheme (see Section 2.3.7 and Appendix A in [4] for a discussion). The simulated, enhanced boron delivery is a result of increased core flow due to feedwater flow and higher level. For all three cases the core boron inventory increases after level recovery, which begins at 2180 s. The effective injection boron

concentration (an output of the boron transport model that accounts for re-mixing of boron in the lower plenum) for the 75% flow case is shown in Figure 2.35. The temporary increases in injected boron concentration above the nominal (0.02369 kg-B/kg-water) take into account the re-mixing of settled boron in the lower plenum of the reactor vessel. The re-mixing is assumed to be a function of coolant flow in the lower plenum (see Appendix A in [4] for a discussion of the re-mixing model).

The core reactivities calculated by PARCS are shown in Figure 2.36 and Figure 2.37 for the 75% flow and the 85% flow cases, respectively (see Figure 4.113 in [4] for the corresponding plot for the 105% flow case). In all three cases the general trend of the reactivities is similar. There is a decrease in core reactivity after depressurization due to voiding in the core and a recovery of reactivity after refilling of the core. As the transient progresses, only the injected boron contributes negative reactivity to the core. Both the fuel (Doppler) and coolant (moderator density) reactivities are positive. Restoration of water level at 2180 s causes a positive increase in the moderator density reactivity, but that is more than compensated for by a corresponding increase in the negative contribution from the boron reactivity. Therefore, the reactor is maintained in a subcritical state during level recovery.

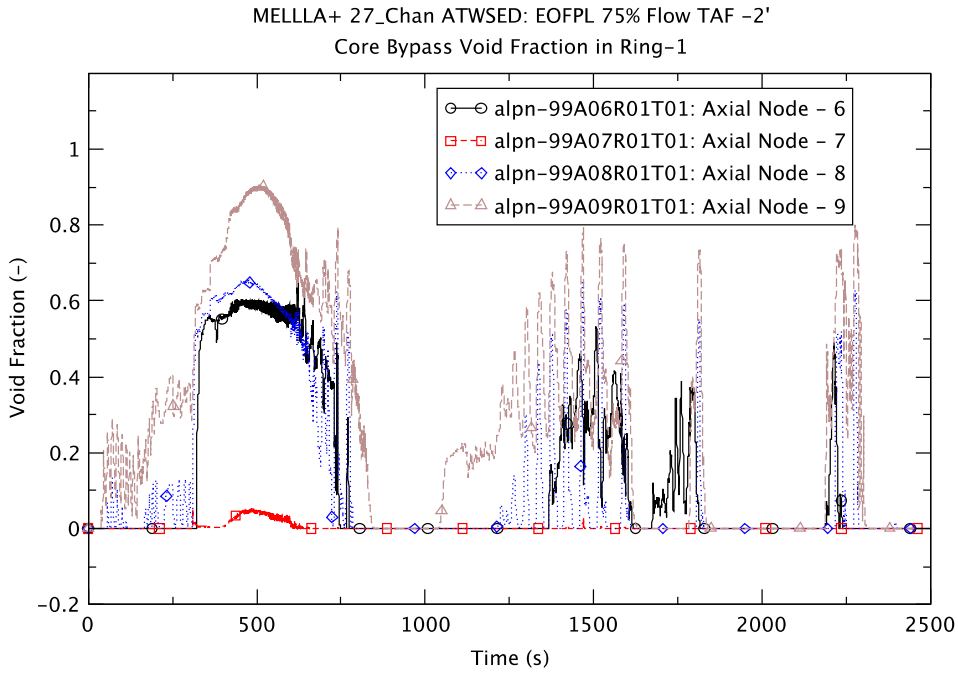

Figure 2.33 Void Fraction in Core Bypass (Ring 1) – EOFPL TAF-2 75% Flow

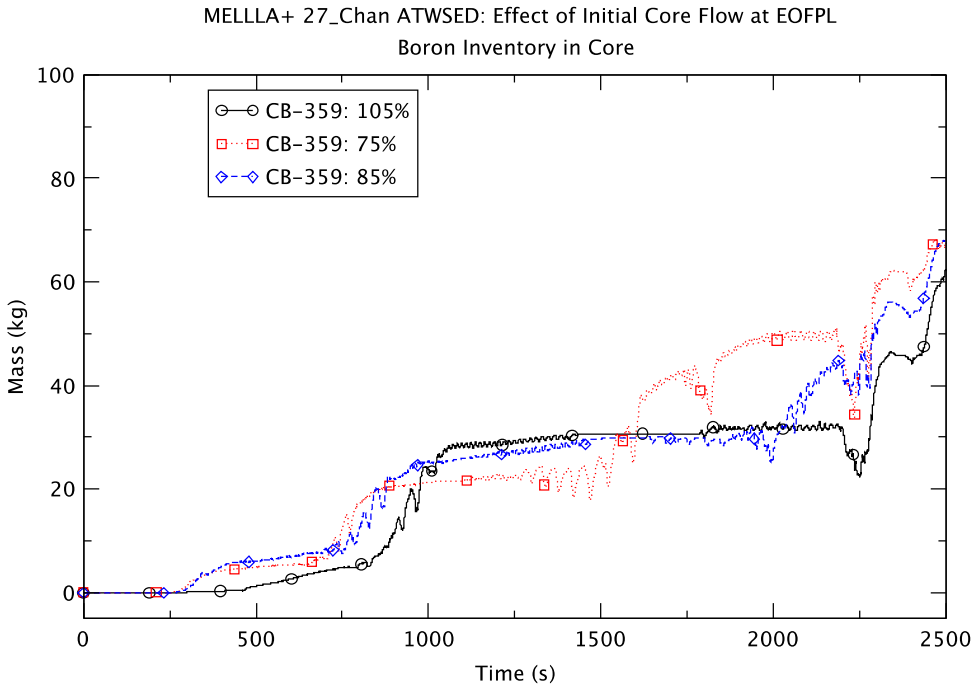

Figure 2.34 Boron Inventory in the Core Region – EOFPL TAF-2 Cases

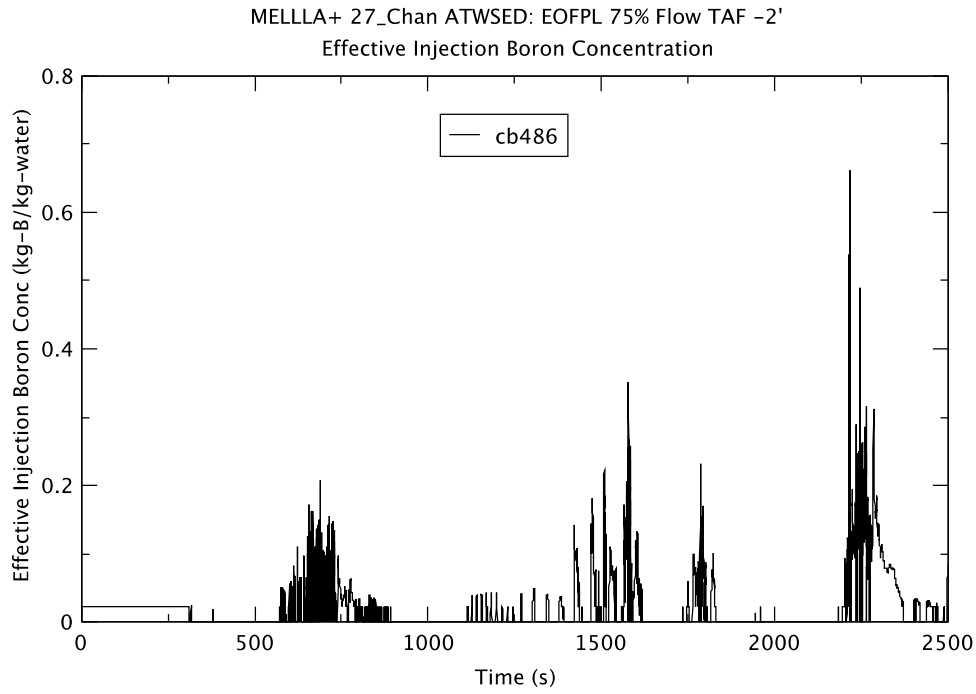

Figure 2.35 Effective Injection Boron Concentration – EOFPL TAF-2 75% Flow

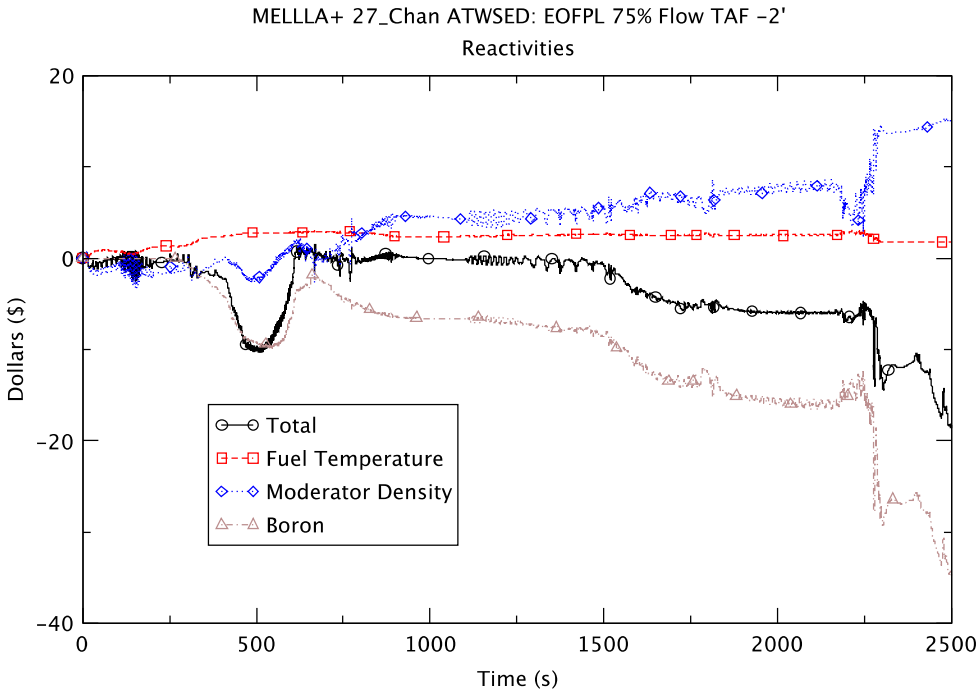

Figure 2.36 Core Reactivity – EOFPL TAF-2 75% Flow

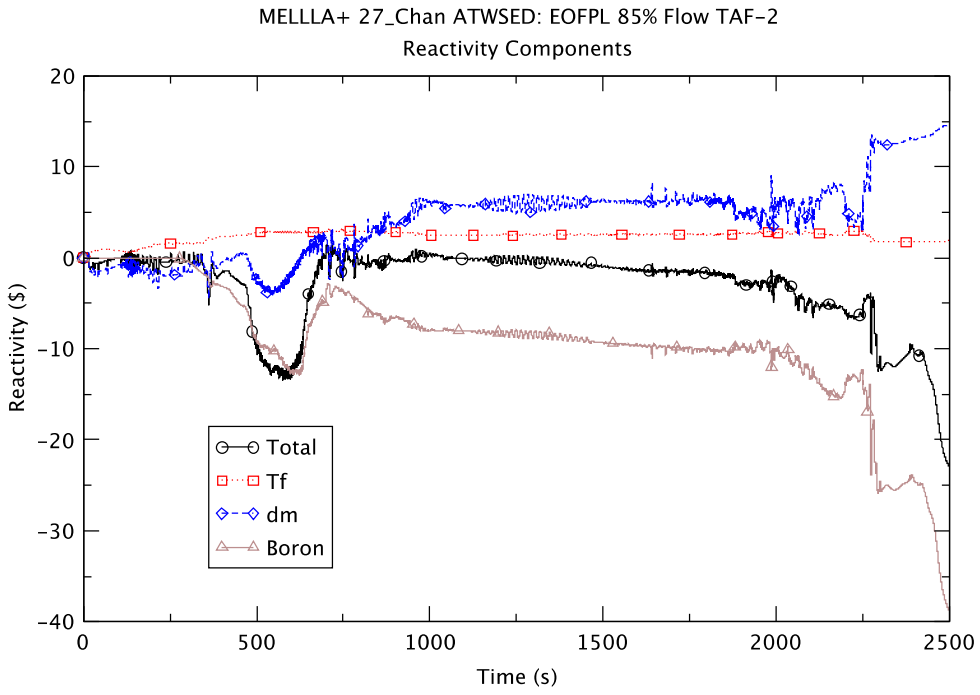

Figure 2.37 Core Reactivity – EOFPL TAF-2 85% Flow

One of the more distinguishing differences among the three cases is the maximum PCT, shown in Figure 2.38. The 75% flow case and the 85% flow case reach a temperature of 1380.5 K and 979.7 K, respectively, compared to 639.0 K for the reference case. For the two sensitivity cases, the maximum PCT occurs early; right after level control is initiated when core flow is still relatively high. In the sensitivity cases, the fuel experiences dryout with failure to rewet, leading to high PCT early in the transient. For the reference case (105% flow), the fuel does not experience extended heatup (because the power is lower) during the early transient, but there is a delayed heatup of the core at a time when the reduction in core flow after depressurization has created substantial voiding in the core. Core voiding also causes transient increase in the maximum PCT for the two sensitivity cases, at around 600 s. For the two sensitivity cases, a higher power post 2RPT leads to earlier dryout compared to the reference case. For the two sensitivity cases it appears that unstable DWO is the cause of PCT that occurs at a time when the reactor power to flow ratio is high.

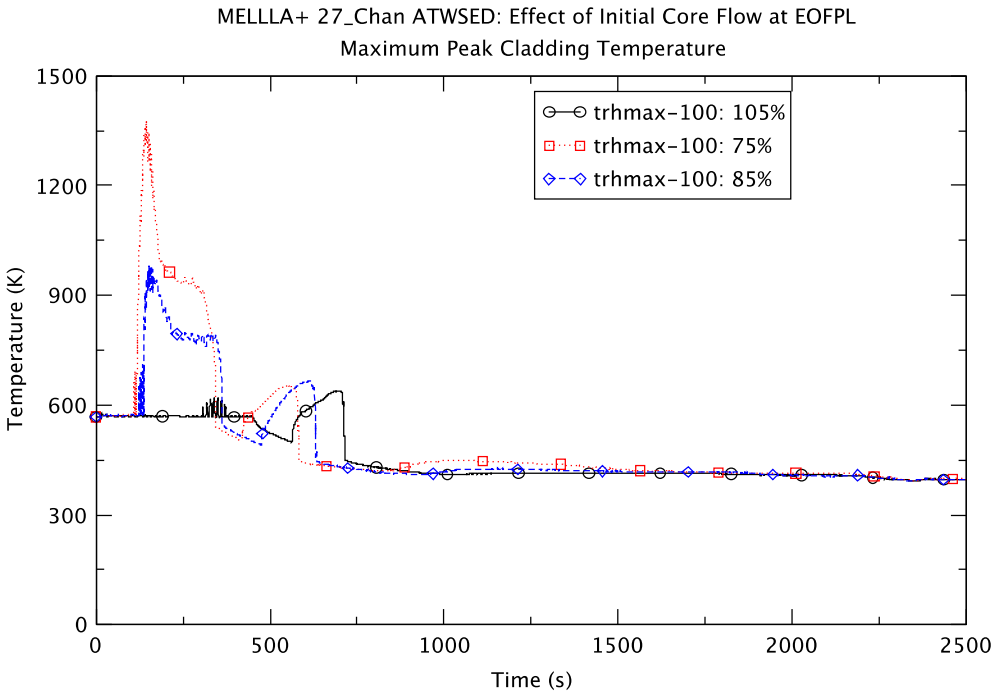

Figure 2.38 Peak Clad Temperature – EOFPL TAF-2 Cases

The suppression pool water temperature (Figure 2.39) provides an indication of energy relieved to the pool via the SRVs. The 75% flow case has the highest pool temperature followed by the 85% flow case and the reference case. In all three cases the pool temperature stays below the limit (i.e., saturation temperature at one atmosphere of pressure).

The drywell pressure (Figure 2.40) exhibits a similar trend to the suppression pool water temperature. In all three cases the maximum drywell pressure is low enough so as not to be of concern for containment integrity.

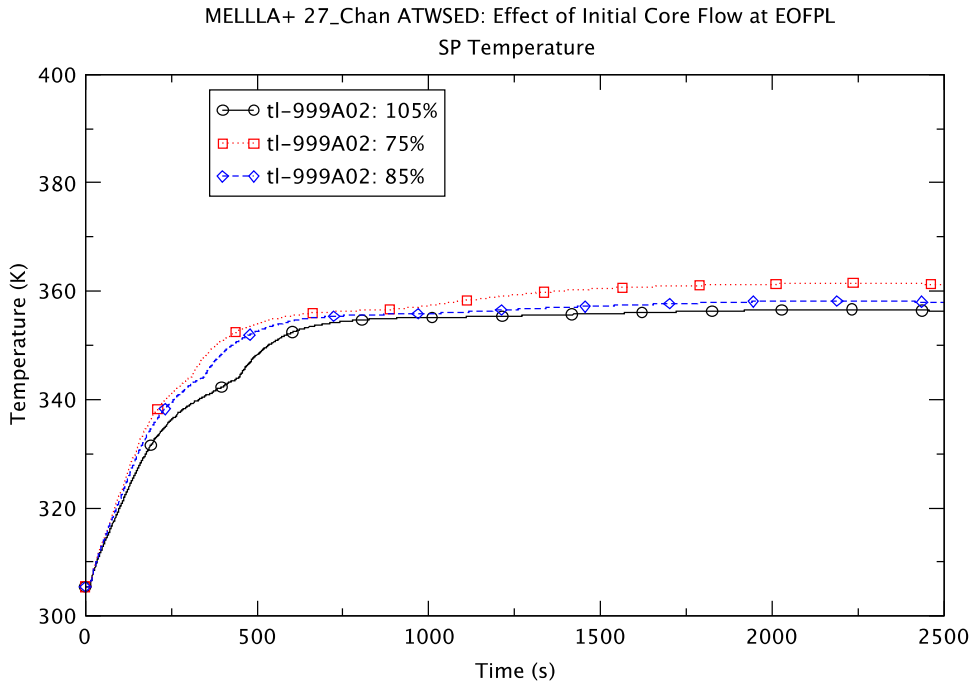

Figure 2.39 Suppression Pool Temperature – EOFPL TAF-2 Cases

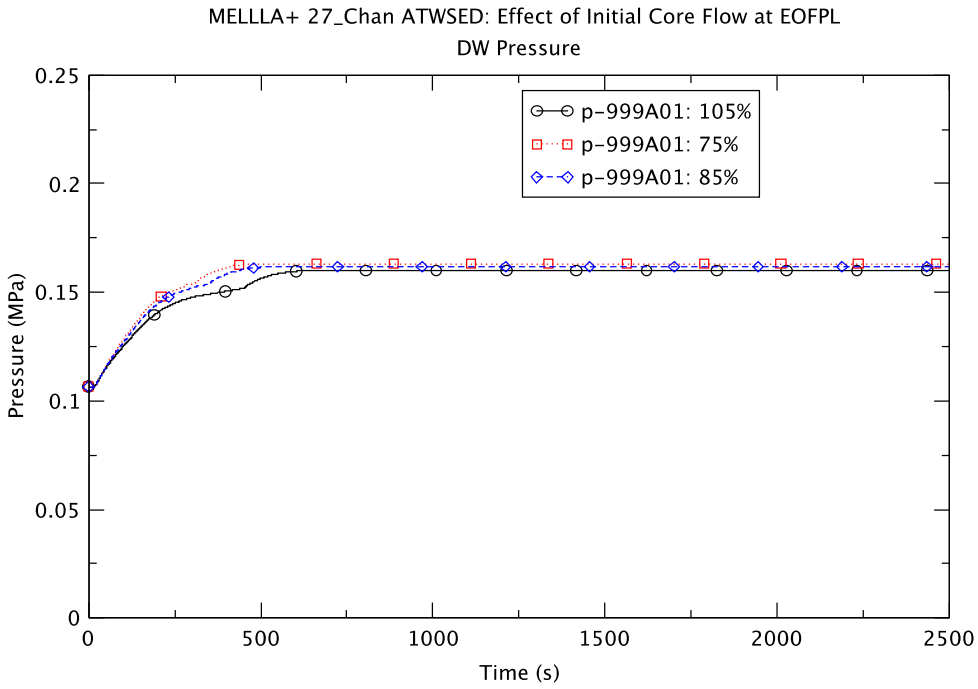

Figure 2.40 Drywell Pressure – EOFPL TAF-2 Cases

2.5 Effect of Level Control for the EOFPL with Reduced Core Flow

Three sensitivity cases at a reduced initial core flow of 85% rated have been done at EOFPL to evaluate the effect of level control to TAF+5, TAF and TAF-2. An initial core flow at 85% of the rated flow is near the lower range of the MELLLA+ operating domain. Compared to the base reference case at 105% flow, the reduced flow case has an initial axial power distribution that peaks lower (nearer to the core inlet).

In general the transient responses to water level control for the 85% flow sensitivity cases are very similar to the corresponding base cases (at EOFPL 105% flow; see Section 4.4.3 in [4]). Key results of the three sensitivity cases are summarized in Table 2.8.

Table 2.8 Comparison of Key Results for EOFPL 85% Flow Cases

Key Event	TAF	TAF-2	TAF+5
Maximum PCT (trhmax-100)	705.9 K (149.8 s)	979.7 K (151.4 s)	706.5 K (150.8 s)
Core Boron Inventory (CB 359) > 0.01 kg	249 s	255 s	245 s
Emergency Depressurization	354.8 s	346.8 s	310.0 s
Maximum Drywell Pressure	0.162 MPa (546 s)	0.162 MPa (541 s)	0.169 MPa (789 s)
Reactor Shutdown (Power Remains < 3.25% of Initial Power)	1278 s	1188 s	983 s
Maximum Suppression Pool Temperature	359.8 (2223 s)	358.2 K (2205 s)	367.4 K (2132 s)

The most significant difference between the sensitivity cases and the base cases (with the three different water level strategies) is the higher transient reactor power in the former. This is reflected in the higher maximum PCT and earlier depressurization time for the sensitivity cases (see Table 4.10 in [4] for the corresponding results for the EOFPL base cases). Another difference is the early timing of the maximum PCT at TAF-2 for the sensitivity case (at 699.3 s for the base case).

Similar to the base cases, the sensitivity cases at TAF and TAF-2 exhibit several characteristics that are different from the TAF+5 sensitivity case:

- there is flashing in the lower plenum and the core after the emergency depressurization

- natural circulation is broken after the ED and reactor power decreases further

- boron dilution is observed when the refilling of the lower plenum and the core region occurs
- core boron inventory does not increase monotonically

A complete set of plots for all three sensitivity cases is available in Appendix C. A select set of plots (Figure 2.41 to Figure 2.56) is used to compare and contrast the transient responses of the three EOFPL sensitivity cases with level control to TAF, TAF-2 and TAF+5.

The transient response of the reactor power for all three cases is shown in Figure 2.41. All three power traces show similar responses, a power spike after MSIV closure and power decreases after recirculation pump trip (2RPT), lowering of water level and depressurization. Figure 2.42 shows the reactor power for the first 600 s of the ATWS-ED transient. Between roughly 110 s and 170 s the reactor power oscillates with a frequency of ~0.4 Hz until water level reduction has successfully suppressed reactor power. The transient increase in oscillatory reactor power before water level reduction is attributed partly to a decrease in core inlet temperature (see discussion in Section 4.2.2 in [4]). The oscillatory reactor power between roughly 110 s and 170 s appears to be caused by density-wave oscillations (DWO).

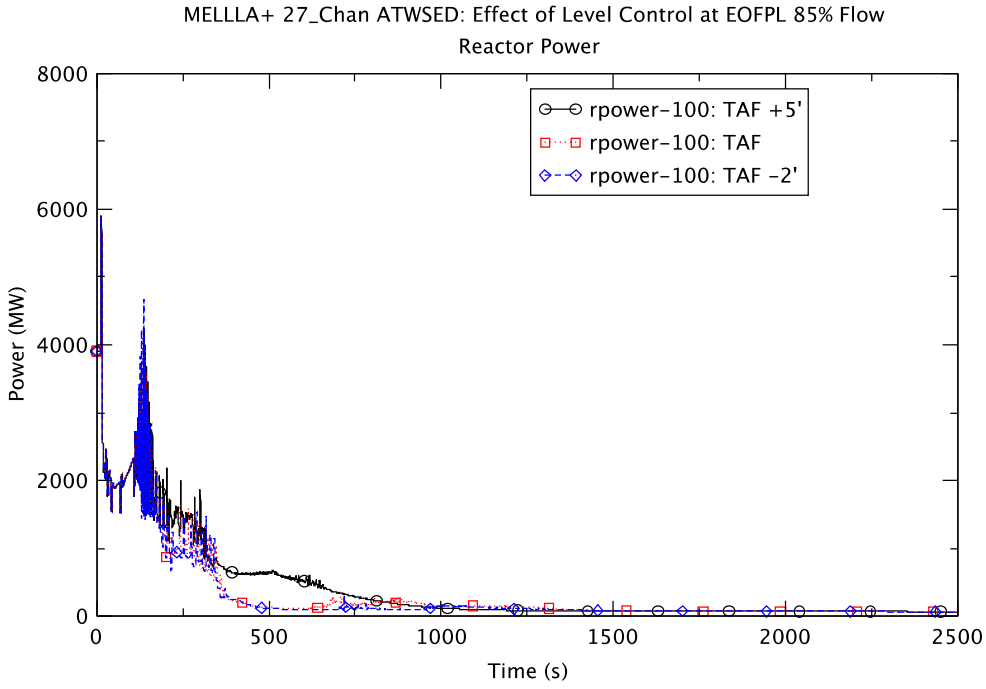

Figure 2.41 Reactor Power – EOFPL 85% Flow Cases

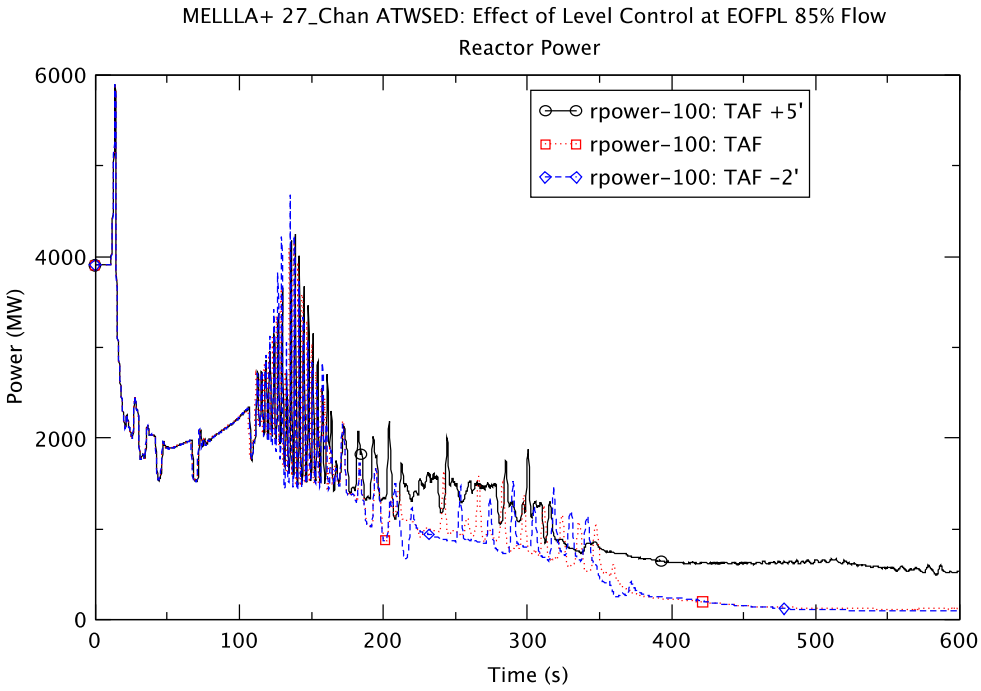

Figure 2.42 Reactor Power (0 to 600 s) – EOFPL 85% Flow Cases

With a higher reactor power after the initiation of level control, the TAF+5 case has the earliest ED time. The TAF-2 case has an earlier depressurization time than the TAF case. This has been attributed to a lower boron reactivity in the TAF-2 case and thus a slightly higher power, up to the time of the depressurization (see Section 4.2.3 in [4] for a more detailed discussion). The reactor pressure for the three sensitivity cases is shown in Figure 2.43. The initial rate of depressurization for all three cases is similar but the TAF+5 case takes longer to depressurize below 2 MPa. The TAF and TAF-2 cases show lower plenum voiding flashing after the ED and natural circulation flow in these two cases is "broken," resulting in practically zero core flow (see Figure 2.44) and noticeable level swell in the downcomer (see Figure 2.45). The lower core flow resulting from the break in natural circulation for the TAF and TAF-2 cases explains the lower reactor power level compared to the TAF+5 case (see Figure 2.42).

For the TAF+5 case, natural circulation persists after the ED and the downcomer level swell is very minor. Since the core flow remains higher for the TAF+5 case, the reactor power level likewise remains higher. During the depressurization stage, the higher power in the TAF+5 case, and hence the higher steam generation rate in the RPV, slows down the rate of depressurization compared to the other cases (see Figure 2.43).

For the TAF and TAF-2 cases the fluctuations in core flow and water level between roughly 500 s and 800 s is due to the transient flow condition created by refilling of the lower plenum and the core region. The void fraction in the core bypass region is shown in Figure 2.46 for the TAF-2 case to illustrate the refilling of the core region. From about 1000 s onward, the core power in all three cases has dropped sufficiently for the core

region to be refilled with water. This sets up a manometer-type oscillation in the downcomer water level. The oscillation is evident in the fluctuations in the water level (Figure 2.45) between about 1000 s and 1500 s. During that time period the oscillating core flow (Figure 2.44) also shows a decreasing trend for the TAF+5 case. The oscillatory condition in the core is observable from the average core void fraction as reported by the PARCS calculation (see Figure 2.47).

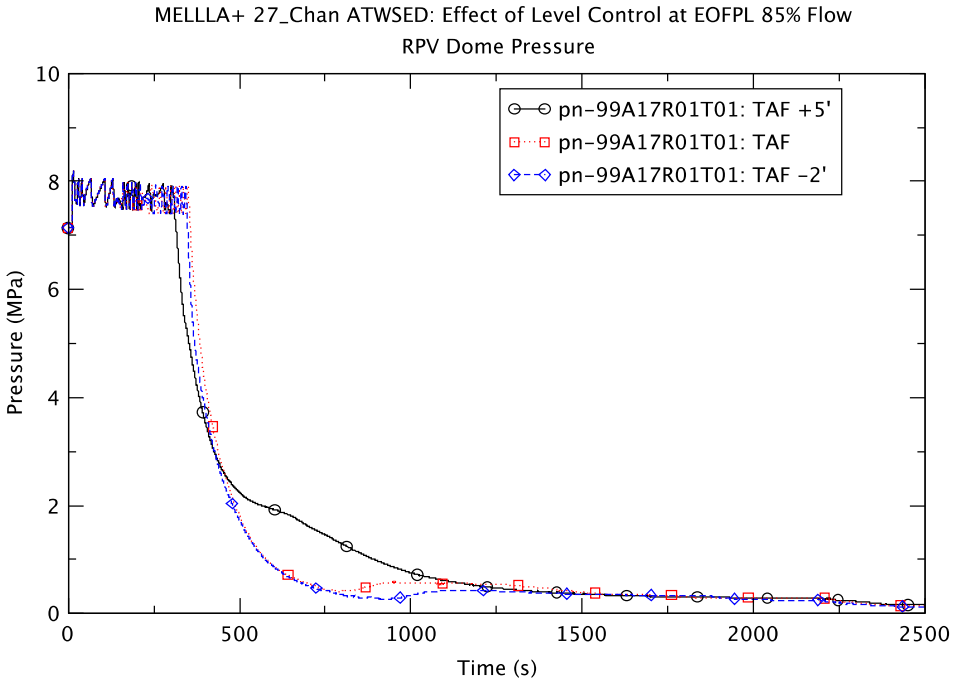

Figure 2.43 Reactor Pressure – EOFPL 85% Flow Cases

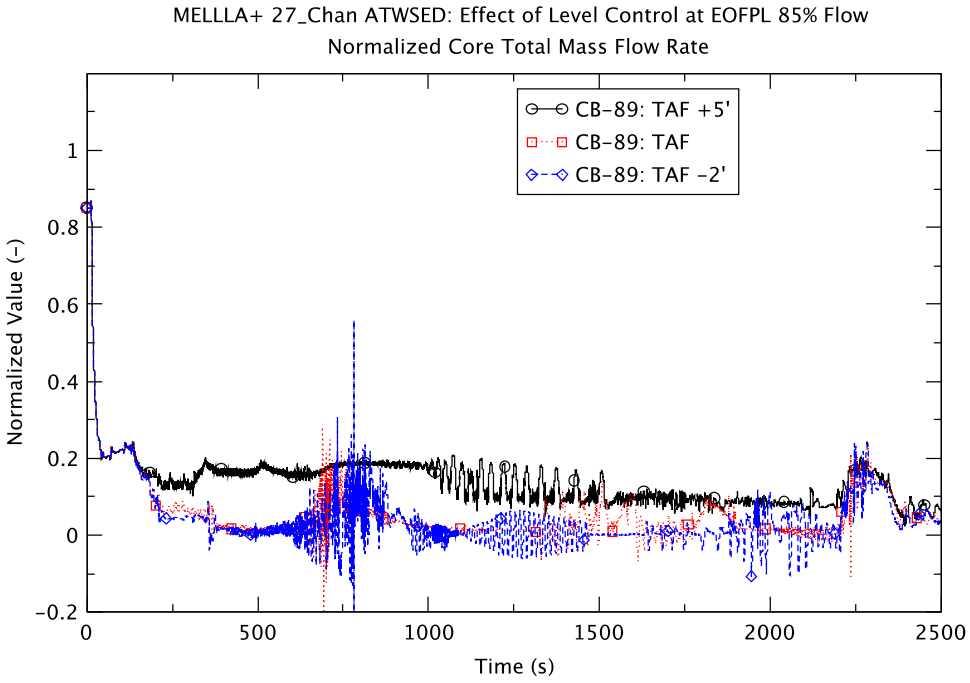

Figure 2.44 Core Flow – EOFPL 85% Flow Cases

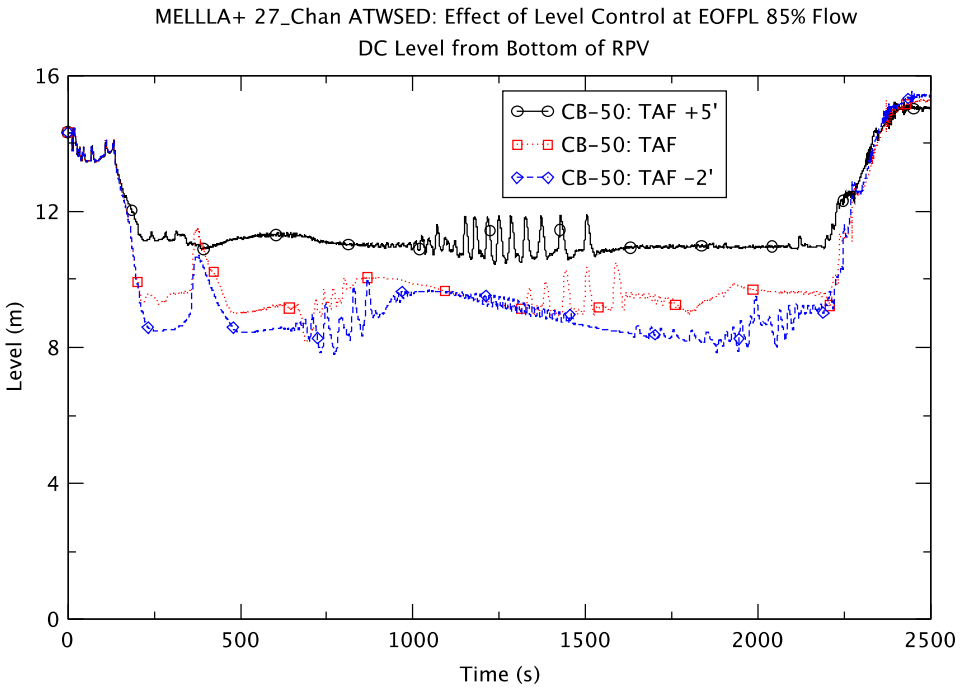

Figure 2.45 Downcomer Water Level – EOFPL 85% Flow Cases

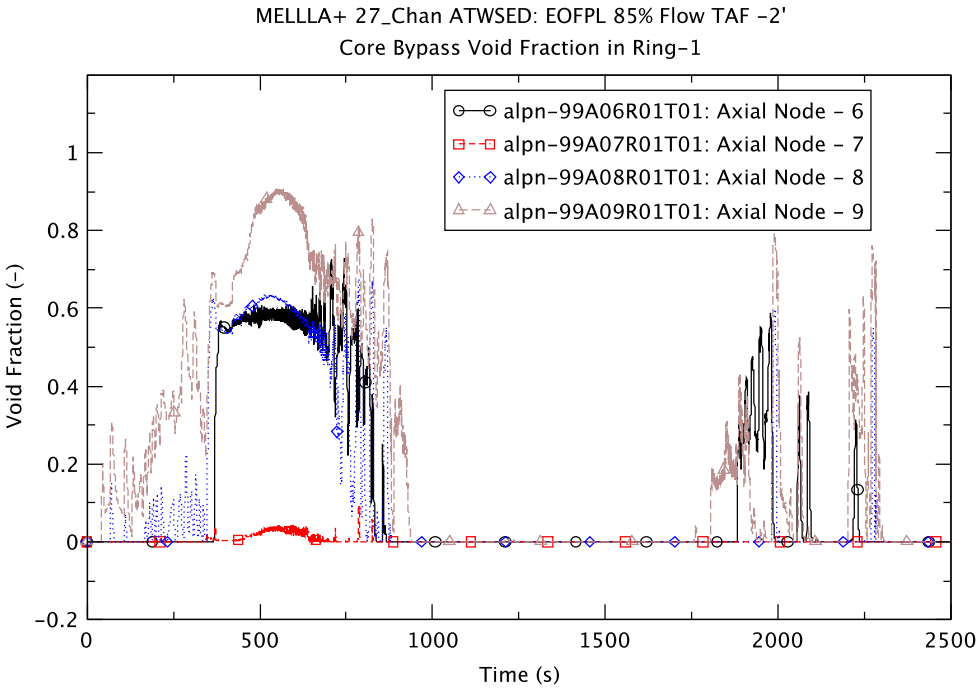

Figure 2.46 Void Fraction in Core Bypass (Ring-1) – EOFPL TAF-2 85% Flow

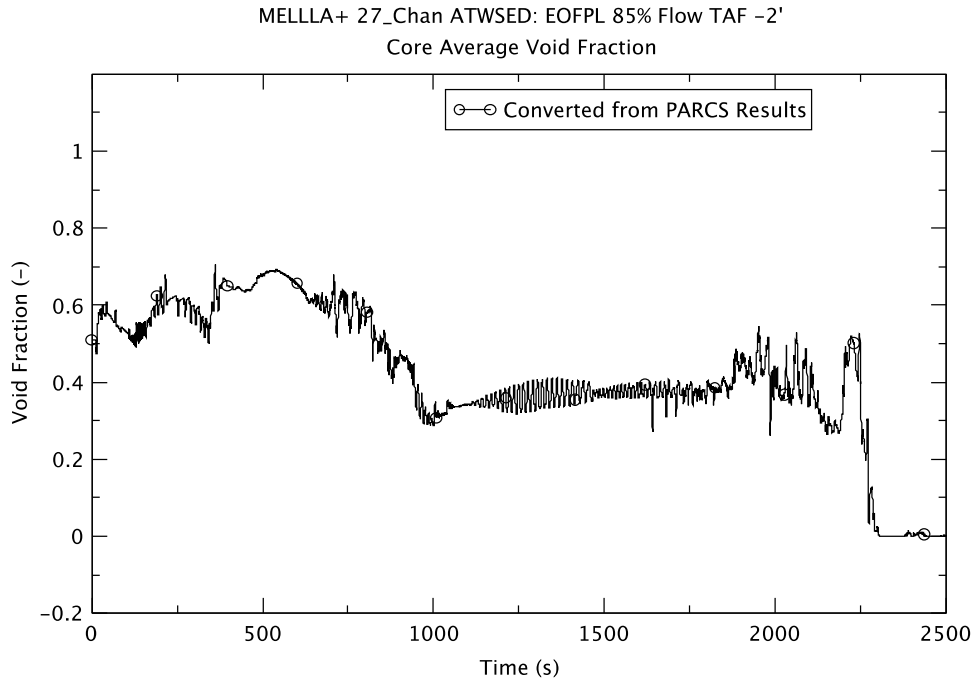

Figure 2.47 Core Average Void Fraction – EOFPL TAF-2 85% Flow Case

For the TAF+5 case, the continuation of natural circulation after ED translates to a slower decay in reactor power. A slower depressurization rate then follows after the reactor pressure has dropped to about 2.5 MPa (see Figure 2.43). The substantial core flow in the TAF+5 case also promotes boron mixing in the core. This is seen in the monotonic increase in the core boron inventory, shown in Figure 2.48. The buildup of boron in the core ultimately adds enough negative reactivity to shutdown the reactor in the TAF+5 case. The reactor power for the TAF+5 case is seen in Figure 2.41 to begin an exponential decay at about 500 s.

For the TAF and TAF-2 cases, at about 750 s, coincident with the refilling of the lower plenum, there is a marked increase in the core boron inventory. The subsequent increase in boron at 1500 s and 2000 s for the TAF case and the TAF-2 case, respectively, is associated with re-mixing of stratified boron in the bottom of the lower plenum. The re-mixing is treated with an increase in the concentration of the injected boron, as calculated by the boron transport control scheme (see Section 2.3.7 and Appendix A in [4] for a discussion). The enhanced boron concentration is a result of increased core flow due to feedwater flow and higher level. For all three cases the boron inventory increases after level recovery, which begins at 2180 s. The effective injection boron concentration for the three sensitivity cases is shown in Figure 2.49 - Figure 2.51. The increases in boron concentration above nominal are attributed to the re-mixing of settled boron in the lower plenum of the reactor vessel. It is noted that the re-mixing is assumed to be a function of coolant flow in the lower plenum.

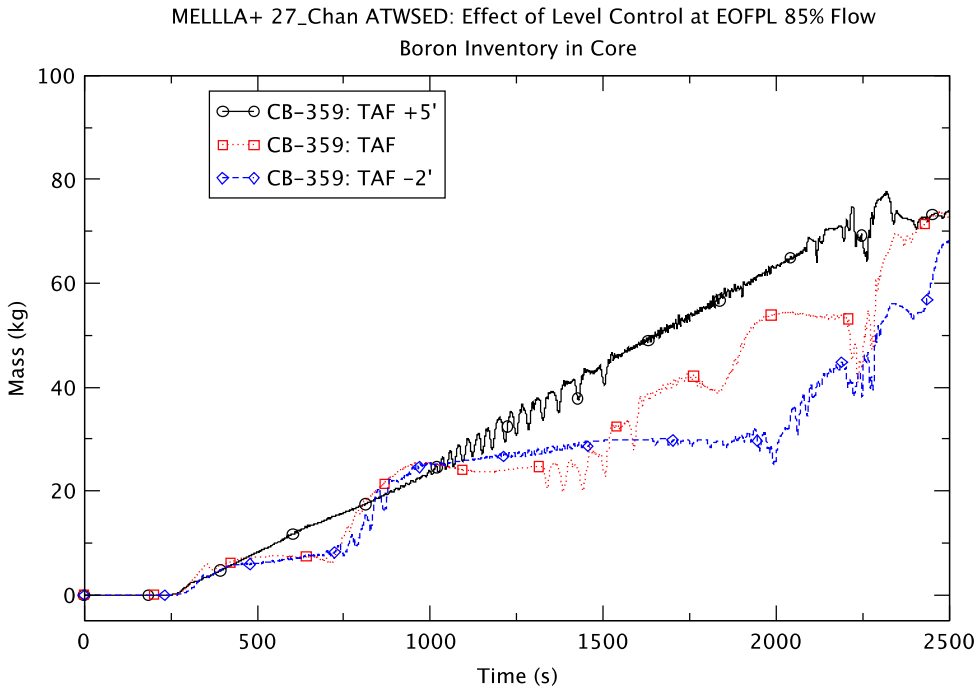

Figure 2.48 Boron Inventory in the Core Region – EOFPL 85% Flow Cases

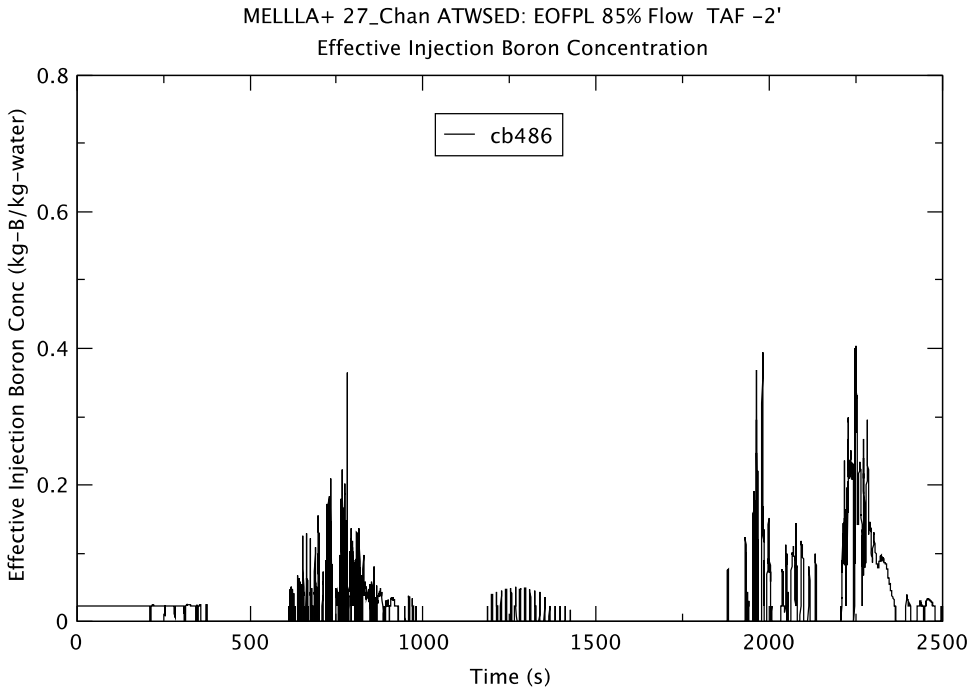

Figure 2.49 Effective Injection Boron Concentration – EOFPL TAF-2 85% Flow

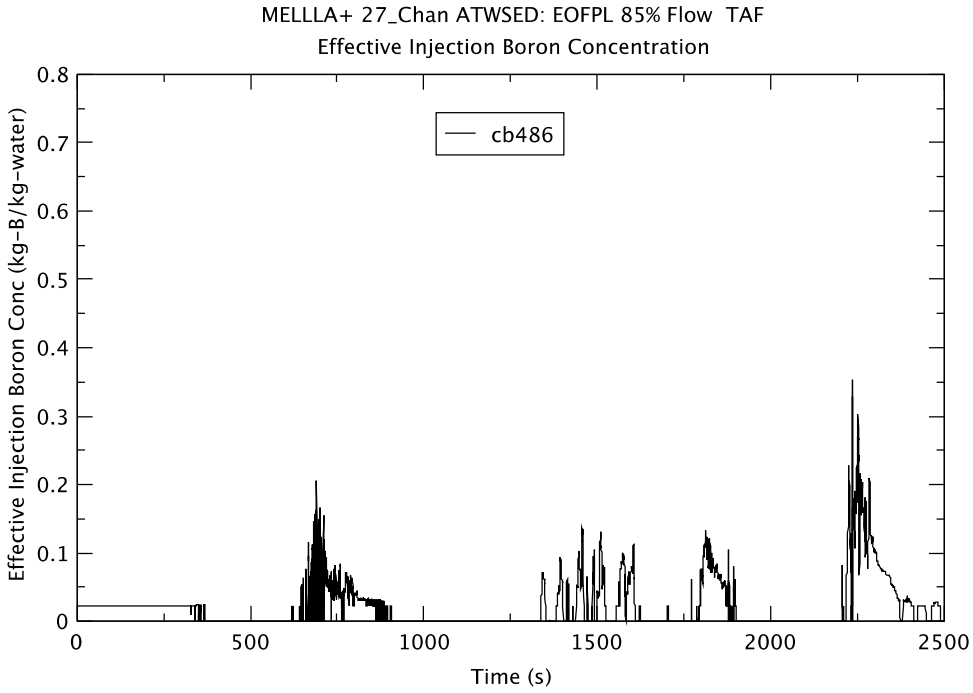

Figure 2.50 Effective Injection Boron Concentration – EOFPL TAF 85% Flow

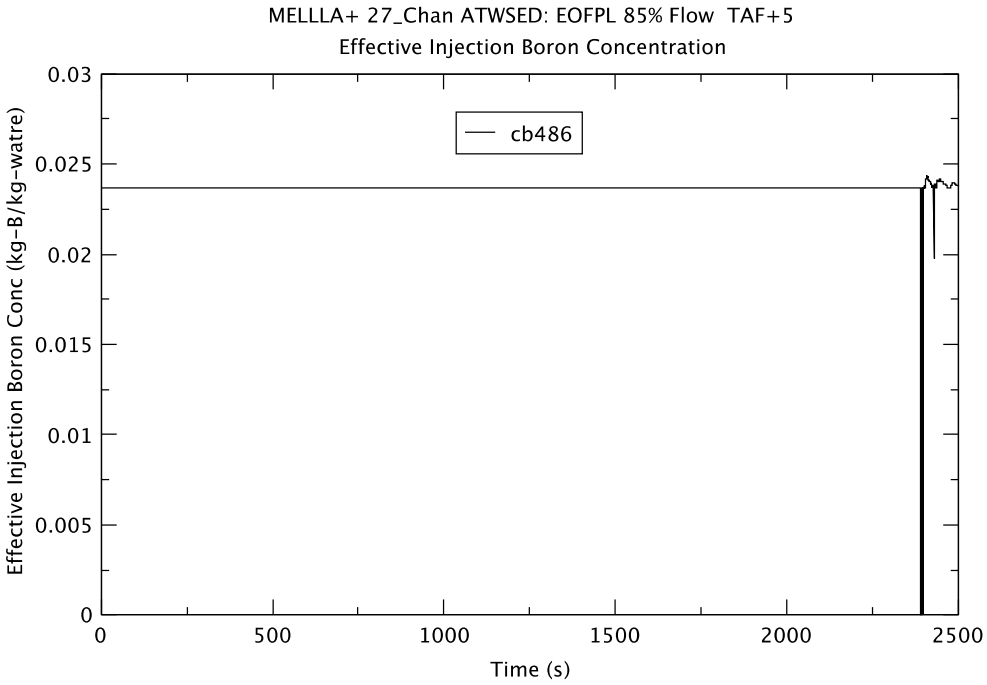

Figure 2.51 Effective Injection Boron Concentration – EOFPL TAF+5 85% Flow

For the TAF+5 case the boron transport model predicts 100% mixing for almost the entire time of the simulated transient (see Figure 2.51). The exception is a momentary drop in the mixing coefficient after the initiation of level recovery. This is caused by a drop in core flow subsequent to the displacement of voids in the core by coolant flow from the downcomer after the water level recovery.

The core reactivities calculated by PARCS are shown in Figure 2.52 and Figure 2.53 for the TAF+5 and the TAF cases, respectively (see Figure 2.37 for the corresponding plot for the TAF-2 case). For the TAF and TAF-2 cases there is a decrease in core reactivity after depressurization due to voiding in the core and a recovery of reactivity after refilling of the core. For the TAF+5 case the total core reactivity stays relatively unchanged until about 1000 s. As the transient progresses only the injected boron contributes negative reactivity to the core. Both the fuel (Doppler) and coolant (moderator density) reactivities are positive. It is observed in the figures that restoration of water level at 2180 s causes a positive increase in the moderator density reactivity, but that is more than compensated for by a corresponding increase in the negative contribution from the boron reactivity. Therefore, the core remains subcritical during the level recovery.

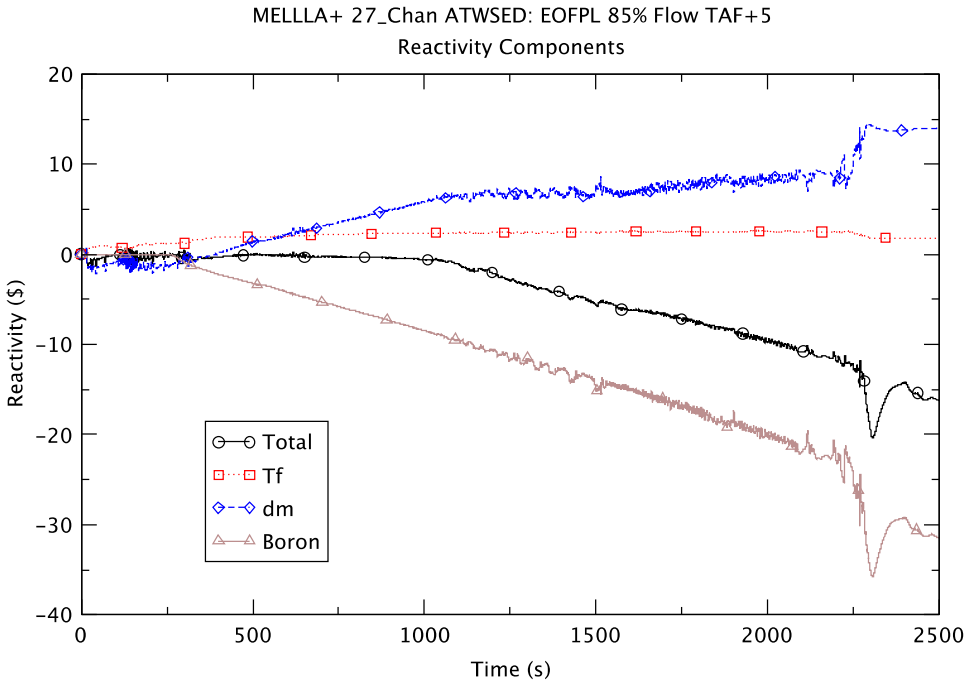

Figure 2.52 Core Reactivity – EOFPL TAF+5 85% Flow

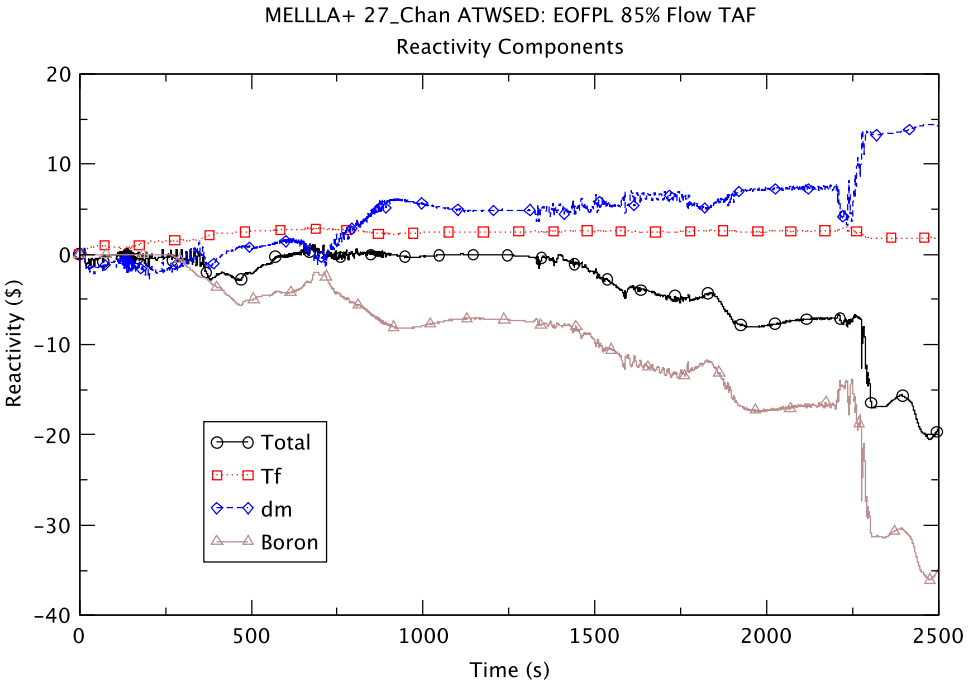

Figure 2.53 Core Reactivity – EOFPL TAF 85% Flow

The PCT for the three sensitivity cases is shown in Figure 2.54. In all three cases the maximum PCT occurs shortly after the initiation of water level control at 130 s and before the emergency depressurization. It appears that unstable DWO is the cause of PCT that occurs at a time when the reactor power to flow ratio is high. In the TAF-2 case, the fuel is predicted to dryout, fail to rewet, and experience heatup. The flow is lowest for the TAF-2 case; which contributes to higher PCT. For the TAF-2 sensitivity case there is a second, lower, peak for the PCT after the ED when the lower plenum and the core are refilled, a time when the peak PCT occurs in the corresponding base case (105% flow). For the TAF and TAF+5 base cases (at 105% flow), the maximum PCT occurs much earlier (shortly after MSIV closure; see Table 2.6) than the corresponding sensitivity cases.

The suppression pool water temperature (Figure 2.55) indicates that the TAF+5 case has the highest energy input to the water in the suppression pool, followed by the TAF case and the TAF-2 case, respectively. These differences are attributed to the fact that the power trends downward more slowly for higher RPV level (see Section 2.5 for additional discussion). In all three cases the pool temperature stays below the limit (i.e., saturation temperature at one atmosphere of pressure).

The drywell pressure (Figure 2.56) exhibits a similar trend to the suppression pool water temperature. In all three cases the maximum drywell pressure is low enough as not to be of concern for containment integrity.

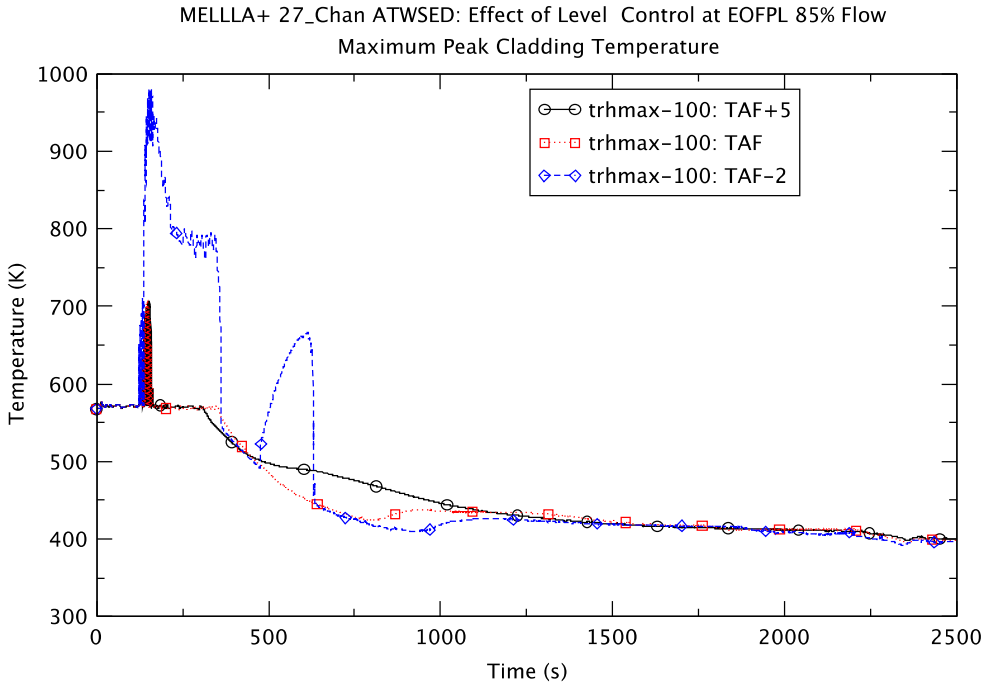

Figure 2.54 Peak Clad Temperature – EOFPL 85% Flow Cases

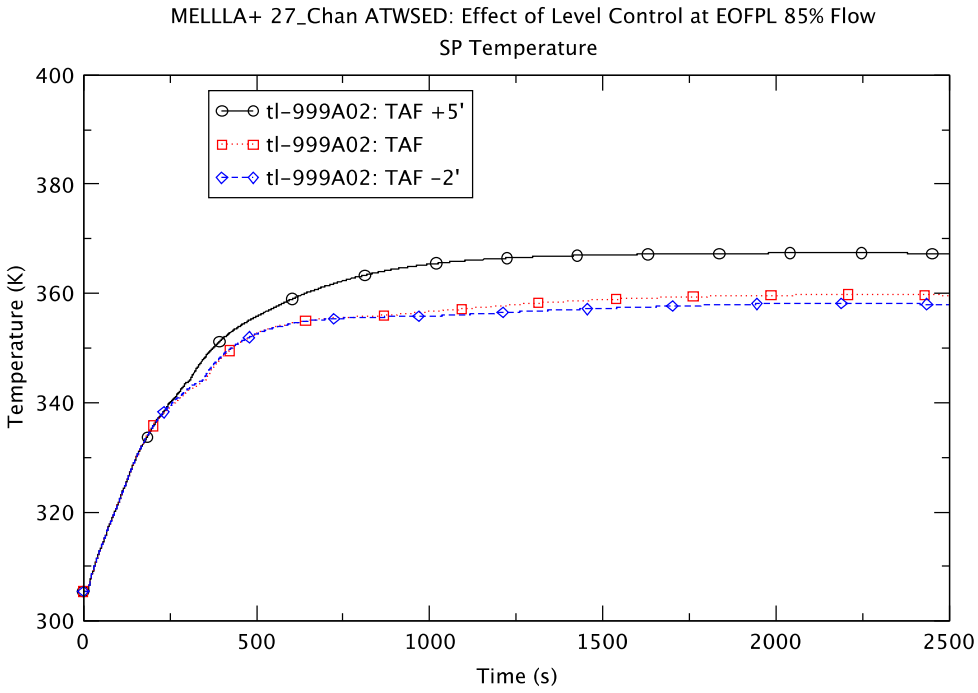

Figure 2.55 Suppression Pool Temperature – EOFPL 85% Flow Cases

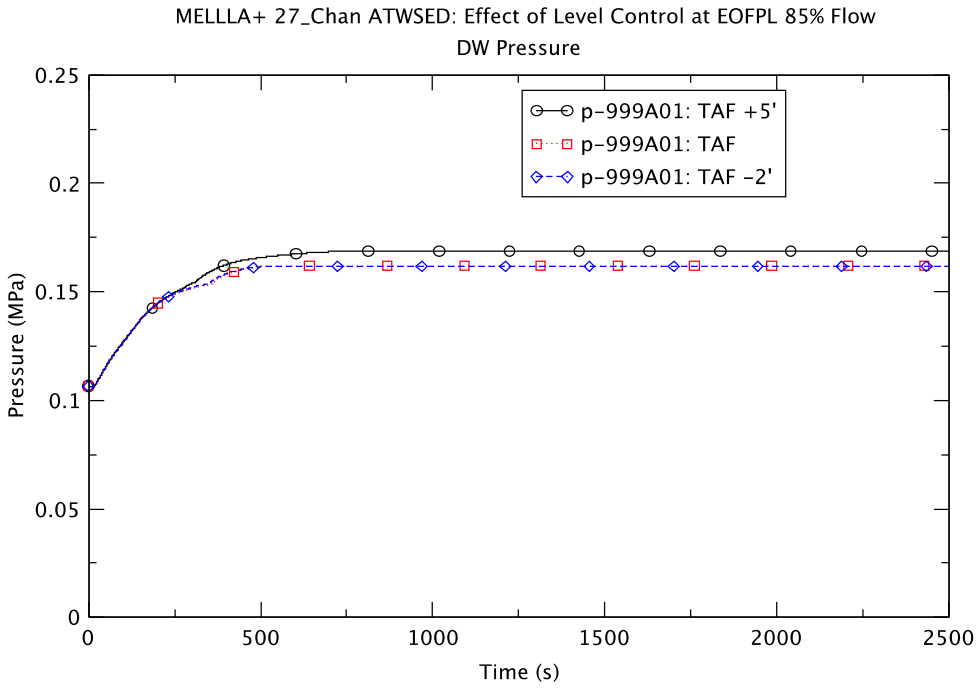

Figure 2.56 Drywell Pressure – EOFPL 85% Flow Cases

3 SUMMARY AND CONCLUSIONS

This chapter provides a summary of results and conclusions for this sensitivity study; which is a continuation of a previous study [4] of ATWS-ED events (i.e., those initiated by closure of main steam isolation valves (MSIVs) and leading to emergency depressurization (ED) once the heat capacity temperature limit (HCTL) of the suppression pool is exceeded). In the present study, the objective is to understand the sensitivity of ATWS-ED events to operating core flow and spectrally corrected moderator density history (void history) in a typical BWR/5 operating in an expanded operating domain under MELLLA+ conditions. For the simulation of ATWS-ED events the TRACE BWR/5 model was modified to become a BWR/4-like model with lower plenum SLCS injection.

In this report, results of the sensitivity cases listed in Table 1.1 are compared with results of the corresponding reference cases presented in a previous report [4]. This chapter is divided into two sections, a section on what has been learned about the sensitivity cases and a section related to the calculational tool that was used, namely TRACE/PARCS.

3.1 ATWS Events Initiated by MSIV Closure – Sensitivity Cases

The sensitivity study was conducted by using the same methodology and ATWS-ED scenario as reported in [4]. The six ATWS-ED cases listed in Table 1.1 are to investigate the sensitivity of ATWS-ED events to operating core flow and spectrally corrected moderator density history (void history) in a typical BWR/5 operating in an expanded operating domain under MELLLA+ conditions. For the typical BWR/5 under consideration the nominal core flows for the beginning of cycle (BOC) and the end of full-power life (EOFPL) conditions are 85% and 105% of rated flow, respectively. The sensitivity studies on core flow assumed operating flows of 75% (for BOC and EOFPL) and 85% (for EOFPL) of rated flow. The correction to the moderator history is to take into account the impact of factors such as leakage or control state on the neutron energy spectrum. For the EOFPL 85% flow condition the sensitivity study also considered different water level control strategies: top of active fuel (TAF), TAF+5' and TAF-2' respectively.

The results show:

- The ATWS-ED transient (EOFPL, TAF+5) is not sensitive to the void history model. Results of the sensitivity case using the spectrally corrected void history (UHSPH) are essentially the same as the base case (the UH case).

- Reducing operating core flow shifts the boiling boundary and power generation towards the inlet of the core.

- Transient reactor power is higher in the reduced (initial) flow cases than in the corresponding reference cases. The fractional decrease in core flow as a result of the recirculation pump trip (2RPT) is lower for the reduced flow cases leading to a relatively lower reduction in reactivity as compared to the reference cases.

- Higher core power in the reduced flow cases results in

    - higher PCT
    - more energy relieved to the suppression pool via the SRVs
    - earlier depressurization time
    - higher drywell pressure
    - higher suppression pool temperature.

- In all reduced flow cases the reactor remains shutdown by the injected boron.

    - There is no recriticality observed due to either repressurization of the reactor vessel or dilution of boron.
    - The maximum PCT is below 1478 K (2200°F), the limit chosen for this study.
    - Both the drywell pressure and the suppression pool temperature stay low enough as not to be of safety concern.

- The progression of the BOC, TAF+5 case at 75% flow generally follows the same trend as the reference case at 85% flow. As noted above, the sensitivity case at reduced core flow has higher reactor power and PCT than the reference case.

- Reactor power DWO with increasing amplitude at a frequency of ~0.4 Hz is observed in the EOFPL 75% and 85% flow cases, after the 2RPT and before level reduction has successfully suppressed the reactor power. Evaluation of reactor instability is outside the scope of this sensitivity study.

- For the EOFPL reduced flow cases, the magnitude of the power oscillation after the 2RPT is higher for a lower operating flow.

- For the EOFPL reduced flow cases (75% and 85% flow) the maximum PCT occurs shortly after the initiation of level control at 130 s when the core flow is still relatively high. For the TAF-2 sensitivity cases there is a second peak in the PCT after the depressurization at a time when the reactor is at or close to decay heat level. Though the second peak in the PCT is much lower than the first one, it is calculated to be higher than the maximum PCT for the corresponding reference case (EOFPL, 105% flow, TAF-2). For the two reduced flow cases, it appears that unstable DWO is the cause of the maximum PCT that occurs at a time when the reactor power to flow ratio is high.

- For the EOFPL reference cases (105% initial flow; see Section 4.4 in [4]), the timing of the maximum PCT depends on the level control strategy. For level

control to TAF and TAF+5, the maximum PCT occurs at 14.3 s when the reactor is still undergoing pressurization, i.e., before the MSIV becomes fully closed. For level control to TAF-2, the maximum PCT occurs at 700 s when core flow is very low and the core is voided resulting in a higher maximum PCT than the other two cases.

- The effects of level control with reduced core flow for the EOFPL condition are generally similar to the trends exhibited by the corresponding reference cases at 105% flow. There are two exceptions to the general trend. They are in the timing of the maximum PCT (see earlier discussion) and the condition of core flow after the emergency depression (ED) for the TAF+5 case.

- For the EOFPL sensitivity case (85% flow) at TAF+5, natural circulation flow persists through the ED. For the reference case (105% flow TAF+5), natural circulation flow is broken after the ED and is not re-established until after the lower plenum is refilled at about 750 s.

Similar to the analyses described in [4] results of the sensitivity cases demonstrate the effectiveness of operator actions in mitigating reactor power in an ATWS-ED transient. These actions include reactor water level control, emergency depressurization, and injection of boron. In all cases analyzed, the peak clad temperature (PCT) stayed below the chosen limit of 1478 K (2200°F), no recriticality was predicted, and no overheating of the suppression pool or over-pressurization of the drywell was predicted to occur. In summary the sensitivity study shows that the PCT is the parameter most affected by reduced initial operating flow. Also the magnitude of power oscillation is increased at reduced flow and the frequency of oscillation coincides with that characterized by density-wave oscillation in BWRs.

3.2 Applying TRACE/PARCS to ATWS-ED Events

As an advanced tool for system transient analysis the TRACE/PARCS package has numerous modeling parameters that the analyst can select to overcome some of the numerical difficulties encountered in the simulation of a transient scenario. This is also the case in this sensitivity study. TRACE/PARCS input options specific to the simulation of ATWS-ED events have been discussed previously in [4]. However, code updates were found necessary to enable the completion of all six sensitivity cases. Three TRACE executables, as summarized in Table 2.2, were used in the current work. Appendix A provides additional background information on the use of different versions of TRACE. Results in the appendix demonstrate that the updated version of the code is capable of duplicating major features predicted by the old version for the same ATWS-ED transient.

The sensitivity of the ATWS-ED results to the time-step size and the choice of numerical method (stability enhanced two step (SETS) versus semi-implicit (S-I)) is examined in Appendix B. In using the SETS method it is shown that the results are not sensitive to a

reduction of the maximum time-step size from 0.05 s to 0.025 s. Calculations discussed in the appendix also demonstrate that by judicious choice of the maximum time-step size, SETS and S-I produce essentially identical results. A scoping calculation described in Appendix B suggests that there is bifurcation in results when the computation is started from slightly different initial conditions. The nature of the parameter(s) that drives the solution to a certain path is unclear, however, results seem to be sensitive to modeling and numerical method differences.

4 REFERENCES

1. “General Electric Boiling Water Reactor Maximum Extended Load Line Limit Analysis Plus,” NEDC-33006P-A, Rev. 3, General Electric Nuclear Energy, June 2009.
2. L-Y. Cheng et al., “BWR Anticipated Transients Without Scram in the MELLLA+ Expanded Operating Domain – Model Development and Events Leading to Instability,” BNL-97068-2012, Brookhaven National Laboratory, March 30, 2012.
3. L-Y. Cheng et al., “BWR Anticipated Transients Without Scram in the MELLLA+ Expanded Operating Domain – Part 2: Sensitivity Studies for Events Leading to Instability,” BNL-98525-2012-IR, Brookhaven National Laboratory, October 26, 2012.
4. L-Y. Cheng et al., “BWR Anticipated Transients Without Scram in the MELLLA+ Expanded Operating Domain – Part 3: Events Leading to Emergency Depressurization,” BNL-98584-2012-IR, Brookhaven National Laboratory, November 27, 2012.
5. P. Yarsky, “Applicability of TRACE/PARCS to MELLLA+ BWR ATWS Analyses,” U.S. Nuclear Regulatory Commission, Office of Nuclear Regulatory Research, draft August 10, 2011.
6. NRC, “Standard Review Plan,” Section 15.8, NUREG 0800, U.S. Nuclear Regulatory Commission, March 2007.

APPENDIX A

Comparison of TRACE Executables

This Appendix provides additional background information on the use of three versions of the TRACE/PARCS executable in the analysis of the six ATWS-ED sensitivity cases. The objective is to confirm that the three versions of the executable are capable of producing similar results for a given ATWS-ED case. The version of the executable used for each sensitivity case is indicated in Table A.1.

Table A.1 Version of TRACE Executable Used

Case ID	Exposure	Core Flow Rate, %	Reactor Water Level Strategy	TRACE Executable
4B	BOC	75	TAF+5	V5.540_fxValveChoke.x
10D	EOFPL	75	TAF-2	V5.0p3P32m07co_x64.exe
10A	EOFPL	85	TAF+5	V5.540_fxValveChoke.x
11A	EOFPL	85	TAF	V5.540_fxValveChoke.x
12A	EOFPL	85	TAF-2	V5.0p3P32m07co.x
10C	EOFPL UHSPH	105	TAF+5	V5.540_fxValveChoke.x

The Linux and Windows executables are identified by filename extensions ".x" and ".exe" respectively. All eleven of the base reference cases were analyzed using V5.540_fxValveChoke.x, a version that is very similar to the latest released version of TRACE (V5.541 is V5 Patch 3). However, this version of the executable failed to complete two of the EOFPL cases at reduced flow (75% and 85%) with water level reduction to TAF-2. The difficulty appears to be related to failure of PARCS to converge when the reactor power is at decay heat levels. A revised version of TRACE, V5.0p3P32m07co, was subsequently used to complete the two TAF-2 sensitivity cases.

Two of the relevant changes made in the PARCS module of TRACE that enable the completion of the TAF-2 simulations are:

1. A limiter was added to the ADF adjustment factor, on the left and right faces of the considered node.
2. For the NEM kernel, a limit was also placed on the lowest value for the surface flux.

An EOFPL base case was rerun with this new version of the executable to confirm that the two versions of the executable are equivalent. Results from the two executables are compared in the first part of this appendix.

The new version of the TRACE executable successfully completed the EOFPL TAF-2 85% flow case. However, using the Linux executable V5.0p3P32m07co.x to run the same case but starting with a 75% core flow, an anomalous power spike was observed at about 700 s. The Windows version of the new executable, V5.0p3P32m07co_x64.exe, completed the case without the power spike. Results from

the Linux and Windows version of the executable are compared in the second part of this appendix. The two executables produce identical results until the occurrence of the power spike.

The following figures (Figure A.1 to Figure A.11) are from the execution of the EOFPL TAF-2 base case (105% flow) by the two versions of the TRACE executable, namely, V5.540_fxValveChoke.x (the old version) and V5.0p3P32m07co.x (the new version). Both runs were done with the semi-implicit numerical scheme and a maximum time step size of 0.02 s. A comparison of the results from the two executables demonstrates that the new version of TRACE is capable of duplicating major features predicted by the old version for an ATWS-ED transient. These features include:

- power spike after MSIV closure
- power and flow decrease after recirculation pump trip (2RPT)
- level control
- timing of ED
- reactor pressure
- level swell after ED
- boron inventory in the core region

Any minor differences in the results produced by the two executables will not lead to different conclusions of the sensitivity study.

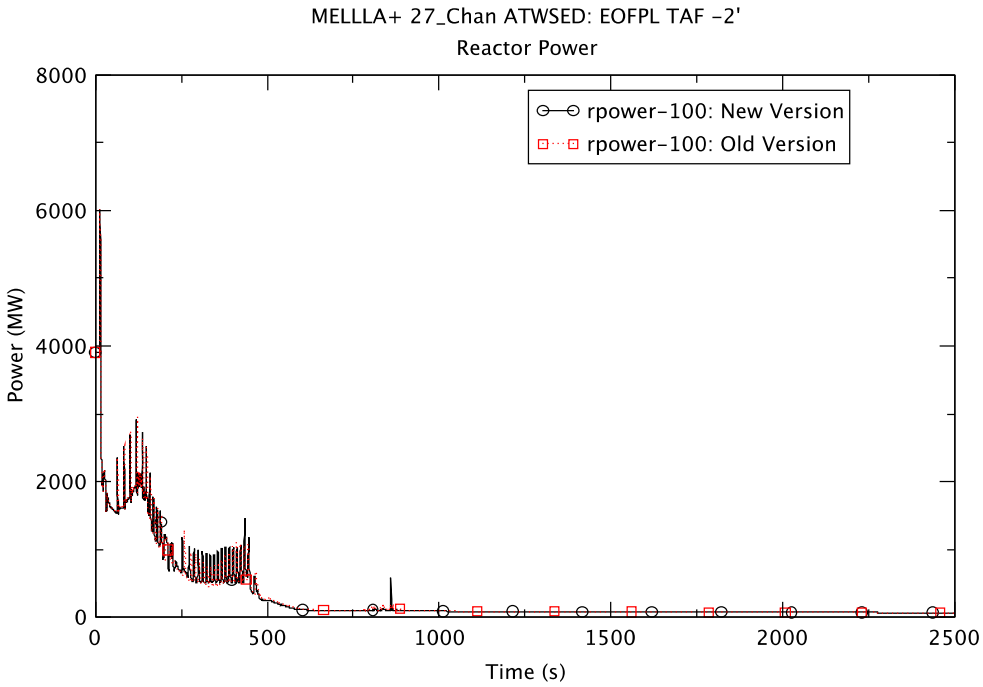

Figure A.1 Reactor Power – EOFPL TAF-2

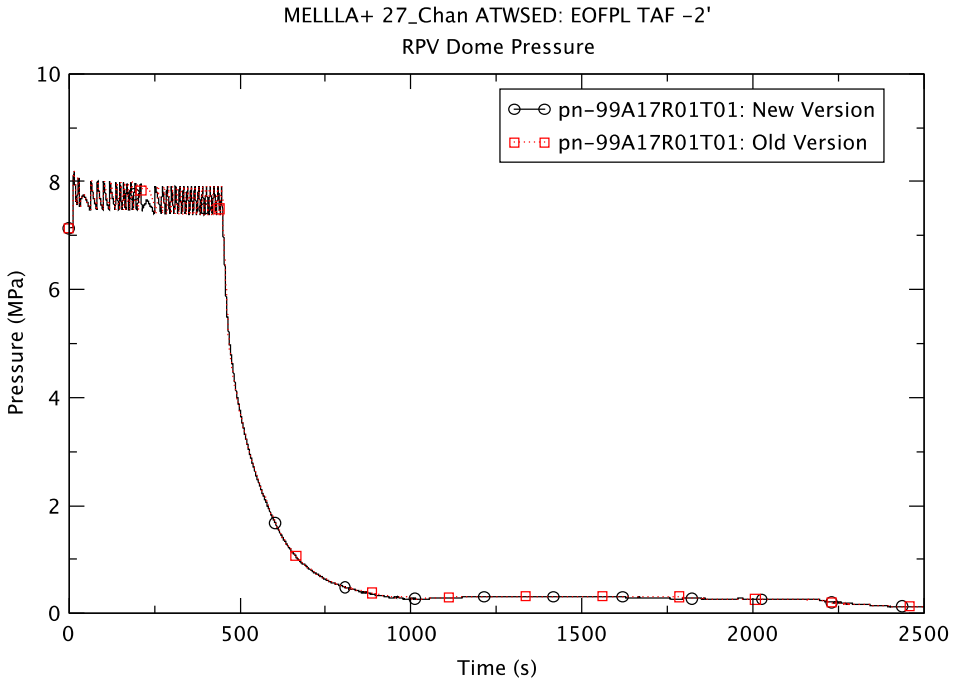

Figure A.2 Reactor Pressure – EOFPL TAF-2

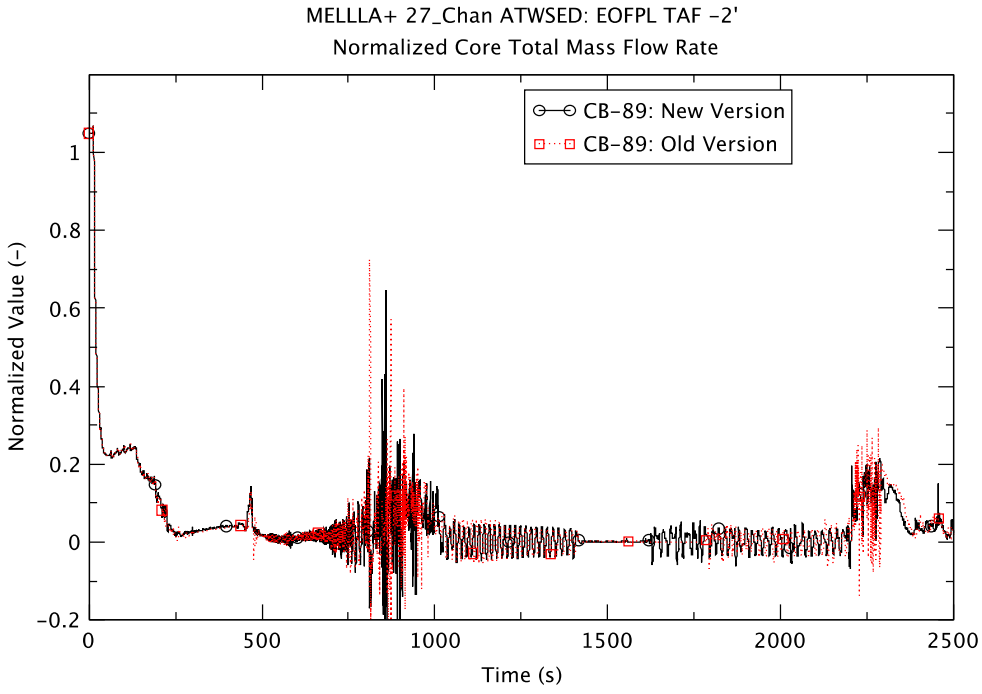

Figure A.3 Core Flow – EOFPL TAF-2

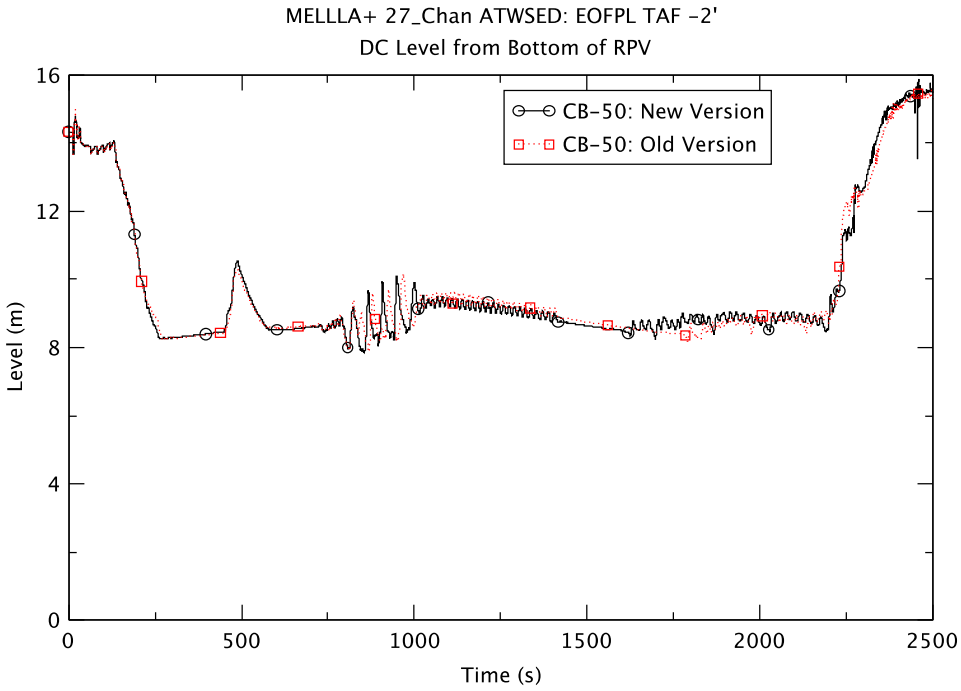

Figure A.4 Downcomer Water Level – EOFPL TAF-2

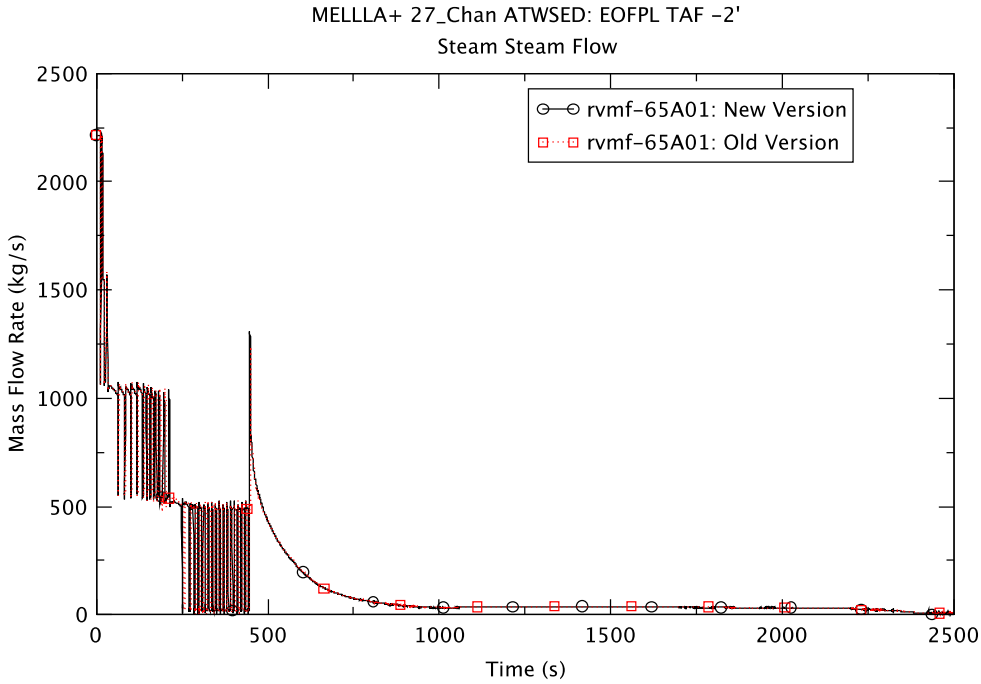

Figure A.5 Steamline Flow – EOFPL TAF-2

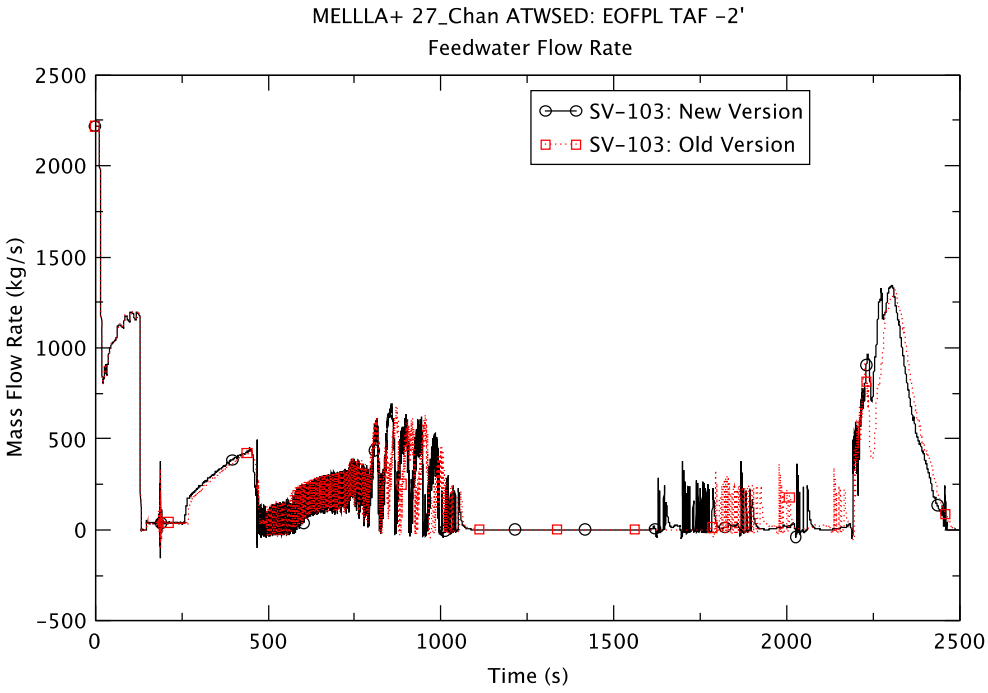

Figure A.6 Feedwater Flow Rate – EOFPL TAF-2

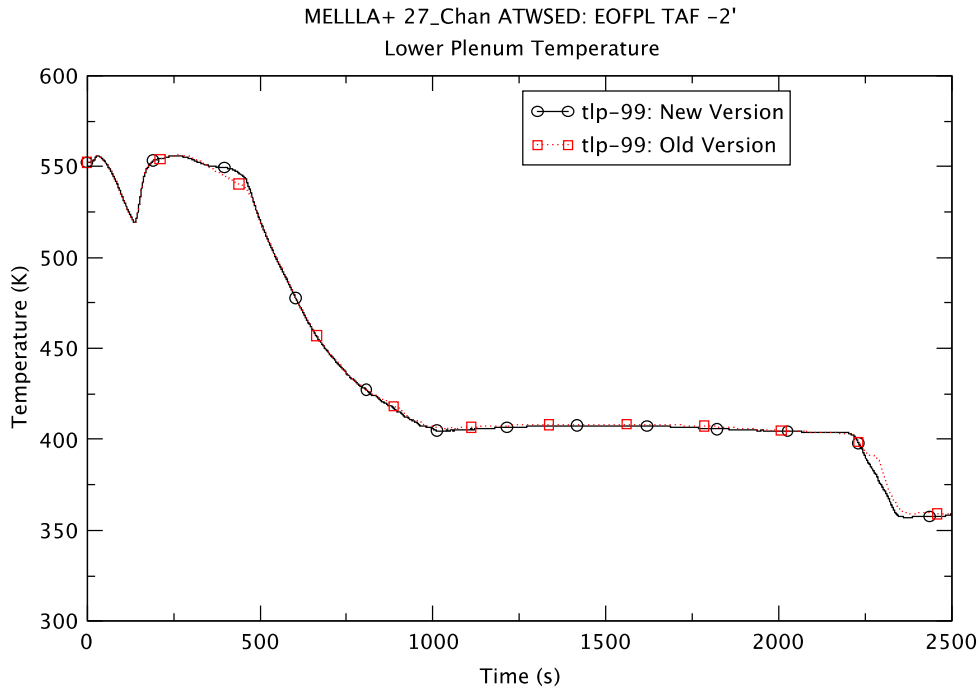

Figure A.7 Lower Plenum Temperature – EOFPL TAF-2

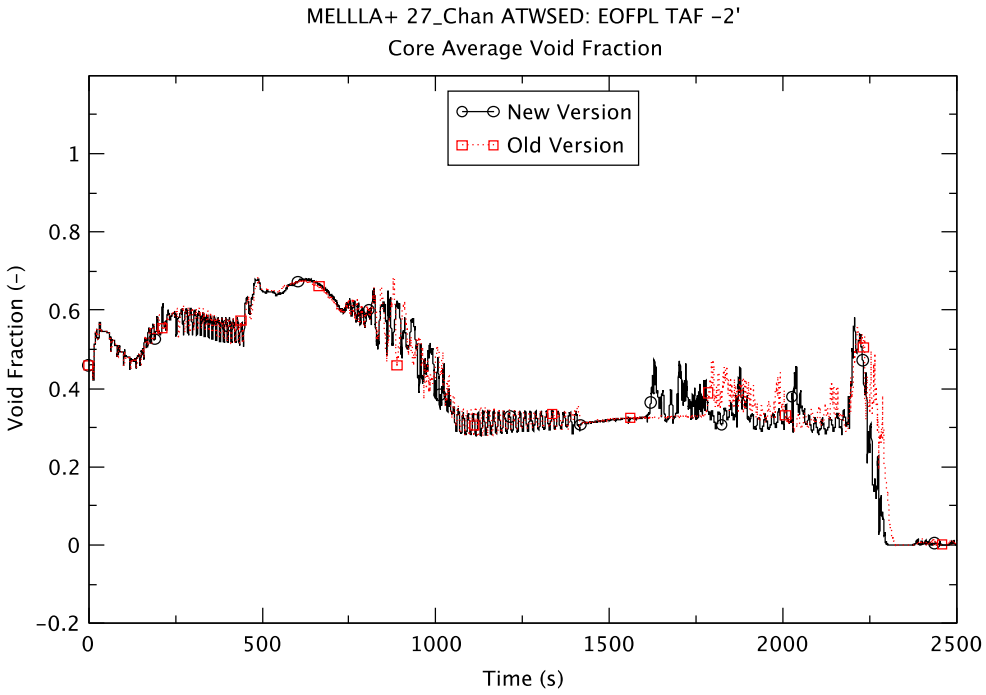

Figure A.8 Core Average Void Fraction –EOFPL TAF-2

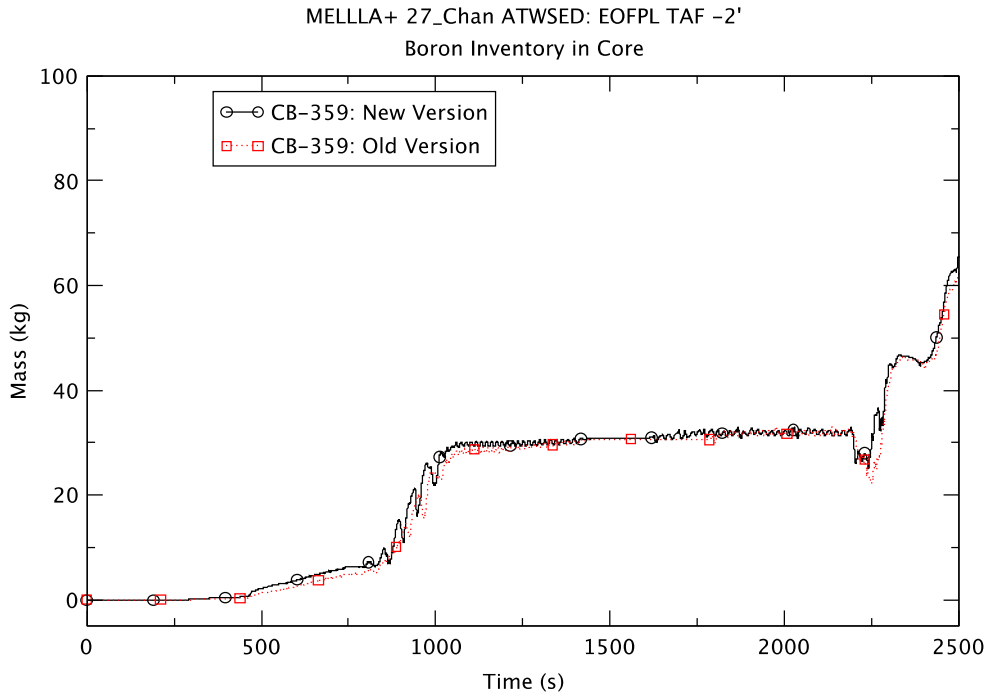

Figure A.9 Boron Inventory in the Core Region – EOFPL TAF-2

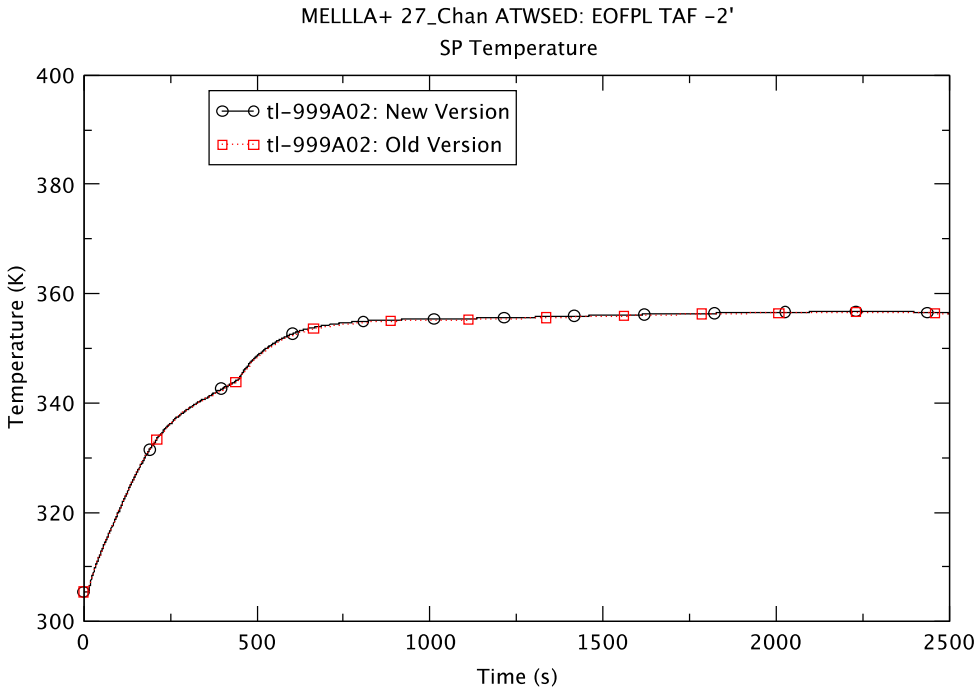

Figure A.10 Suppression Pool Temperature – EOFPL TAF-2

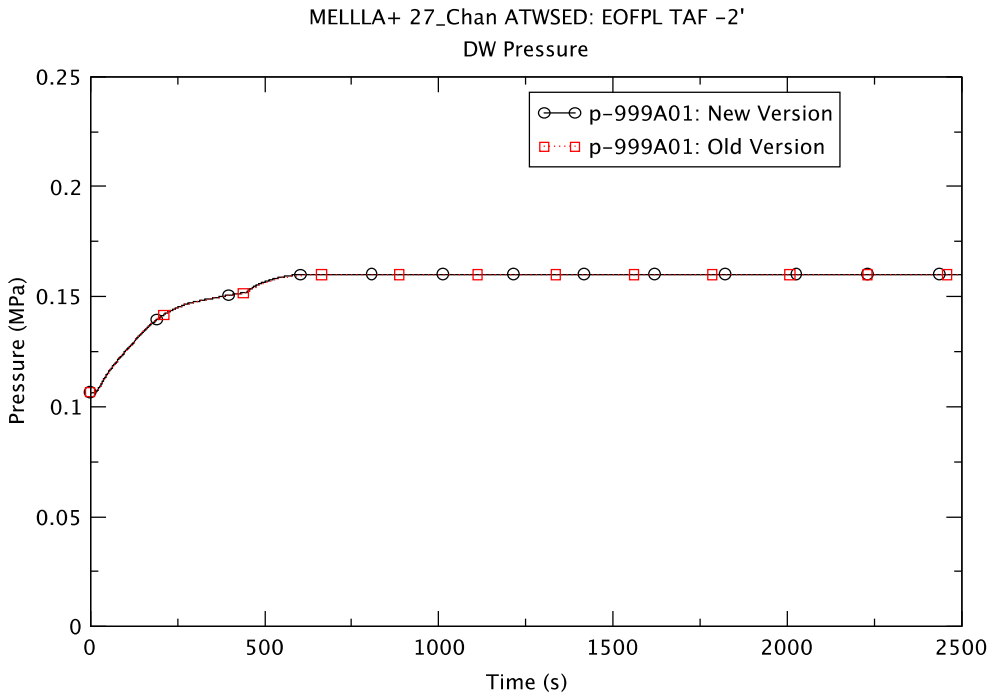

Figure A.11 Drywell Pressure – EOFPL TAF-2

The following figures (Figure A.12 to Figure A.19) are from the execution of the EOFPL TAF-2 75% flow case using two TRACE executables. They are from the same code modification cycle (V5.0p3P32m07co), but are for two different computer platforms, namely, Linux and Windows. Both runs were done with the semi-implicit numerical scheme and a maximum time step size of 0.02 s. Preceding the power spike some differences between the two executables are observed at around 650 s, e.g. in the downcomer water level (Figure A.13). A comparison of the overall results from the two executables demonstrates that both versions of TRACE produce essentially identical results until shortly before the appearance of the power spike at ~700 s. It is thus reasonable to apply the equivalent executable for the Windows platform, namely V5.0p3P32m07co_x64.exe to simulate the EOFPL TAF-2 75% flow case while the cause of the anomaly in the Linux version is under investigation.

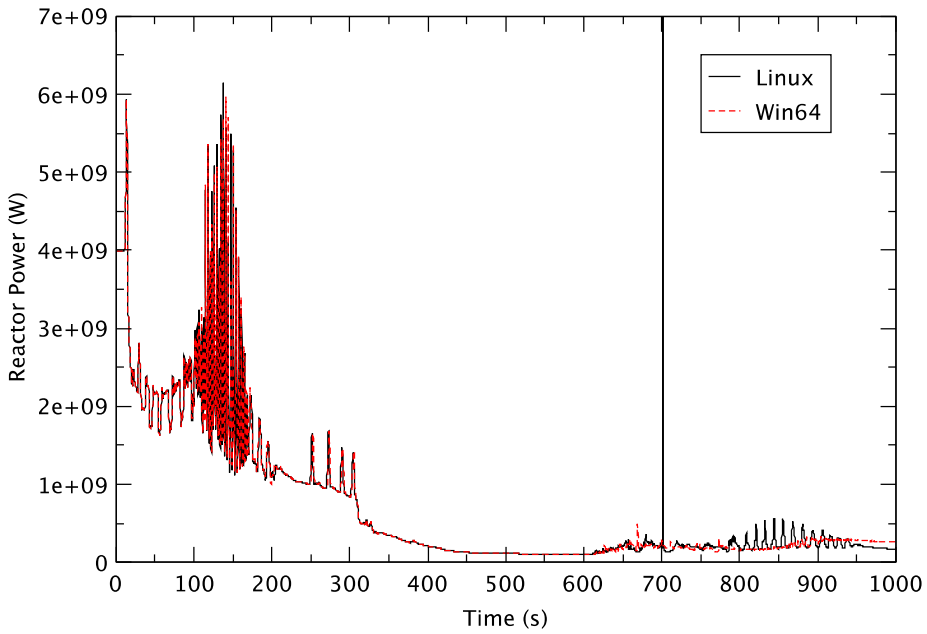

Figure A.12 Reactor Power – EOPFL TAF-2 75% Flow Case

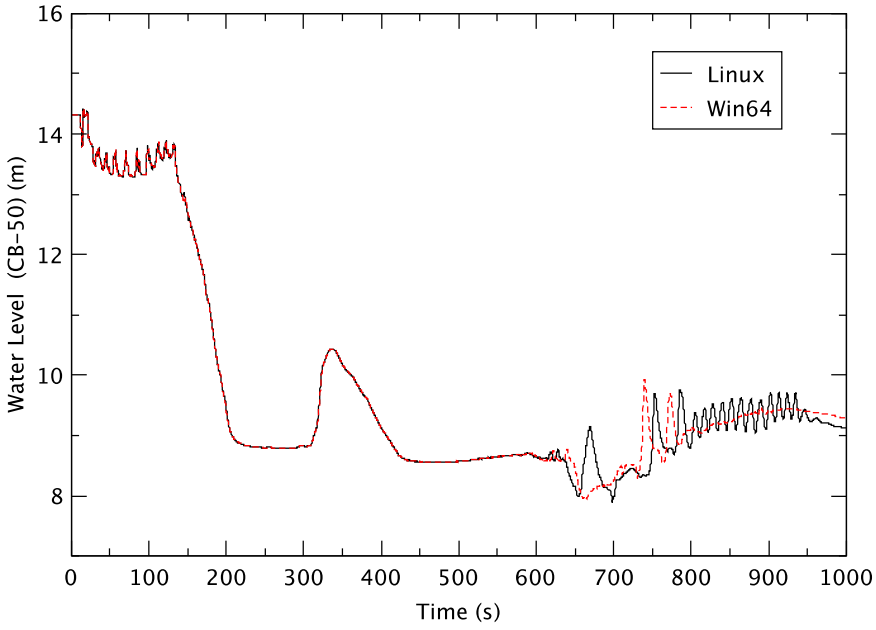

Figure A.13 Downcomer Water Level – EOFPL TAF-2 75% Flow Case

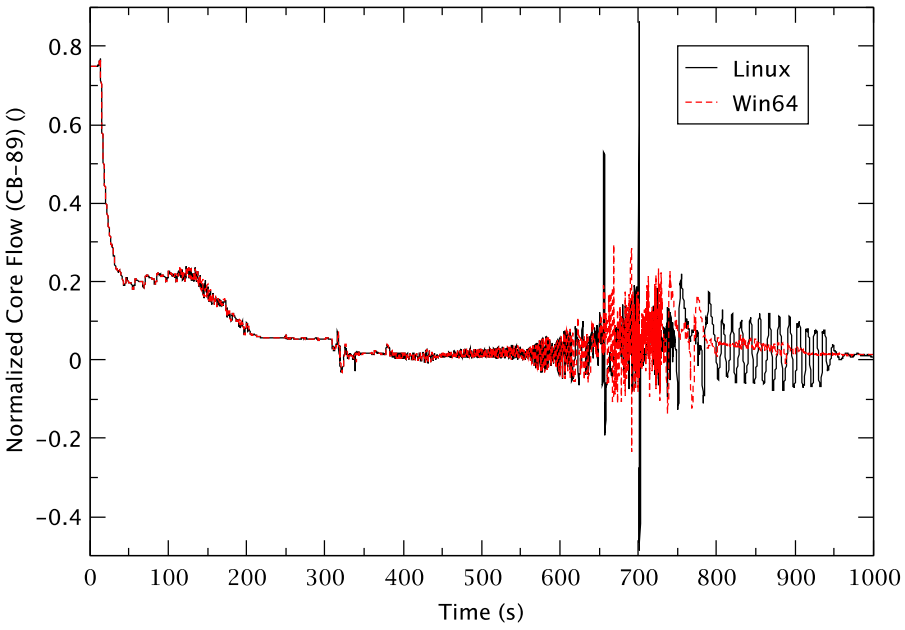

Figure A.14 Core Flow – EOFPL TAF-2 75% Flow Case

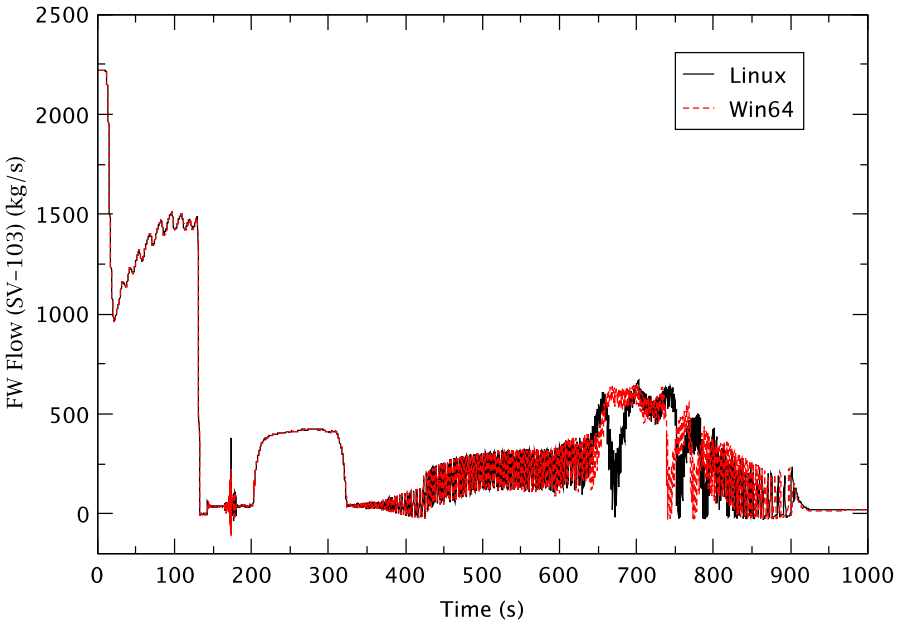

Figure A.15 Feedwater Flow Rate – EOFPL TAF-2 75% Flow Case

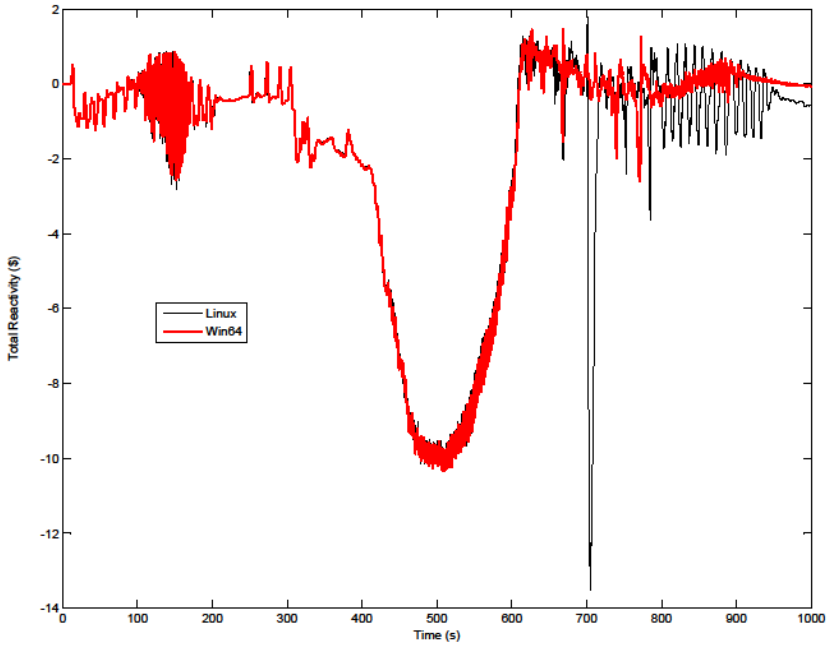

Figure A.16 Total Core Reactivity – EOFPL TAF-2 75% Flow Case

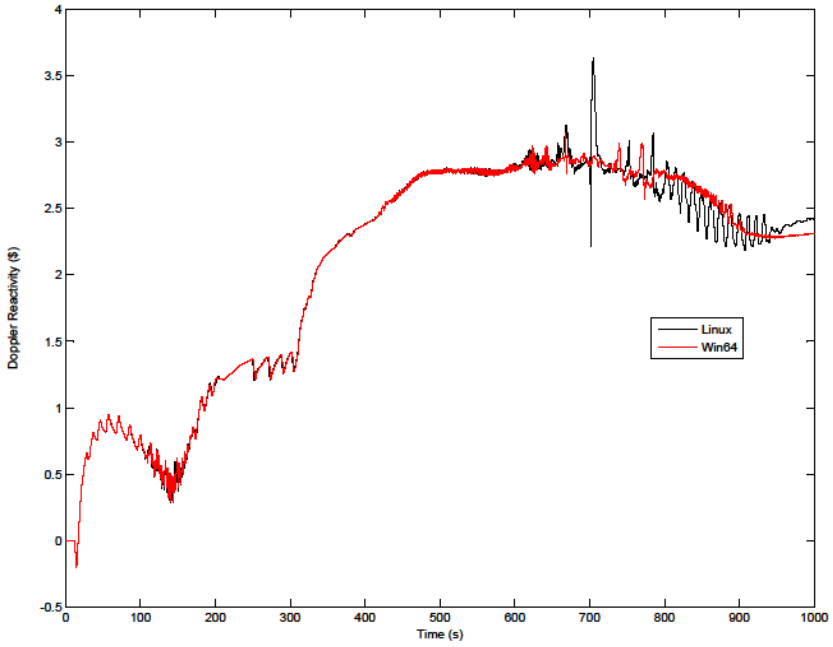

Figure A.17 Doppler Reactivity – EOFPL TAF-2 75% Flow Case

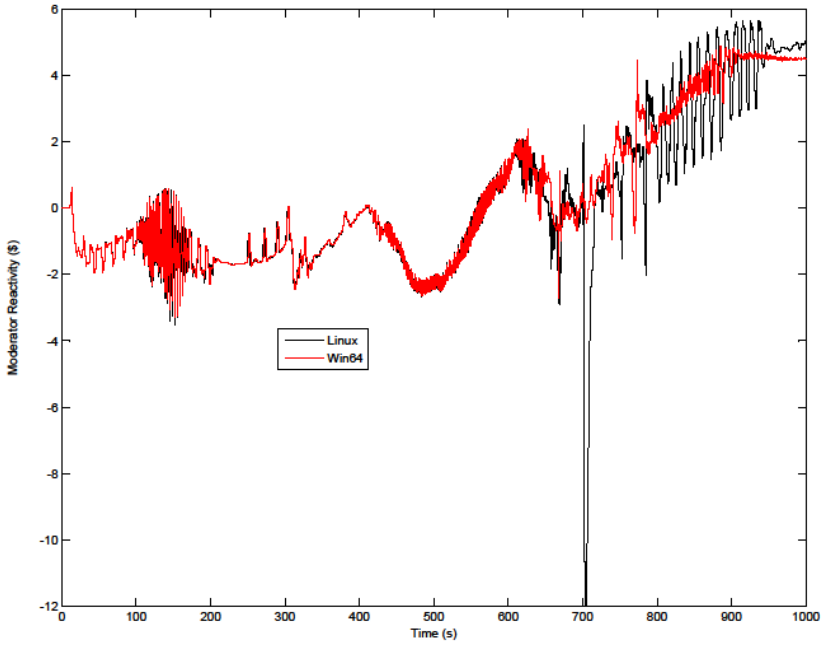

Figure A.18 Moderator Reactivity – EOFPL TAF-2 75% Flow Case

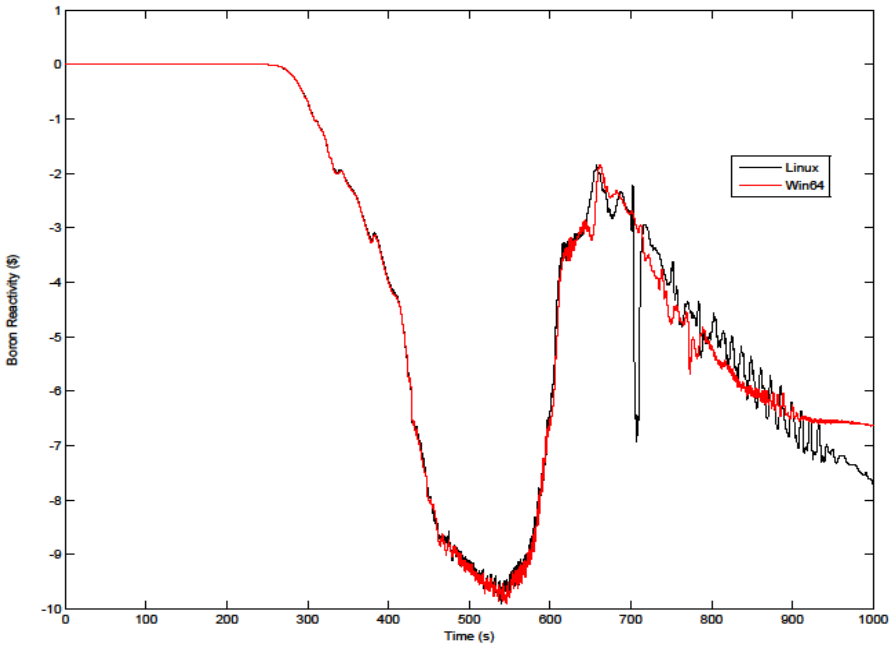

Figure A.19 Boron Reactivity – EOFPL TAF-2 75% Flow Case

APPENDIX B

Selection of Time-Step Size and Numerical Method

This appendix provides additional background information on the selection of numerical method and time-step size for the analysis of ATWS-ED cases by TRACE.

TRACE contains the option to select one of two related numerical methods for solution of the fluid-dynamics equations in the spatial one-dimensional (1D), and three-dimensional (3D) components. The default Stability Enhancing Two-Step (SETS) method has the advantage of avoiding Courant stability limits on time-step size but the disadvantage of relatively high numerical diffusion. A namelist input option permits selection of a semi-implicit (S-I) method that can have substantially less numerical diffusion but has time-step sizes restricted to a material Courant limit. This should be the method of choice for BWR stability analysis. For the current work of analyzing ATWS-ED cases the primary objective is to assess the response of key components to operator actions and not reactor stability. Since the SETS method allows violation of the Courant limit to the time step size, it is possible to simulate long transients such as ATWS with larger time step sizes. The larger time step sizes allow calculations for such transients, generally, to be performed in a reasonable period of real time. Therefore, it has been chosen to be the default method for the analysis of ATWS-ED cases. However SETS loses its efficiency when the problem requires time-step size reductions to very small values. In that case it is appropriate to use the more robust S-I method to solve the problem.

The following is the general guideline used in the current work for the selection of time-step size and the decision to apply the S-I method.

1) Apply SETS with a maximum time-step size of 0.05 s
2) If problem failed, reduce time-step size to 0.025 s
3) If problem still failed, reduce time-step size to 0.01 s sometime before last failure
4) If problem again failed, apply S-I with a maximum time-step size of 0.02 s

It has been found that it took about the same amount of CPU time to complete a 2500 s ATWS-ED transient using either the S-I method or the SETS method with a maximum time-step size of 0.01 s.

The maximum time-step size and the numerical method applied in the 17 ATWS-ED cases are summarized in Table B.1 .

Table B.1 Summary of Time-Step Size and Numerical Method for ATWS-ED

Case ID	Exposure	Flow Rate %	RWL Strategy	SLCS Injection	Comment
6	BOC	85	TAF-2	Lower Plenum	Terminated at 1816 s (SETS 0.025 s) Re-ran successfully with 0.01 s max time-step after 1500 s
7	PHE	85	TAF+5	Lower Plenum	Completed (SETS 0.05 s)
4	BOC	85	TAF+5	Lower Plenum	Completed (SETS 0.05 s)

7C	PHE	85	TAF+5	Upper Plenum	Completed (SETS 0.05 s)
5	BOC	85	TAF	Lower Plenum	Terminated at 1291 s (SETS 0.05 s) Completed (SETS 0.025 s)
10	EOFPL	105	TAF+5	Lower Plenum	Completed (SETS 0.05 s)
12	EOFPL	105	TAF-2	Lower Plenum	Terminated at 768 s (SETS 0.025 s) Re-run with 0.01 s max time-step after 500 s; failed at 800.937 s Completed (S-I 0.02 s)
EDSI	BOC	85	TAF	Lower Plenum	Completed (S-I 0.02 s)
9	PHE	85	TAF-2	Lower Plenum	Terminated at 1760 s (SETS 0.025 s) Re-ran successfully with 0.01 s max time-step after 1500 s
8	PHE	85	TAF	Lower Plenum	Completed (SETS 0.05 s)
11	EOFPL	105	TAF	Lower Plenum	Terminated at 2058 s (SETS 0.05 s) Re-run with 0.025 s max time-step; failed at 817.775 s Re-ran successfully with 0.05 s (SETS) max time-step to 1500 s; 0.025 s max time-step to 2000s and 0.01 s max time-step to 2500 s
4B	BOC	75	TAF+5	Lower Plenum	Completed (SETS 0.05 s)
10D	EOFPL	75	TAF-2	Lower Plenum	Terminated at 618 s (SETS 0.025 s) Re-run with 0.01 s max time-step after 500 s; failed at 615.447 s Re-run with S-I and 0.02 s max time-step; terminated at 628 s. Completed (S-I 0.02 s) (1)
10A	EOFPL	85	TAF+5	Lower Plenum	Completed (SETS 0.05 s)
11A	EOFPL	85	TAF	Lower Plenum	Completed (SETS 0.025 s)
12A	EOFPL	85	TAF-2	Lower Plenum	Terminated at 669 s (SETS 0.025 s) Re-run with 0.01 s max time-step after 500 s; failed at 693.926 s Re-run with S-I and 0.02 s max time-step; terminated at 707 s. Completed (S-I 0.02 s) (2)
10C	EOFPL UHSPH	105	TAF+5	Lower Plenum	Terminated at 1757 s (SETS 0.05 s) Completed re-run with max time-step reduced to 0.025 s after 1500 s

(1) Completed using Windows executable V5.0p3P32m07co_x64.exe. See Appendix A for additional discussion.

(2) Completed using Linux executable V5.0p3P32m07co.x. The CSTEP input for the CONTAN component was changed from 1.0 to 0.5 to avoid failure in the thermal-hydraulic calculation.

In the process of completing the 17 ATWS-ED cases a series of assessment runs have been performed. User experience in selecting time-step size and numerical method is presented in the following discussions.

Effect of Time-Step Size

An EOFPL base case with level control to TAF is used to illustrate the effect of time-step size on the simulation of an ATWS-ED transient. The completion of the case required some adjustments to the time-step size during the course of the execution. As summarized in Table B.1 a run with a 0.05 s maximum time-step size failed at 2058 s while a 0.025 s case failed even earlier at 817 s. The following plots compare the results from the two runs.

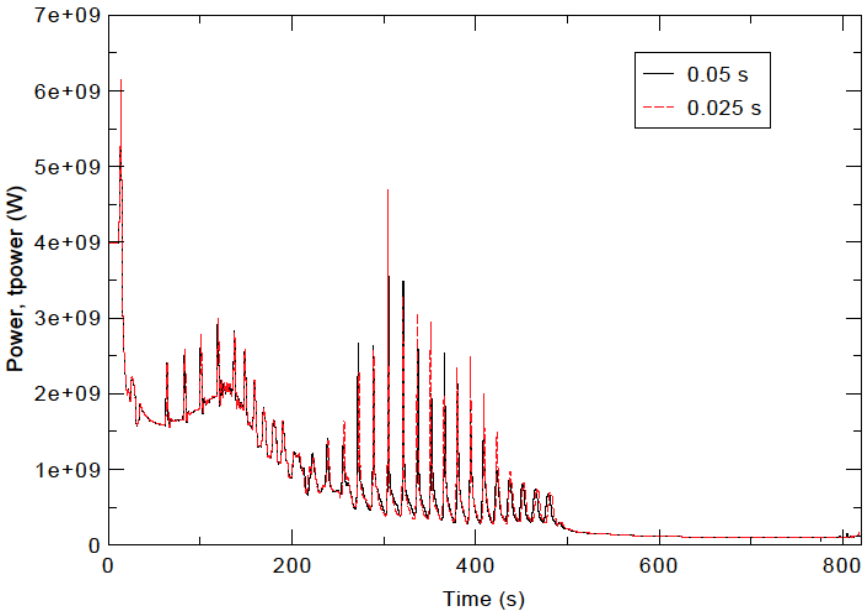

Figure B.1 Case 11 – Reactor Power

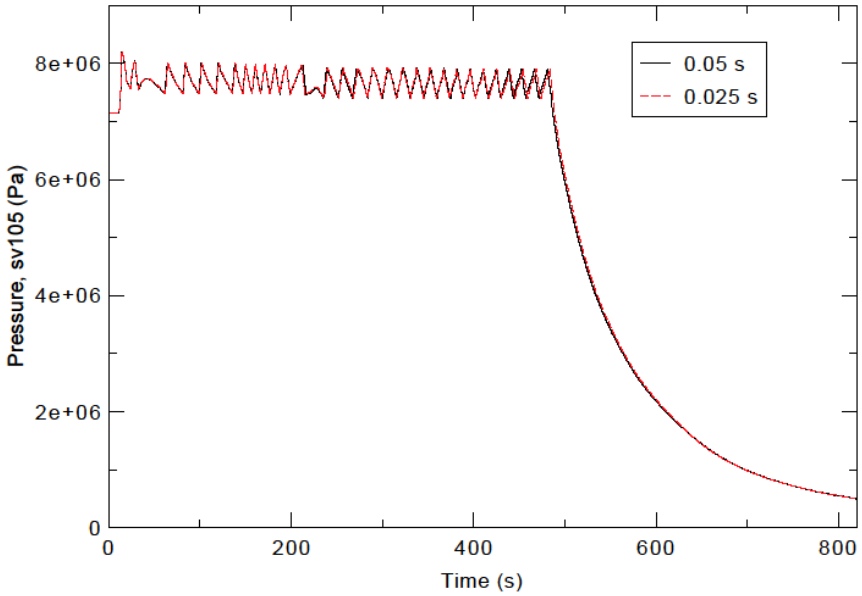

Figure B.2 Case 11 – Reactor Pressure

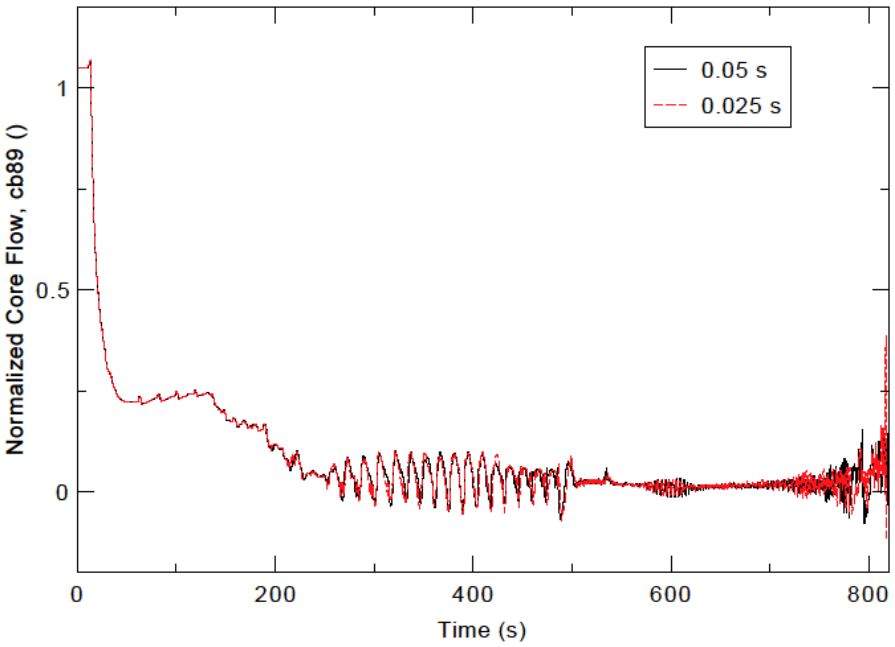

Figure B.3 Case 11 – Core Flow

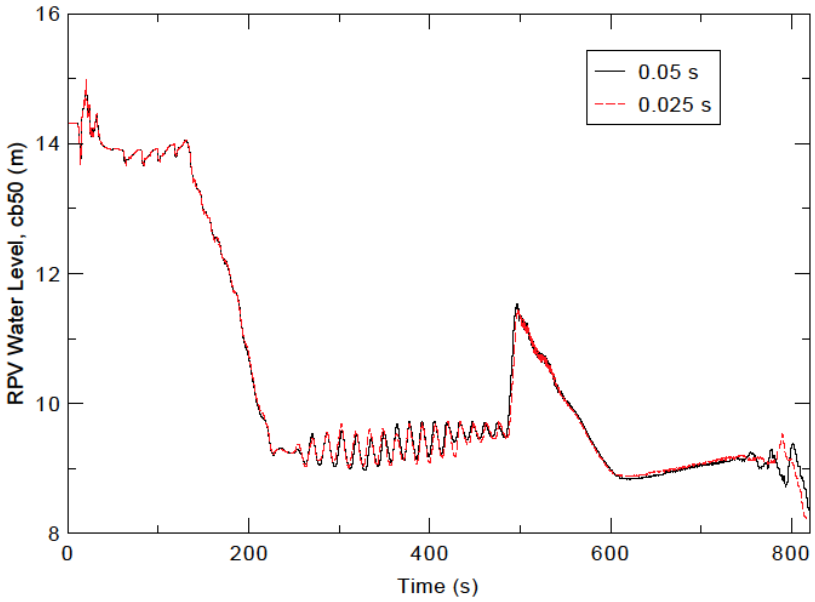

Figure B.4 Case 11 – Downcomer Water Level

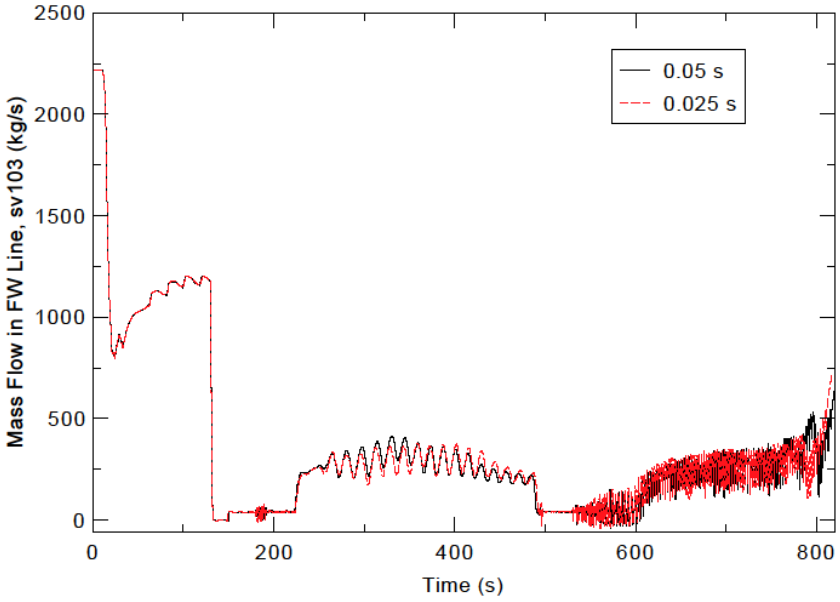

Figure B.5 Case 11 – Feedwater Flow Rate

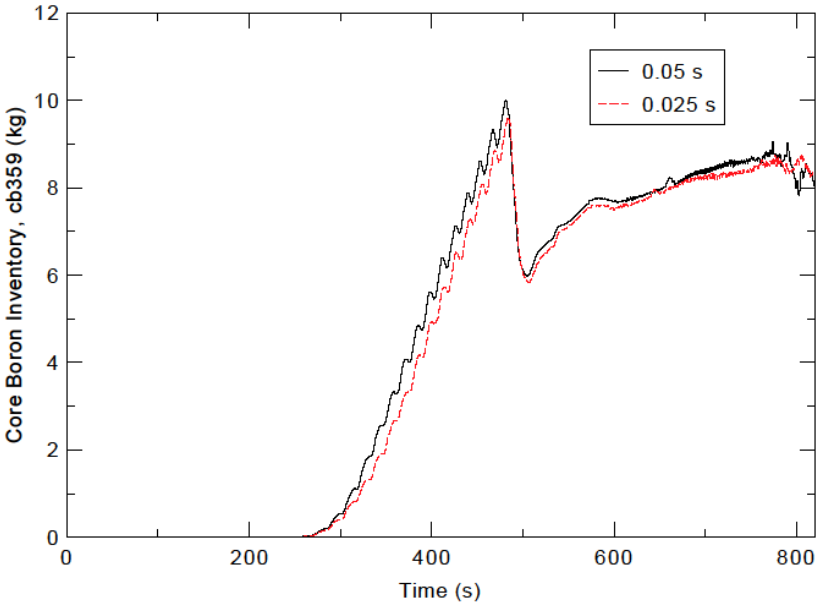

Figure B.6 Case 11 – Boron Inventory in the Core Region

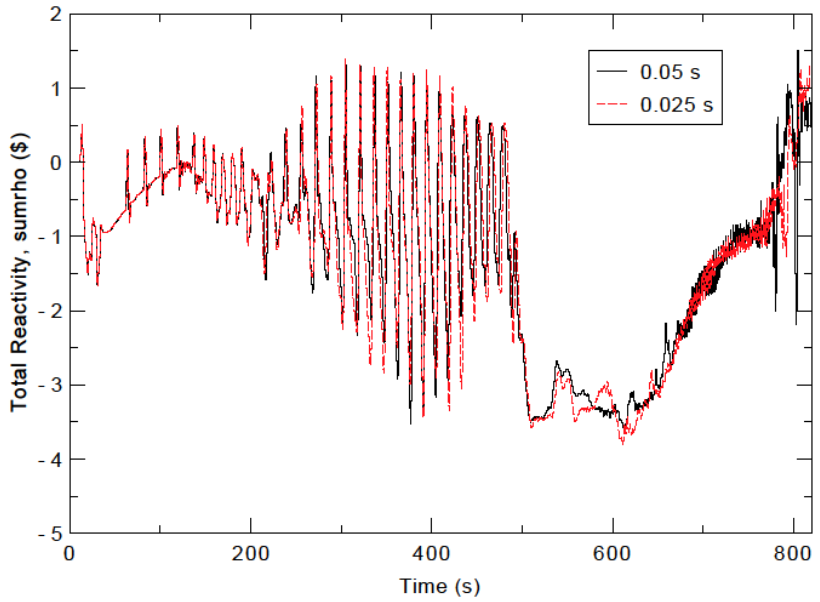

Figure B.7 Case 11 – Core Reactivity

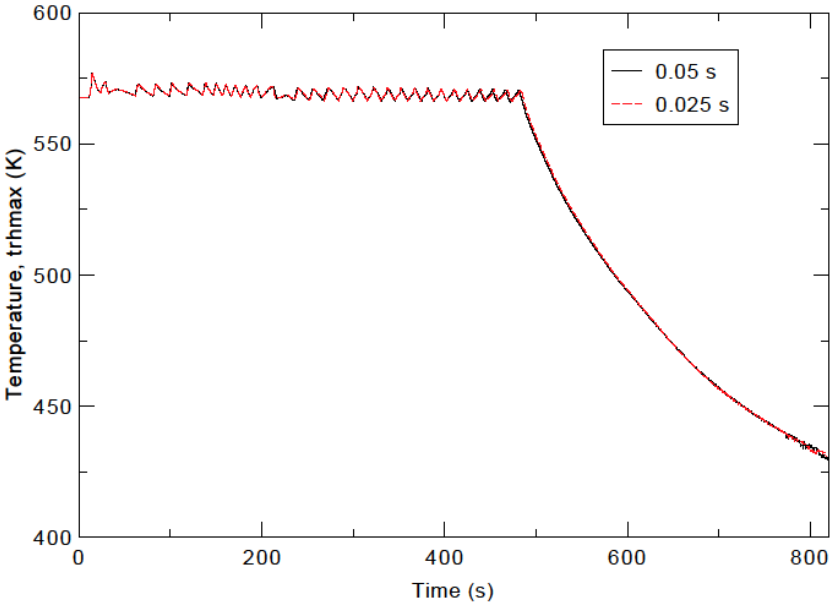

Figure B.8 Case 11 – Peak Clad Temperature

Up to the failure point, the two cases compare favorably. However, the immediate cause of failure appears to be different for the two cases. The 0.025 s case terminated when PARCS outer iteration failed to converge after the set number of iterations (750) and passed bad power (NaN) information to TRACE. The 0.05 s case terminated on TRACE outer iteration failure when the time step reduction reached the limit of 1E-8. In all the ATWS-ED transients analyzed, the power transient is dominated by events occurring in the first few hundred seconds and the later part of the transient is not too important. The plots show that the results in the first few hundred seconds are not sensitive to the time-step size. By judicious choice of time-step sizes during the course of the transient (see Table B.1) the TAF case completed the 2500 s simulation successfully.

Effect of Numerical Method

A BOC base case with level control to TAF (Case 5) is used to demonstrate the effect of numerical method, SETS versus semi-implicit (S-I), on the ATWS-ED results. The case was run using the Windows executable, and the result from the first 500 s is shown in the following figures. It is noted that the SETS case had a maximum time-step size of 0.05 s while the S-I case had a corresponding limit set to 0.02 s.

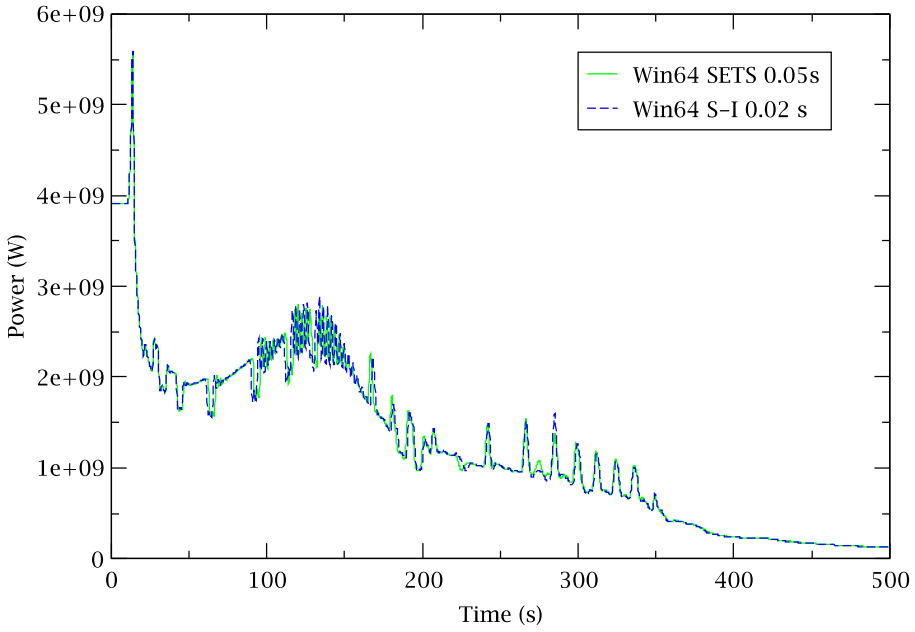

Figure B.9 Case 5 – Reactor Power

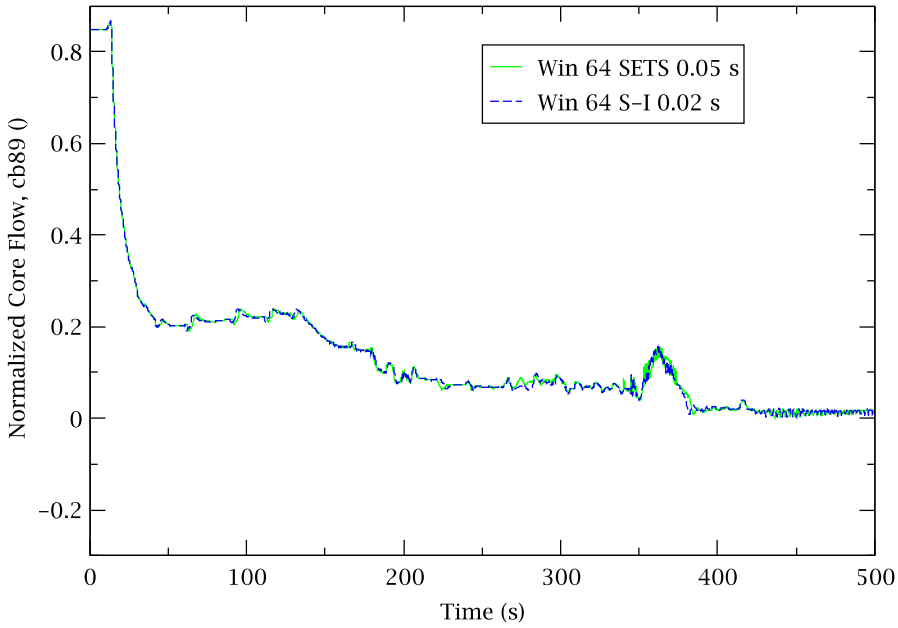

Figure B.10 Case 5 – Core Flow

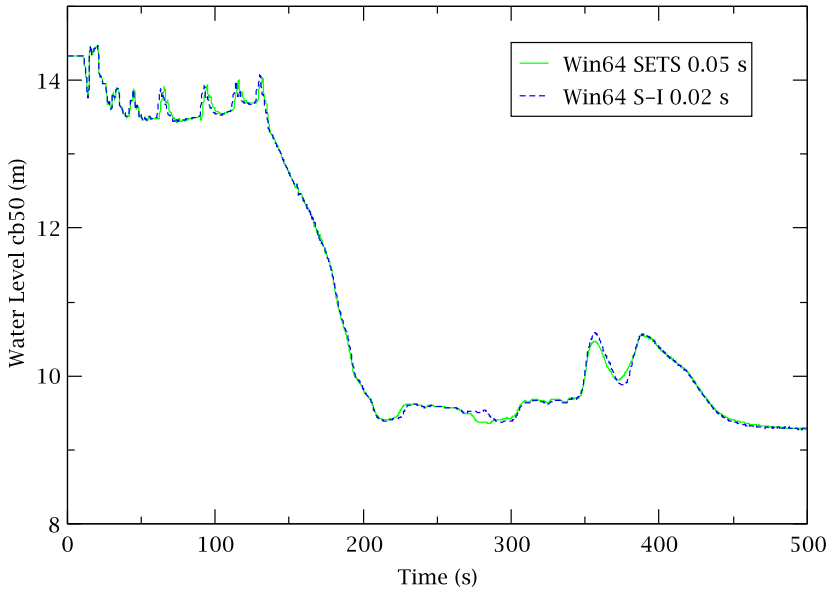

Figure B.11 Case 5 – Downcomer Water Level

The two numerical methods provide almost identical results, as shown in Figure B.9 - Figure B.11.

Effect of Initial Steady-State

All ATWS-ED transient cases were run as a restart from a coupled steady-state (see Section 2.1 in [4] for a discussion of the work flow of executing a TRACE analysis). It is observed that there is bifurcation in results when the computation is started from slightly different initial conditions. Two BOC base cases with level control to TAF were run using the S-I numerical method. Each case was started from a slightly different initial steady state. Two coupled steady-states were generated, one using the S-I method and a maximum time-step size of 0.01 s (initial condition SS1) and the other using the SETS method and a maximum time-step size of 0.02 s (initial condition SS2). Results of the two cases are shown in Figure B.12 and Figure B.13. At ~350 s the two cases start to go on slightly different paths. Both paths seem to be possible in the calculations and which path it takes seems to be sensitive to modeling and numerical method differences. For the case with the SS1 steady-state the natural circulation flow was maintained after the emergency depressurization whereas for the case with the SS2 steady-state the natural circulation was broken. In both cases the reactor power was decaying and the difference does not appear to have significant impact on the outcome of the transient.

It is noted that a similar pattern of an ATWS-ED transient diverging into two different solutions was observed in a comparison between the SETS and the S-I method for a

BOC TAF case [4]. A preliminary explanation[b] for the source of the diverging results, use of different PARCS options (the exponential extrapolation option (Expo_opt) and the implicitness option (THETA), has been shown not to be the case. The controlling factor in the diverging result is the initial steady-state.

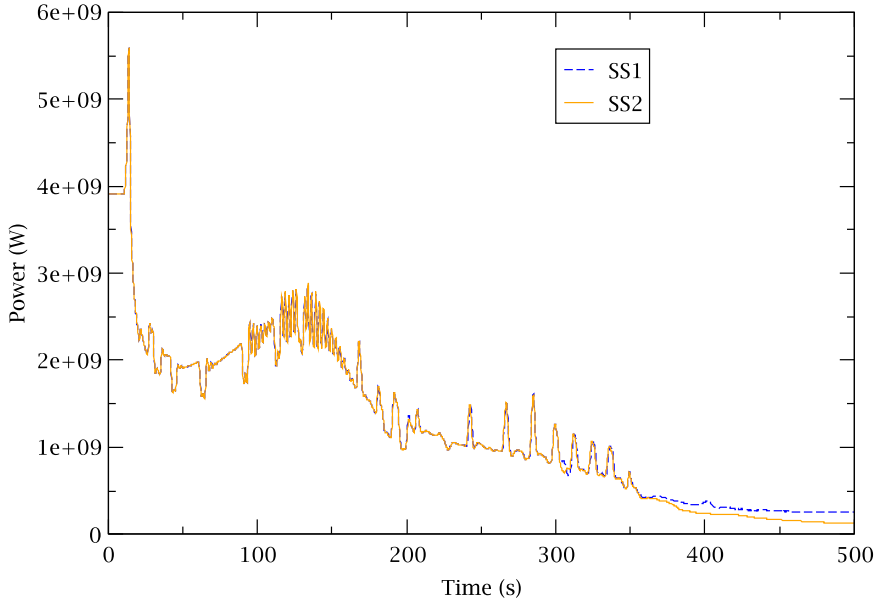

Figure B.12 Core Power – Different Initial Steady-State

[b] J. Staudenmeir, Email to P. Yarsky, U.S. Nuclear Regulatory Commission, May 18, 2012.

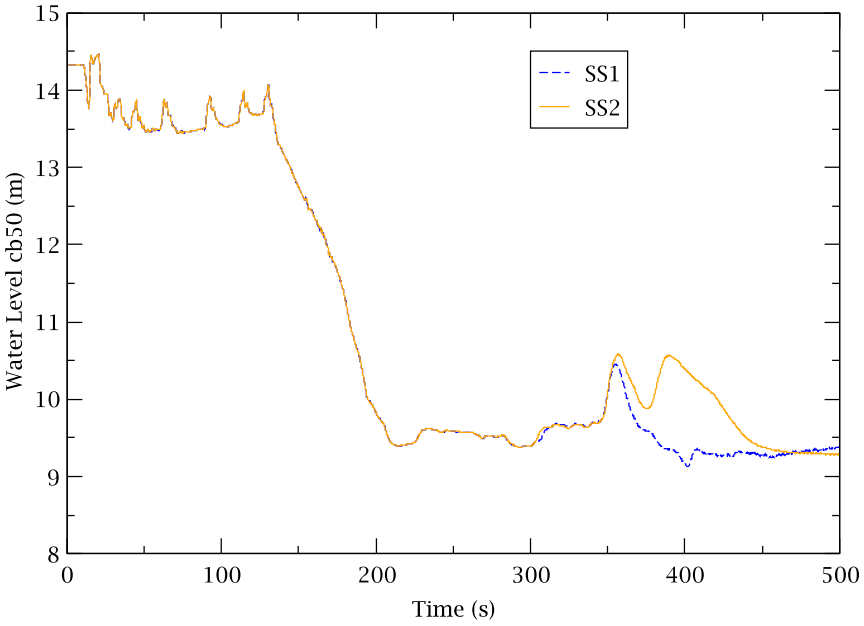

Figure B.13 Downcomer Water Level – Different Initial Steady-State

APPENDIX C

Inputs and Outputs (on CD)

1. ATWS-ED Stand-alone Steady-State File Names
2. ATWS-ED Coupled Steady-State File Names
3. ATWS-ED Transient Input File Names
4. Basic Outputs, available for All ATWS-ED Cases
5. Additional TRACE Outputs
6. Comparison Plots
7. Appendix A Plots
8. Appendix B Plots

Table C.1 ATWS-ED Stand-alone Steady-State File Names

Case ID	TRACE Input File Name
4B	**BOC 75% Flow** boc75-atwsED13.inp
10C	**EOFPL UHSPH** eofpl27ch-atwsED13.inp
10D	**EOFPL 75% Flow** eofpl75-atwsED13.inp
10A/11A	**EOFPL 85% Flow** eofpl85-atwsED13.inp
12A (*)	**EOFPL 85% Flow** eofpl85-atwsED13-12A.inp

(*) Minor update to CONTAN component (CSTEP=0.5) with respect to the input for cases 10A and 11A. The change was needed to be able to run the transient calculation on a Linux platform.

Table C.2 ATWS-ED Coupled Steady-State File Names

Case ID	TRACE/PARCS Input File Names
4B	**BOC 75% Flow** boc75-atwsED13-rc.inp boc75-atwsED13-rc.parcs_inp full-boc.dep mapping27.map bwr5-full-rev4.geom
10C	**EOFPL UHSPH** eofplUH-atwsED13-rc.inp eofplUH-atwsED13-rc.parcs_inp full-SPH-eohf.dep mapping27.map bwr5-full-rev4.geom
10D	**EOFPL 75% Flow** eofpl75-atwsED13-rc.inp eofpl75-atwsED13-rc.parcs_inp full-eohf.dep mapping27.map bwr5-full-rev4.geom
10A/11A/12A	**EOFPL 85% Flow** eofpl85-atwsED13-rc.inp eofpl85-atwsED13-rc.parcs_inp full-eohf.dep mapping27.map bwr5-full-rev4.geom

Table C.3 ATWS-ED Transient Input File Names

Case ID	TRACE/PARCS Input File Names
4B	**BOC 75% Flow TAF+5** boc75TAF+5-atwsED13L-tr.inp boc75TAF+5-atwsED13L-tr.parcs_inp
10C	**EOFPL UHSPH TAF+5** eofplUHTAF+5-atwsED13L-tr.inp eofplUHTAF+5-atwsED13L-tr.parcs_inp
10D (*)	**EOFPL 75% Flow TAF-2** eofpl75TAF-2-atwsED13L-tr.inp eofpl75TAF-2-atwsED13L-rc.parcs_inp
10A	**EOFPL 85% Flow TAF+5** eofpl85TAF+5-atwsED13L-tr.inp eofpl85TAF+5-atwsED13L-rc.parcs_inp
11A	**EOFPL 85% Flow TAF** eofpl85TAF-atwsED13L-tr.inp eofpl85TAF-atwsED13L-rc.parcs_inp
12A	**EOFPL 85% Flow TAF-2** eofpl85TAF-2-atwsED13L-tr.inp eofpl85TAF-2-atwsED13L-rc.parcs_inp

(*) Two sets of outputs for this case: one using the Linux executable and one for Windows.

Table C.4 Basic TRACE Outputs, available for all ATWS-ED Cases

File Names	Description
Reactivities_PDF.pdf (*)	Components of Reactivity ($)
TR-Boron-Concent-LP-R1_PDF.pdf	Boron Concentration in Lower Plenum of Ring-1 (-)
TR-Boron-Concent-LP-R2_PDF.pdf	Boron Concentration in Lower Plenum of Ring-2 (-)
TR-Boron-Inv-Core_PDF.pdf	Boron Inventory in Core (kg)
TR-CladT_PDF.pdf	Cladding Temperatures (Axial) (K)
TR-Core-Avg-VFrac_PDF.pdf (*)	Core Average Void Fraction (-)
TR-Core-Bypass-VFrac-R1_PDF.pdf	Core Bypass Void Fraction in Ring-1 (-)
TR-Core-Bypass-VFrac-R2_PDF.pdf	Core Bypass Void Fraction in Ring-2 (-)
TR-Core-Flow_PDF.pdf	Normalized Core Total Mass Flow Rate (-)
TR-DC-Level_PDF.pdf	DC Level from Bottom of RPV (m)
TR-DW-P_PDF.pdf	DW Pressure (MPa)
TR-FCT_PDF.pdf	Fuel Centerline Temperatures (Axial) (K)
TR-FW-Flow_PDF.pdf	Feedwater Flow Rate (kg/s)

TR-FW-Temp_PDF.pdf	Feedwater Temperature (K)
TR-Max-PCT_PDF.pdf	Maximum Peak Cladding Temperatures (K)
TR-P-RPV_PDF.pdf	RPV Dome Pressure (MPa)
TR-Reactor-Power_PDF.pdf	Reactor Power (MW)
TR-Recir-Flow_PDF.pdf	Recirculation Flow Rate (kg/s)
TR-RPV-Level_PDF.pdf	RPV Level (m)
TR-SP-Temp_PDF.pdf	SP Temperature (K)
TR-SRV-Chok-A_PDF.pdf	SRV Choking Flag at SRV A (-)
TR-SRV-Chok-B_PDF.pdf	SRV Choking Flag at SRV B (-)
TR-SRV-Chok-C1_PDF.pdf	SRV Choking Flag at SRV C1 (-)
TR-SRV-Chok-C2_PDF.pdf	SRV Choking Flag at SRV C2 (-)
TR-SRV-Chok-D_PDF.pdf	SRV Choking Flag at SRV D (-)
TR-SRV-Flow-A_PDF.pdf	SRV Flow through SRV A (kg/s)
TR-SRV-Flow-B_PDF.pdf	SRV Flow through SRV B (kg/s)
TR-SRV-Flow-C1_PDF.pdf	SRV Flow through SRV C1 (kg/s)
TR-SRV-Flow-C2_PDF.pdf	SRV Flow through SRV C2 (kg/s)
TR-SRV-Flow-D_PDF.pdf	SRV Flow through SRV D (kg/s)
TR-SRV-P-A_PDF.pdf	Pressure Upstream and Downstream of SRV A (MPa)
TR-SRV-P-B_PDF.pdf	Pressure Upstream and Downstream of SRV B (MPa)
TR-SRV-P-C1_PDF.pdf	Pressure Upstream and Downstream of SRV C1 (MPa)
TR-SRV-P-C2_PDF.pdf	Pressure Upstream and Downstream of SRV C2 (MPa)
TR-SRV-P-D_PDF.pdf	Pressure Upstream and Downstream of SRV D (MPa)
TR-Steam-Flow_PDF.pdf	Steam Flow (kg/s)
TR-Temp-LP_PDF.pdf	Lower Plenum Temperature (K)
TR-Void-LP-R1_PDF.pdf	Lower Plenum Void Fraction in Ring-1 (-)
TR-Void-LP-R2_PDF.pdf	Lower Plenum Void Fraction in Ring-2 (-)

(*) The information used to generate this plot is output from PARCS.

Table C.5 Additional TRACE Outputs

File Name	Description
Boron injection conc EOFPL 75F TAF-2.pdf	Effective Injection Boron Concentration – EOFPL 75% Flow TAF-2' (kg-B/Kg-water)
Effective Boron Conc EOFPL 85F TAF.pdf	Effective Injection Boron Concentration – EOFPL 85% Flow TAF (kg-B/Kg-water)
Effective Boron Conc EOFPL 85F TAF+5.pdf	Effective Injection Boron Concentration – EOFPL 85% Flow TAF+5' (kg-B/Kg-water)
Effective Boron Conc EOFPL 85F TAF-2.pdf	Effective Injection Boron Concentration – EOFPL 85% Flow TAF-2' (kg-B/Kg-water)

Table C.6 Comparison Plots

File Name	Description
Boron-Inv-Core_PDF.pdf	Core Boron Inventory (kg)
Core-Flow_PDF.pdf	Normalized Total Core Flow (-)
DC-Level_PDF.pdf	Downcomer Level (m)
DW-P_PDF.pdf	Drywell Pressure (MPa)
P-RPV_PDF.pdf	RPV Pressure (MPa)
Reactor-Power_PDF.pdf	Reactor Power (MW)
SP-Temp_PDF.pdf	Suppression Pool Temperature (K)
Reactor-Power_zoom.pdf (*)	Reactor Power (MW) (0 to 600 s)
PCT_PDF.pdf (*)	Maximum Peak Clad Temperature (K)
SS_axial.pdf (**)	Normalized Steady-State Axial Power Distribution (-)
SS_axialdensity.pdf (***)	Axial Moderator Density Distribution (kg/m^3)
Total-Reactivity.pdf (for Section 2.2 only))	Total Reactivity ($)

(*) Not available for Section 2.3.
(**) Not available for Section 2.5.
(***) Available for Sections 2.2 and 2.4.

Table C.7 Appendix A Plots

File Name	Description
TR-Boron-Inv-Core_PDF.pdf	Boron Inventory in the Core (kg) EOFPL TAF-2 (old vs. new)
TR-Core-Avg-VFrac_PDF.pdf (*)	Core Average Void Fraction (-) EOFPL TAF-2 (old vs. new)
TR-Core-Flow_PDF.pdf	Normalized Core Flow (-) EOFPL TAF-2 (old vs. new)
TR-DC-Level_PDF.pdf	Downcomer Water Level (m) EOFPL TAF-2 (old vs. new)
TR-DW-P_PDF.pdf	Drywell Pressure (MPa) EOFPL TAF-2 (old vs. new)
TR-FW-Flow_PDF.pdf	Feedwater Flow Rate (kg/s) EOFPL TAF-2 (old vs. new)
TR-P-RPV_PDF.pdf	Reactor Pressure (MPa) EOFPL TAF-2 (old vs. new)
TR-Reactor-Power_PDF.pdf	Reactor Power (MW) EOFPL TAF-2 (old vs. new)
TR-SP-Temp_PDF.pdf	Suppression Pool Temperature (K) EOFPL TAF-2 (old vs. new)
TR-Steam-Flow_PDF.pdf	Steam Flow Rate (kg/s) EOFPL TAF-2 (old vs. new)
TR-Temp-LP_PDF.pdf	Lower Plenum Temperature (K) EOFPL TAF-2 (old vs. new)
Boron.pdf (*)	Boron Reactivity ($) (Linux and Win64)
CoreFlow.pdf	Normalized Total Core Flow (-) (Linux and Win64)
Doppler.pdf (*)	Doppler Reactivity ($) (Linux and Win64)
FWFlow.pdf	Feedwater Flow (kg/s) (Linux and Win64)
moderator.pdf (*)	Moderator Density Reactivity ($) (Linux and Win64)
Rxpower.pdf	Reactor Power (MW) (Linux and Win64)
TotalReactivity.pdf (*)	Total Reactivity ($) (Linux and Win64)
WaterLevel.pdf	Downcomer Water Level (m) (Linux and Win64)

(*) The information used to generate this plot is output of PARCS.

Table C.8 Appendix B Plots

File Name	Description
tpower.pdf	Reactor Power (W) (0.05 s and 0.025 s)
pressure.pdf	Reactor Pressure (Pa) (0.05 s and 0.025 s)
core flow.pdf	Normalized Core Flow (-) (0.05 s and 0.025 s)
wl.pdf	Downcomer Water Level (m) (0.05 s and 0.025 s)
fw.pdf	Feedwater Flow Rate (kg/s) (0.05 s and 0.025 s)
boron inv.pdf	Boron Inventory in the Core (kg) (0.05 s and 0.025 s)
sumrho.pdf (*)	Core Reactivity ($)(0.05 s and 0.025 s)
trhmax.pdf	Peak Clad Temperature (K) (0.05 s and 0.025 s)
SETS-S-I Rx Power.pdf	Reactor Power (s) (SETS 0.05 s and S-I 0.02 s)
SETS-S-I Core Flow.pdf	Normalized Core Flow (-) (SETS 0.05 s and S-I 0.02 s)
SETS-S-I Water Level.pdf	Downcomer Water Level (m) (SETS 0.05 s and S-I 0.02 s)
SS Power.pdf	Reactor Power (W) (different steady-state)
SS Water Level.pdf	Downcomer Water Level (m) (different steady-state)

(*) The information used to generate this plot is output of PARCS.